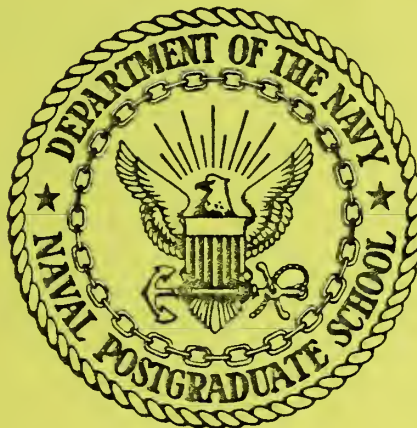


NAVAL POSTGRADUATE SCHOOL

Monterey, California



FINAL TECHNICAL REPORT OF NSF GRANT DES 75-10719

"TROPICAL WAVE DYNAMICS"

by

Chih-Pei Chang and Roger T. Williams

March 1978

Final Report for Period October 1975 - March 1978

Approved for public release; distribution unlimited.

NAVAL POSTGRADUATE SCHOOL
Monterey, California

Rear Admiral Tyler F. Dedman
Superintendent

J. R. Borsting
Provost

The work reported herein was supported by the National Science Foundation, Atmospheric Research Section, under Grant DES 75-10719.

Reproduction of all or part of this report is authorized.

This report was prepared by:

U N C L A S S I F I E D

SECURITY CLASSIFICATION OF THIS PAGE (When Data Entered)

REPORT DOCUMENTATION PAGE		READ INSTRUCTIONS BEFORE COMPLETING FORM
1. REPORT NUMBER NPS 63Cj78031	2. GOVT ACCESSION NO.	3. RECIPIENT'S CATALOG NUMBER
4. TITLE (and Subtitle) Final Technical Report of NSF Grant DES 75-10719 "Tropical Wave Dynamics"		5. TYPE OF REPORT & PERIOD COVERED Final Report for Oct 1975 - Mar 1978
		6. PERFORMING ORG. REPORT NUMBER
7. AUTHOR(s) Chih-Pei Chang and Roger T. Williams		8. CONTRACT OR GRANT NUMBER(s) NSF DES 75-10719
9. PERFORMING ORGANIZATION NAME AND ADDRESS Naval Postgraduate School Monterey, California 93940		10. PROGRAM ELEMENT, PROJECT, TASK AREA & WORK UNIT NUMBERS
11. CONTROLLING OFFICE NAME AND ADDRESS National Science Foundation Washington, D.C. 20550		12. REPORT DATE March 1978
		13. NUMBER OF PAGES 65
14. MONITORING AGENCY NAME & ADDRESS (If different from Controlling Office)		15. SECURITY CLASS. (of this report) Unclassified
		15a. DECLASSIFICATION/DOWNGRADING SCHEDULE
16. DISTRIBUTION STATEMENT (of this Report) Approved for public release; distribution unlimited.		
17. DISTRIBUTION STATEMENT (of the abstract entered in Block 20, if different from Report)		
18. SUPPLEMENTARY NOTES		
19. KEY WORDS (Continue on reverse side if necessary and identify by block number) Tropical Waves Tropical Meteorology Tropical Dynamics Monsoon Barotropic Instability		
20. ABSTRACT (Continue on reverse side if necessary and identify by block number) This research may be divided into the following three parts: a) waves forced by condensation heating in the troposphere, b) the local barotropic instability produced by a spatially varying basic flow, c) the numerical modeling of the wave-basic flow interacting system. In the first part, the problem of the vertical structure of tropical waves generated by cumulus heating is treated for the following two cases: 1) heating is controlled by large-scale low-level convergence and 2) heating receives no feedback from		

large-scale motion. In the first case it is shown that waves which have a short vertical wavelength relative to the vertical scale of heating are stable, and the structure of the most unstable solution is computed. In the second case it is shown that the forcing is most efficient for the longest zonal wavelength and that the most favored vertical wavelength is about twice the vertical scale of the heating. The effect of cumulus damping on planetary-scale Kelvin-like oscillation gives solution which resembles certain observed tropical circulation.

The second portion of the research treats waves in a barotropically unstable jet, which varies in x and y . Numerical solutions are obtained in a channel with time periodic forcing on the east side and a radiation condition on the west side. The solutions, which are periodic in time with the forcing frequency, show the spatial growth and decay of the waves as they move through the channel.

In the third portion of the research a 3-level primitive equation model is used to simulate the interaction between the planetary-scale monsoon circulation and the synoptic waves. The heating is specified from the 200-mb time-mean divergence field analyzed by Krishnamurti and Rogers. The interactions are examined with a constant heating and with a heating with a ten day period. The model properly simulates certain aspects of the summer monsoon circulation but also reveals certain problems in the vorticity damping mechanism.

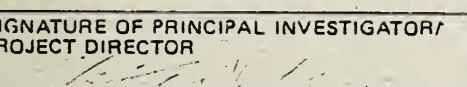
NATIONAL SCIENCE FOUNDATION Washington, D.C. 20550		SUMMARY OF COMPLETED PROJECT		Form Approved OMB No. 99R0013	
<i>Please read instructions on reverse carefully before completing this form.</i>					
1. INSTITUTION AND ADDRESS Naval Postgraduate School Monterey, Calif 93940		2. NSF PROGRAM Meteorology		3. PRINCIPAL INVESTIGATOR(S) Chih-Pei Chang Roger T. Williams	
4. AWARD NUMBER DES 75-10719	5. DURATION (MOS) 30	6. AWARD PERIOD from 10/1/75 to 3/31/78	7. AWARDEE ACCOUNT NUMBER 56522		
8. PROJECT TITLE <div style="text-align: center; padding: 10px;">Tropical Wave Dynamics</div>					
9. SUMMARY (ATTACH LIST OF PUBLICATIONS TO FORM) <p> This research may be divided into the following three parts: a) waves forced by condensation heating in the troposphere, b) the local barotropic instability produced by a spatially varying basic flow, c) the numerical modeling of the wave-basic flow interacting system. In the first part, the problem of the vertical structure of tropical waves generated by cumulus heating is treated for the following two cases: 1) heating is controlled by large-scale low-level convergence and 2) heating receives no feedback from large-scale motion. In the first case it is shown that waves which have a short vertical wavelength relative to the vertical scale of heating are stable, and the structure of the most unstable solution is computed. In the second case it is shown that the forcing is most efficient for the longest zonal wavelength and that the most favored vertical wavelength is about twice the vertical scale of the heating. The effect of cumulus damping on planetary-scale Kelvin-like oscillation gives solution which resemble certain observed tropical circulations. </p> <p> The second portion of the research treats waves in a barotropically unstable jet, which varies in x and y. Numerical solutions are obtained in a channel with time periodic forcing on the east side and a radiation condition on the west side. The solutions, which are periodic in time with the forcing frequency, show the spatial growth and decay of the waves as they move through the channel. </p> <p> In the third portion of the research a 3-level primitive equation model is used to simulate the interaction between the planetary-scale monsoon circulation and the synoptic waves. The heating is specified from the 200-mb time-mean divergence field analyzed by Krishnamurti and Rogers. The interactions are examined with a constant heating and with a heating with a ten day period. The model properly simulates certain aspects of the summer monsoon circulation but also reveals certain problems in the vorticity damping mechanism. </p>					
9. SIGNATURE OF PRINCIPAL INVESTIGATOR/ PROJECT DIRECTOR 		TYPED OR PRINTED NAME Chih-Pei Chang		DATE 	

TABLE OF CONTENTS

1. Description of Research and Results - - - - - 5

2. List of Publications - - - - - 12

3. Theses - - - - - 13

4. Scientific collaborators - - - - - 13

5. Comments - - - - - 13

6. Appendix (reprints) - - - - - 14

Initial Distribution List - - - - - 65

1. DESCRIPTION OF RESEARCH AND RESULTS

The research goal of this project may be summarized into the following three parts

a) Waves forced by condensation heating in the troposphere

We have studied the problem of the vertical structure of tropical waves generated by cumulus heating for two cases: 1) heating is controlled by large-scale low-level convergence (CISK model) and 2) heating receives no feedback from large-scale motion (forced model). In the first case the internal wave-CISK system is treated and upper and lower bounds for the vertical wavelength of the unstable waves under normal heating conditions are established through analysis of the frequency equation. The lower bound excludes the possibility of excitation or maintenance of short vertical wavelengths relative to the vertical scale of heating. The vertical structure of the most unstable waves is also computed. These results were reported in Chang (1976a). In the second case the problem of scale-selection of Kelvin waves in the stratosphere is analyzed using an inviscid linear model. The results modify Holton's (1973) theory in that 1) the forcing is most efficient for the longest zonal wavelength even if the heat sources are distributed randomly, and 2) the most favored vertical wavelength of the excited waves is about twice the vertical scale of heating. These results were reported in Chang (1976b). We have also treated the linear model with friction added which is called for by several budget studies of cumulus-related tropical weather systems, including the monsoon (Holton and Colton, 1972), the cloud clusters (Williams and Gray, 1973), and the

easterly waves (Reed and Recker, 1971; Wallace, 1971, Reed and Johnson, 1974; Chu, 1976). This friction is believed to be due to vertical cumulus transports. Our analysis shows that this damping has a strong influence at low frequencies on the forced equatorial waves and results in two types of dispersive relationships. The first type is characteristic of the regular internal gravity waves which have fast phase speeds and weak vertical attenuation. The second type is dominated by the viscous damping time scale and has slow phase speed and strong vertical trapping. This theory predicts that the stratospheric oscillations may be identified with the first type and the tropospheric oscillations with the second type. In the case of Kelvin waves the results can be used to explain consistently both the observed stratospheric Kelvin waves and the planetary-scale Kelvin-like oscillations in the troposphere including the 40-50 day oscillation and the winter monsoon and Walker circulations. These results are described in Chang (1977a).

b) The local barotropic instability produced by the spatially varying basic flow.

Here we have studied the behavior of waves superimposed upon a barotropically unstable mean wind field, which varies in x and y . This mean wind field roughly simulates the 200 mb easterly jet south of the Tibetan high during the northern hemisphere summer. The barotropic vorticity equation is linearized and a linear damping term is added. The following mean u component is used

$$\bar{u}(x,y) = -U(x) \operatorname{sech}^2(y/d(x)) - U_0 ,$$

where $d(x)$ is a measure of the width of the jet. The quantity $U(x)$ and \bar{u} are chosen in such a way that the mean flow is non-divergent. A rectangular domain is employed with a time periodic boundary condition on the east and a radiation condition on the west, which simulates the propagation of small amplitude waves through the easterly jet region. The vorticity equation is solved with the use of finite differences, and when the boundary conditions are properly adjusted the waves move smoothly across the region and out the western boundary. After a certain time interval of numerical integration, the solution becomes periodic everywhere, with the frequency that is specified on the eastern boundary. As the waves move through the domain they grow or decay spatially in reaction to the local basic flow, even though at each point the variation is purely harmonic. We have developed a simple mechanistic analytical model which describes the main features of the spatial variation. The simple model uses growth rates and phase velocities which are computed from a parallel flow model with the wavelengths taken from the full numerical model. These wavelengths increase to a maximum at the point where the jet is most unstable, and then decrease; the phase velocity has a similar behavior. The maximum amplitude in the numerical solution occurs downstream from the most unstable part of the jet, at the point where the growth rate in the parallel flow model becomes zero. The above results are grossly similar to that expected from the parallel flow theory of barotropic instability. However, in the unstable region the resultant structure of the waves causes a spatial growth rate greater than predicted by the local growth rates

computed with a parallel flow model. In the stable region, the structure leads to a strong dynamic damping which is apparently due to the presence of the continuous spectrum modes (Case, 1960; Pedlosky, 1964). When a uniform advective velocity is added to a variable mean flow, the difference between the behavior of the computed waves and that implied by the parallel flow theory is somewhat reduced. However, in this case a stronger zonal asymmetry in the spatial growth rate with respect to the jet maximum occurs as a result of slower adjustment of the wave structure to the local stability conditions. Chang and Williams (1976) presented the analytic model and discussed some other analytical aspects of the problem. The numerical model results and comparisons with the analytic model will be reported by Tupaz, Williams and Chang (1978).

c) The numerical modeling of the wave-basic flow interacting system.

In this part we adopted a simple numerical model formulated by Monaco and Williams (1975) to simulate the planetary-scale monsoon circulation and the interaction with synoptic waves. In order to concentrate on the vorticity dynamics, the heating is specified with a horizontal distribution given by the time-mean 200-mb divergence of the 1967 summer analyzed by Krishnamurti and Rogers (1970). The domain of the model extends from 18°S to 46°N and there are three σ -levels in the vertical. Topography is not included although its thermal effect is implied in the heating function. Two preliminary experiments have been carried out to study the vorticity budget of the planetary scales and the non-linear barotropic energy conversions. In one experiment the

heating is fixed in time while in the other it fluctuates with a period of 10 days. The time-mean fields with moderate damping in both experiments show a significant westward phase shift of the Tibetan high, which suggests that the correlation of the fluctuations of the divergence and vorticity as suggested by Holton and Colton (1972) is probably not sufficient for the required planetary-scale vorticity sink. However, the integration period is only three times the fluctuation period in the second experiment and the amplitude of fluctuation is about half that observed. So the full effect of the fluctuation may not have been properly represented in the experiment. A longer integration with larger fluctuation is probably necessary to assess fully the effect of the fluctuating heating. On the other hand, the positions of the simulated tropical upper tropospheric troughs in our model agree quite well with those observed. This may suggest that damping due to cumulus transport is more likely to account for the vorticity sink in the Tibetan high area. We also found significant transient wave activities at the upper levels in both experiments and they appear to be drawing energy from the planetary scale barotropically, in accordance with the observation by Krishnamurti (1971). It is possible that they play an important role in reducing the amplitudes of the long waves which agree quite well with those observed despite the phase problem. This point is borne out by comparison with the excessively large amplitude found in Holton and Colton's linear model when strong damping is excluded. In addition, these short waves are most active in the fluctuating heating case, suggesting that local barotropic instability at

upper levels may be more important than that implied by the time-mean wind. These results have been reported by Chang and Williams (1976b) and Chang and Pentimonti (1977).

Some of the results concerning the planetary-scale monsoon, including the interpretation of the stationary equatorial winter monsoon circulation as a viscous, thermally-forced Kelvin wave (part a), the preliminary result of the study of barotropic instability of the upper-tropospheric summer monsoon basic flow (part b), and the preliminary result of the planetary scale vorticity budget using forced numerical model (part c) are included in a review paper by Chang (1977b). The research on these problems is being continued under NSF Grant ATM77-14821 which began on 15 September 1977.

REFERENCES

- Case, K.M., 1960: Stability of inviscid plane Couette flow. Phys. of Fluids, 3, 143-157.
- Chang, C.-P., 1976a: Vertical structure of tropical waves maintained by internally-induced cumulus heating. J. Atmos. Sci., 33, 729-739.
- Chang, C.-P., 1976b: Forcing of stratospheric Kelvin waves by tropospheric heat sources. J. Atmos. Sci., 33, 740-744.
- Chang, C.-P., 1977a: Viscous internal gravity waves and low-frequency oscillations in the tropics. Submitted to J. Atmos. Sci.
- Chang, C.-P., 1977b: Some theoretical problems of the planetary-scale monsoons, Pure and Appl. Geophys., 115, 1089-1109.
- Chang, C.-P. and R.T. Williams, 1976a: Barotropic instability of a spatially-varying mean flow. Conference on atmospheric waves and stability, Seattle, March-April 1976. Bull. Amer. Meteor. Soc., 57, 101.
- Chang, C.-P. and R.T. Williams, 1976b: Study of planetary and synoptic-scale waves of the northern summer monsoon. GARP Study Conference on tropical numerical modeling, Exeter, England, April 1976.
- Chu, J.-H., 1976: Vorticity in maritime cumulus clouds and its effects on the large-scale budget of vorticity in the tropics. Ph.D. thesis, UCLA, 123 pp.
- Holton, J.R., 1973: On the frequency distribution of atmospheric Kelvin waves. J. Atmos. Sci., 30, 499-501.
- Holton, J.R. and D.E. Colton, 1972: A diagnostic study of the vorticity balance of 200 mb in the tropics during the northern summer. J. Atmos. Sci., 29, 1124-1128.
- Krishnamurti, T.N., 1971: Tropical east-west circulations during the northern summer. J. Atmos. Sci., 28, 1342-1347.
- Krishnamurti, T.N. and B. Rogers, 1970: 200 millibar wind field June, July and August, 1967. Rept 70-2, Dept. of Meteorology, Florida State University, Tallahassee.
- Monaco, A.V. and R.T. Williams, 1975: An atmospheric global prediction model using a modified Arakawa differencing scheme. Naval Postgraduate School Technical Rept. NPS-51Wu75041, 86 pp.
- Pedlosky, J., 1964: An initial value problem in the theory of barotropic instability. Tellus, 16, 12-17.

- Reed, R. J. and R. H. Johnson, 1974: The vorticity budget of synoptic-scale wave disturbances in the tropical western Pacific, J. Atmos. Sci., 31, 1784-1790.
- Reed, R.J. and E.E. Recker, 1971: Structure and properties of synoptic-scale wave disturbances in the equatorial western Pacific J. Atmos. Sci., 28, 1117-1133.
- Tupaz, J.B., R.T. Williams and C.-P. Chang, 1978: A numerical study of barotropic instability in a zonally varying easterly jet. J. Atmos. Sci., 35, (in press).
- Wallace, J.M., 1971: Spectral studies of tropospheric wave disturbances in the tropical western Pacific. Rev. Geophys. Space Phys., 9, 557-612.
- Williams, K.T. and W.M. Gray, 1973: Statistical analysis of satellite-observed trade wind cloud clusters in the western North Pacific. Tellus, 25, 313-336.

LIST OF PUBLICATIONS

- Chang, C.-P., 1976a: Vertical structure of tropical waves maintained by internally-induced cumulus heating. J. Atmos. Sci., 33, 729-739.
- Chang, C.-P., 1976b: Forcing of stratospheric Kelvin waves by tropospheric heat sources. J. Atmos. Sci., 33, 740-744.
- Chang, C.-P., 1976c: Comments on "Instability theory of large-scale disturbances in the tropics." J. Atmos. Sci., 33, 1667-1668.
- Chang, C.-P., 1977a: Viscous internal gravity waves and low-frequency oscillations in the tropics. Submitted to J. Atmos. Sci.
- Chang, C.-P., 1977b: Some theoretical problems of the planetary-scale monsoons. Pure and Appl. Geophys., 115, 1089-1109.
- Chang, C.-P. and R.J. Pentimonti, 1977: A numerical study of time-mean northern summer monsoon with steady and fluctuating heating. Proc. Internatl. Symp. on Monsoons, New Delhi, India.
- Tupaz, J.B., R.T. Williams and C.-P. Chang, 1977: A numerical study of the locally unstable barotropic easterly jet. Proc. Internatl. Symp. on monsoons, New Delhi, India.

THESES

Pentimonti, R.J.: Study of monsoon circulation with steady and fluctuating heating. M.S. thesis. December 1976.

Tupaz, J.B.: A numerical study of barotropic instability of a zonally varying easterly jet. Ph.D. thesis, June 1977.

SCIENTIFIC COLLABORATORS

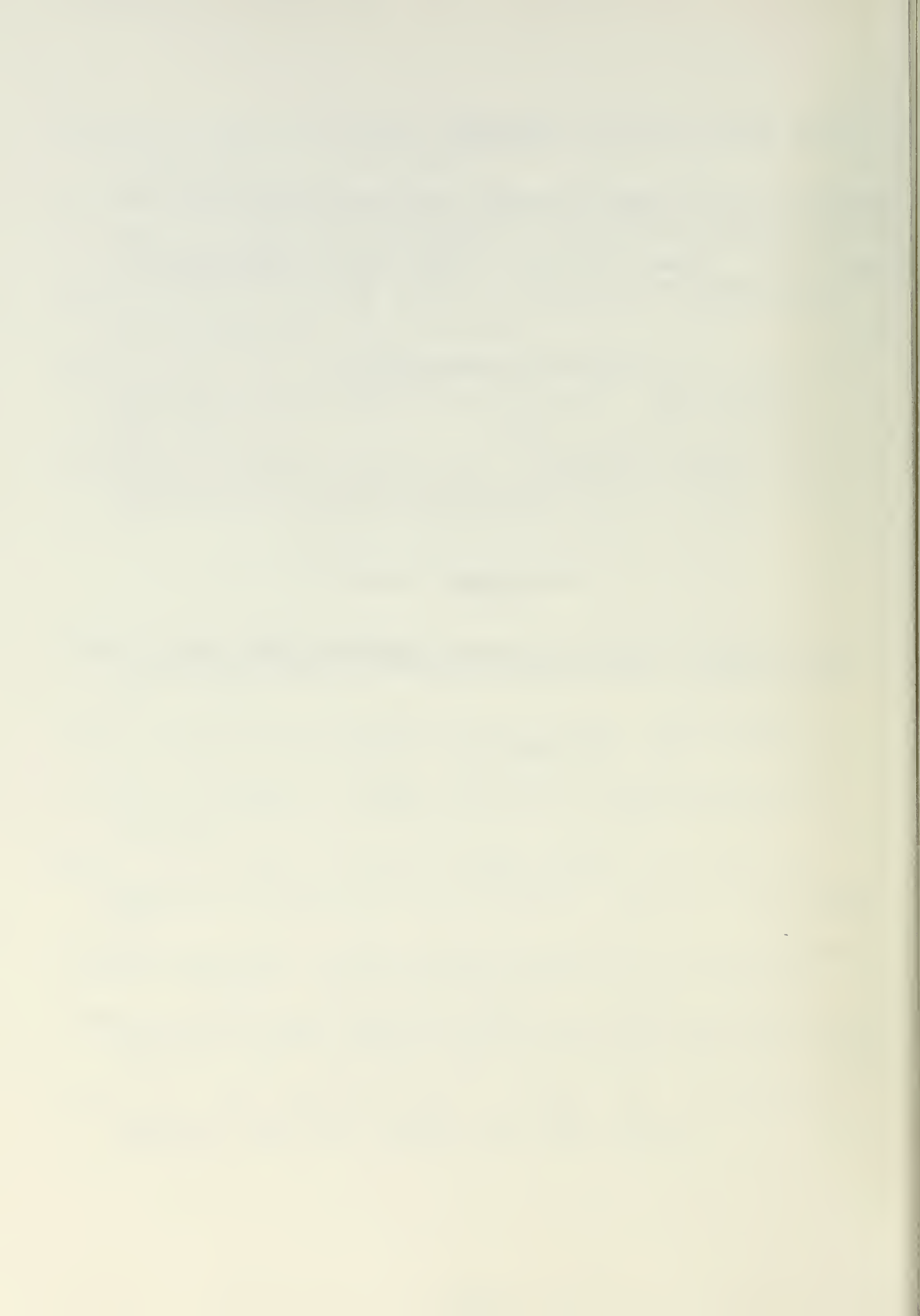
R.J. Pentimonti, graduate student

J.B. Tupaz, graduate student

L.C. Chou, graduate research associate

COMMENTS

This research is being continued under NSF Grant ATM77-14821.



Vertical Structure of Tropical Waves Maintained by Internally-Induced Cumulus Heating

CHIH-PEI CHANG

Department of Meteorology, Naval Postgraduate School, Monterey, Calif. 93940

(Manuscript received 25 November 1975, in revised form 22 January 1976)

ABSTRACT

Solutions to the wave-CISK (conditional instability of the second kind with cumulus heating being induced by low-level internal wave convergence) system are obtained to study the vertical structure of marginally unstable waves. A diabatic heating profile is specified that resembles those observed and those theoretically derived from simple parameterization schemes. Upper and lower bounds for the vertical wavelength of the unstable waves under normal heating conditions are established through analysis of the frequency (stability) equation. The lower bound excludes the possibility of excitation or maintenance of short vertical wavelengths (relative to the vertical scale of heating) by wave-CISK. The calculated growth rates indicate that this result is basically insensitive to the vertical heating profile. The vertical structure of the most unstable waves is also computed and the possible roles played by CISK in large-scale tropical waves are discussed in light of these results.

1. Introduction

The possibility that large-scale waves with short vertical wavelengths may be excited in the tropical atmosphere has been raised by Lindzen (1967), who showed that the equatorially trapped, internal gravity and internal Rossby waves usually have a small positive equivalent depth and therefore a short vertical wavelength. Holton (1969, 1972a) later pointed out that such short vertical wavelengths, if they exist in the troposphere, would cause great difficulties for numerical weather prediction in the equatorial region because of the stringent requirement for high vertical resolution. Whether short vertical-scale waves actually have a significant presence in the tropical troposphere or not is unclear due to inadequate observations. Studies based on conventional radiosonde data (e.g., Wallace, 1971; and others) tend to suggest that most of the variance of the waves in the tropical troposphere is associated with vertical scales comparable to the scale height. However, Madden and Zipser's (1970) analysis of high-resolution rawinsonde data obtained during the Line Island Experiment showed that a quite short vertical wavelength (~ 3 km) existed over the central equatorial Pacific. Further observational studies thus seem necessary to resolve this problem.

Condensation heating due to deep cumulus convection has been recognized as a primary energy source for large-scale tropical motions. Two possible mechanisms which may be responsible for the excitation of large-scale tropical waves by heating have

been investigated. The first is a one-way forcing by the cumulus scale which receives no feedback from the large scale. Numerical study by Holton (1971, 1972a, 1973) and analytical work by Chang (1976) have shown that this mechanism excites tropical waves that have vertical scales comparable to those of the forcing, which are usually 10–14 km. The problem of short vertical wavelengths thus appears unimportant for forced waves. The second possible mechanism is the conditional instability of the second kind (CISK) which involves a feedback to cumulus convection by low-level convergence of large-scale motion. This low-level convergence may be due to frictionally induced cross-isobaric flow, as in the case of typhoons (which shall be called "Ekman-CISK"), or due to the structure of the internal waves (which shall be called "wave-CISK"). The Ekman-CISK has been shown by Chang (1971) and Chang and Piwowar (1974) to possess no preferred horizontal scale for synoptic wave disturbances. Thus Ekman-CISK may not explain the generation of synoptic-scale waves, but it may be quite important in maintaining the waves once they are initiated. The wave-CISK mechanism has been investigated by Hayashi (1970), Lindzen (1974) and Lindzen *et al.* (1975). Although Lindzen (1974) and Lindzen *et al.* (1975) found no direct horizontal scale selection, the most unstable wave-CISK mode has a vertical scale seemingly comparable to the depth of the sub-cloud layer or the low-level convergent moist layer, depending on the particular model aspects. A short vertical scale may therefore

be important for the excited waves. Using the calculated vertical scale they also speculated that, due to the Doppler-shifting effect of the variable basic flow and the small growth rates, a period of ~ 5 days associated with a wavenumber zero, mixed Rossby-gravity mode is likely to dominate the tropical spectra. This periodicity thus provides a basic frequency for tropical systems. Depending on the local basic flow, it may force resonantly higher wavenumbers that may be relevant to the observed waves.

Since the growth rates associated with wave-CISK are usually very small, it may be expected that the CISK waves have properties similar to neutrally forced waves. The difference in the selection of vertical scales between the forced models and the wave-CISK models thus appears to be worth further investigation. In addition to its importance for tropical numerical weather prediction, the vertical scale also determines other properties of the excited internal waves. The purpose of this paper is to examine the growth rates associated with wave-CISK, particularly with regard to the vertical scale selection mechanism.

2. Basic equations

Neglecting the shear of the mean zonal wind, the linearized zonal and meridional momentum, hydrostatic, thermodynamic energy and continuity equations for a single zonal wavenumber k on an equatorial beta-plane may be written

$$i\omega\hat{u} - \beta y\hat{v} = -ik\hat{\phi}, \quad (1)$$

$$i\omega\hat{v} + \beta y\hat{u} = -\frac{\partial\hat{\phi}}{\partial y}, \quad (2)$$

$$\frac{\partial\hat{\phi}}{\partial z} = \frac{R\hat{T}}{H}, \quad (3)$$

$$i\omega\hat{T} + \hat{w}\Gamma = \frac{\hat{Q}}{c_p}, \quad (4)$$

$$ik\hat{u} + \frac{\partial\hat{v}}{\partial y} + e^{z/H} \frac{\partial}{\partial z} (e^{-z/H}\hat{w}) = 0, \quad (5)$$

where \hat{u} , \hat{v} , \hat{w} , \hat{T} , $\hat{\phi}$ and \hat{Q} are the perturbation zonal velocity, meridional velocity, vertical velocity, temperature, geopotential and diabatic heating rate, respectively; ω is the Doppler-shifted frequency, H a constant scale height, Γ the static stability, c_p the specific heat at constant pressure, R the gas constant, β the meridional gradient of the vertical component of earth's vorticity, y the meridional coordinate, and $z = -H \ln(p/p_0)$ is the vertical coordinate with p the pressure and p_0 a reference pressure.

Eqs. (1)–(5) may be combined into a single equation in \hat{w} that may be separated into meridional and

vertical structure equations by assuming that

$$\hat{w} = \sum_n Y_n(y) w_n(z) \exp[z/(2H)],$$

where the density factor $\exp[z/(2H)]$ is separated for convenience. The meridional structure equation is

$$\frac{d^2 Y_n}{dy^2} + \left(\frac{k\beta}{\omega} - k^2 + \frac{\omega^2}{gh_n} - \frac{\beta^2 y^2}{gh_n} \right) Y_n = 0, \quad (6)$$

where g is the gravitational constant and h_n , the equivalent depth, is the separation constant. Matsuno (1966) and Lindzen (1967) have shown that the solutions to (6) which satisfy the boundary condition

$$Y_n \rightarrow 0 \quad \text{as } |y| \rightarrow \infty, \quad (7)$$

and lead to the frequency equation

$$\left(\frac{k\beta}{\omega} - k^2 + \frac{\omega^2}{gh_n} \right) \frac{(gh_n)^{1/2}}{\beta} = 2n+1, \quad n = -1, 0, 1, 2, \dots, \quad (8)$$

are

$$Y_n(y) = \left[\frac{n}{1 - \frac{k}{\omega}(gh_n)^{1/2}} H_{n-1}(\xi) - \frac{1}{2 \left[1 + \frac{k}{\omega}(gh_n)^{1/2} \right]} H_{n+1}(\xi) \right] \times \exp(-\xi^2/2),$$

where $\xi \equiv \beta^{1/2}(gh_n)^{-1/2}y$ and the Hermite polynomials $H_n(\xi)$ have values only for $n \geq 0$. The meridional velocity solution is $v_n(y) \propto H_n(\xi) \exp(-\xi^2/2)$. Lamb (1973) has solved (6) using the more general form of the confluent hypergeometric functions without the restriction of (7). In such a case, the lateral boundary conditions are given by the choice of vanishing meridional velocity at some finite $|y|$ where the confluent hypergeometric functions have a node. The Hermite polynomials are a sub-set of the confluent hypergeometric functions.

The vertical structure equation which is most relevant in the present calculation is

$$\frac{d^2 w_n}{dz^2} + \lambda_n^2 w_n = \frac{Q'_n}{gh_n}, \quad (9)$$

where

$$\lambda_n^2 = \frac{S}{gh_n} - \frac{1}{4H^2}, \quad (10)$$

$$S = \frac{R}{H} \Gamma,$$

$$Q'_n = \frac{R}{c_p H} \hat{Q}_n Y_n^{-1} \exp[-z/(2H)].$$

The parameter λ_n is a measure of the vertical wave-number and is generally complex for unstable waves. In the case of forced modes ω and k are known parameters of the forcing function so that h_n and λ_n are obtained from (8) and (10) respectively. For CISK modes, on the other hand, λ_n is determined as an eigenvalue of (9) and ω is then found from (8) and (10). In the present calculation, the heating function Q' is assumed to possess a white-noise distribution for all Hermite modes (all values of n) so that the calculation of h will be independent of n . The subscript n will therefore be dropped in the subsequent discussions. It is well known that the vertical structure equation (9) can also be derived by considering two-dimensional wave motion only.

As in the forced model by Chang (1976) the following boundary conditions are used to solve (9):

$$w = \begin{cases} 0, & \text{at } z=0 \\ C_1 e^{i\lambda z} + C_2 e^{-i\lambda z}, & \text{at } z=z_t \end{cases} \quad (11a)$$

$$(11b)$$

where

$$C_1 = rC_2.$$

Here z_t is the height of tropopause, C_1, C_2 are constants, and the condition (11b) results from the requirement that latent heating vanishes at z_t . The parameter r is a reflection coefficient which, in the absence of vertical wind shear, is given by the specification of the static stability distribution. If the heating is assumed to vanish below the cloud base (z_c), the solution to (9) may be written in the form

$$w(z) = -\frac{re^{i\lambda z} + e^{-i\lambda z}}{\lambda(1+r)} \int_{z_c}^{z_t} \sin\lambda z \frac{Q'}{gh} dz, \quad z \geq z_t, \quad (12a)$$

$$w(z) = -\frac{\sin\lambda z}{\lambda(1+r)} \int_z^{z_t} (re^{i\lambda z} + e^{-i\lambda z}) \frac{Q'}{gh} dz - \frac{re^{i\lambda z} + e^{-i\lambda z}}{\lambda(1+r)} \times \int_{z_c}^z \sin\lambda z \frac{Q'}{gh} dz, \quad z_t > z > z_c, \quad (12b)$$

$$w(z) = -\frac{\sin\lambda z}{\lambda(1+r)} \int_{z_c}^{z_t} (re^{i\lambda z} + e^{-i\lambda z}) \frac{Q'}{gh} dz, \quad z_c \geq z \geq 0. \quad (12c)$$

The solution procedure using the Green's function technique is the same as in Lindzen (1974).

3. The heating function

The parameterization of the effect of condensation heating due to cumulus convection is a major problem in tropical modeling. Important contributions on this problem have been made by the sophisticated schemes developed by Arakawa and Schubert (1974), Ooyama (1971), and others. On the other hand, in simplified

analytical models, simpler schemes must be used to keep the mathematical analysis tractable. Usually in these models the vertical distribution of the heating is specified as a given function that is invariant in time. The major criticism of this type of parameterization is that the results are sensitive to the specified heating profile such that one can obtain the desired result by simply tuning the heating profile. Another criticism is that the inherent time-variation of the heating function due to the complicated scale interaction cannot be properly included. However, recent observational studies, using both the spectral analysis technique and the composite technique, have produced a consistent picture of the vertical heating profile due to latent heat release over the tropical oceanic areas. The profiles observed by Nitta (1970), Wallace (1971), Reed and Recker (1971) and Williams and Gray (1973) are plotted in Fig. 1. It can be seen that in each case a maximum occurs in the middle troposphere between the 6 and 9 km levels. On the other hand, observational analysis of the divergence and vertical velocity by Schubert and Reed (1975) using recent GATE data has yielded a result that implies a vertical heating profile different from those shown in Fig. 1. They found that the maximum vertical velocity, which usually coincides with the maximum heating, based on scaling arguments (Holton, 1972b), occurs at a much lower level. However, analyses of the same data set by Petrossians *et al.* (1975) and Antsipovich *et al.* (1975) of the USSR Hydrometeorological Center have resulted in profiles which are in close agreement with Fig. 1. In any case, the profiles included in Fig. 1 are

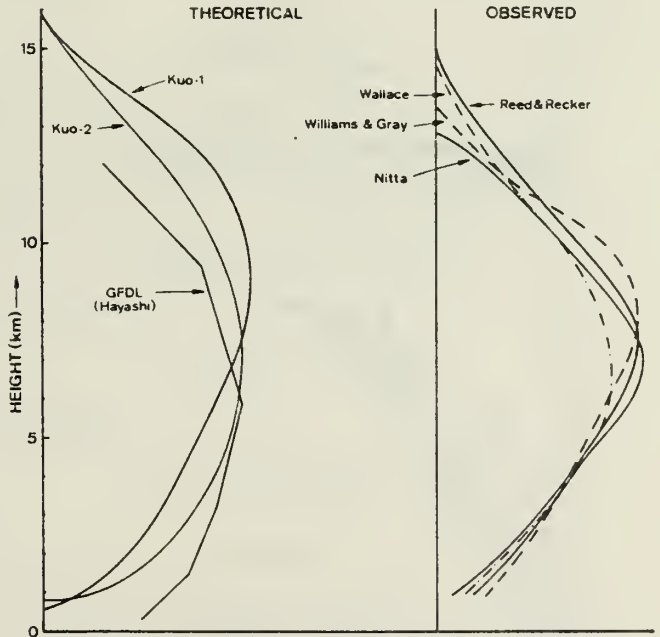


FIG. 1. Vertical heating functions deduced from observations and from simple theoretical parameterization schemes.

based on a much larger sample of data and may be viewed as an indication that the tropical atmosphere, on a *statistical basis*, tends to maintain a similar vertical profile for the large-scale heating function.

Results of a theoretical calculation by Kuo (1965) using his parameterization scheme are also included in Fig. 1. Kuo's parameterization was originally based on the assumption of horizontal mixing between cloud air and environmental air. Recently Kuo (1974) has shown that his formulation is equivalent to the consideration that heating is due to the adiabatic compression of the descending environment. Kuo's scheme has been used in many tropical numerical models with a degree of success not inferior to any other parameterization scheme. It is therefore interesting to compare his heating profiles with those observed. In Fig. 1, the Kuo-1 curve is for the case of no entrainment and the Kuo-2 curve is for the case of moderate entrainment. It is clear that the latter curve, having a maximum near 7 km, agrees quite well with those deduced from observations. The average heating profile obtained from the GFDL general circulation model as calculated by Hayashi (1973) is also included, because the GFDL model uses a different parameterization scheme: the moist convective adjustment. Hayashi decomposed the heating function into components of various equatorial beta-plane modes. Among them, the profile for the Kelvin waves ($n = -1$) at the equator is one of the curves least resembling those observed. This profile is also plotted in Fig. 1. It is seen that even for this highly simplified parameterization scheme the maximum heating still occurs near 6 km, within the range of the other curves.

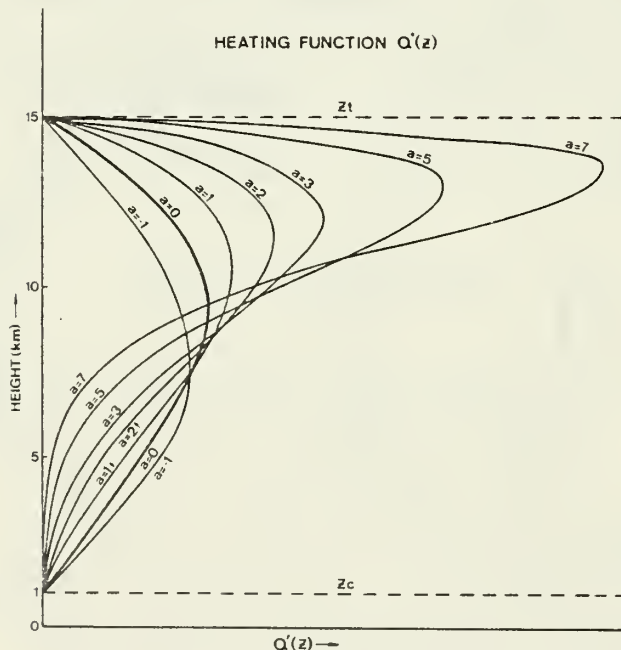


FIG. 2. The specified heating function $Q'(z)$.

Based on the above discussion the heating function for the wave-CISK parameterization is specified as

$$Q'(z) = \frac{1}{2} m N S_t w_b e^{az'} \sin \pi z', \quad z_t \geq z \geq z_c \quad (13)$$

$$Q' = 0, \quad z > z_t \text{ or } z < z_c$$

where

$$z' = \frac{z - z_c}{\Delta z},$$

and $\Delta z = z_t - z_c$ is a measure of the vertical scale of the heating. The coefficient m specifies the strength of the heating and the factor $\frac{1}{2}$ is needed because the amplitude of the Fourier component is one-half of the heating maximum, as only positive condensation heating is permitted. The heating is proportional to the moisture convergence in the moist layer which is represented by the vertical velocity w_b at the top of the moist layer. The tropospheric value of the static stability S_t is included in the proportionality constant. The parameter a is used to vary the maximum heating level to test the sensitivity of the model. The coefficient N is a normalization factor so that when other conditions are equal the total amount of heat release weighted by density in a column would remain the same with different values of a . Thus,

$$N = \frac{\int_0^1 \exp[-z/(2H)] dz'}{\int_0^1 \exp[az' - z/(2H)] \sin \pi z' dz'}$$

$$= \frac{2H \{1 - \exp[-\Delta z/(2H)]\} \{[a - \Delta z/(2H)]^2 + \pi^2\}}{\pi \{\exp[a - \Delta z/(2H)] + 1\}}$$

Profiles of (13) multiplied by the density factor $\exp(z/2H)$ are plotted in Fig. 2 for various values of a . The range of $-1 \leq a \leq 0$, with maximum heating between 7 and 9 km, appears to be representative of the observed and theoretical profiles shown in Fig. 1.

4. Analysis of the stability equation

If the mixed layer with top at z_b ($< z_c$) is assumed to be the moisture layer which provides the convergence for CISK, the most relevant solution in studying the instability is (12c) evaluated at z_b . The solution is

$$w_b = - \frac{\sin \lambda z_b \bar{m} w_b S_t \pi \Delta z}{\lambda \quad 1 + r g h \quad 2} \times \left[\frac{e^{-i\lambda z_c} (e^q + 1) + r e^{i\lambda z_c} (e^{-q} + 1)}{q^2 + \pi^2} \right],$$

where $\bar{m} = mN$ and $q = a - i\lambda \Delta z$. Equating the coefficients of w_b on both sides and using (10) leads to

the stability equation

$$\begin{aligned} \Psi(\lambda) = & -\frac{\pi}{2} \bar{m} z_b \Delta z \\ & \times \frac{\left(\lambda^2 + \frac{1}{4H^2} \right) [(e^q + 1)e^{-i\lambda z_c} + r(e^{-q} + 1)e^{-i\lambda z_c}]}{(1+r)(q^2 + \pi^2)} + 1 = 0, \end{aligned} \quad (14)$$

where we have assumed that $(\sin \lambda z_b)/\lambda \approx z_b$. It can be shown that $q^2 + \pi^2 = 0$ is not a solution to (14). Eq. (14) must be solved for the complex eigenvalue λ using either numerical or graphical methods. However, before doing so some valuable information regarding the range of vertical scale of the unstable solutions may be obtained by analyzing (14).

The complex eigenvalue λ may be written as $\lambda = \lambda_r + i\lambda_i$, where the real part λ_r is the vertical wavenumber while the imaginary part λ_i gives the growth rate of the waves. If the positive λ_r is chosen, the C_2 component in (11b) represents the downward phase upward energy propagation and the C_1 component presents the upward phase or downward energy propagation. It then follows from (10) and (8) that λ_i is negative, the imaginary part of the frequency ω will be negative and the waves will grow exponentially in time. Based on observations, and justified *a posteriori*, we shall consider only the case of marginally unstable waves, or very small growth rates. Thus the conditions applied to (14) may be written

$$\lambda_i = -|\lambda_i|, \quad (15)$$

$$\lambda_i^2 \ll \lambda_r^2. \quad (16)$$

In addition, we shall assume

$$\lambda_r^2 \gg \frac{1}{4H^2}, \quad (17)$$

which is valid for all practical purposes since the scale height H of the atmosphere is ~ 7 km and (17) only places a restriction of ~ 88 km for the maximum vertical wavelength.

Eq. (14) will now be analyzed by assuming that $r=0$ and that the stratosphere ($z > z_t$) and troposphere ($z \leq z_t$) have the same constant static stability S_t . In this case $r=0$ and since $q^2 + \pi^2 \neq 0$ the stability equation may be re-written as

$$\begin{aligned} \Psi(\lambda) = & \Psi(\lambda)(q^2 + \pi^2) = \frac{\pi}{2} \bar{m} z_b \Delta z \left(\lambda^2 + \frac{1}{4H^2} \right) (e^q + 1) \\ & \times \exp(-i\lambda_i z_c) + q^2 + \pi^2 = 0. \end{aligned}$$

Separating $\Psi'(\lambda)$ into its real and imaginary parts

gives two equations:

$$\begin{aligned} \text{Re}(\Psi') &= 0, \\ \text{Im}(\Psi') &= 0. \end{aligned} \quad (18)$$

For $a=0$, (18) may be expanded to give

$$\begin{aligned} \text{Re}(\Psi') = & \left(\lambda_r^2 - \lambda_i^2 + \frac{1}{4H^2} \right) [\exp(\lambda_i z_t) \cos \lambda_r z_t \\ & + \exp(\lambda_i z_c) \cos \lambda_r z_c] + 2\lambda_r \lambda_i [\exp(\lambda_i z_t) \sin \lambda_r z_t \\ & + \exp(\lambda_i z_c) \sin \lambda_r z_c] + \frac{2[\pi^2 - \Delta z^2(\lambda_r^2 - \lambda_i^2)]}{\pi \bar{m} z_b \Delta z} = 0. \end{aligned}$$

Simplifying this equation with the conditions (16) and (17) and using (15) lead to

$$\begin{aligned} \text{Re}(\Psi') \approx & \underbrace{(\lambda_r^2 \cos \lambda_r z_t - 2\lambda_r |\lambda_i| \sin \lambda_r z_t) \exp(-|\lambda_i| z_c)}_{\text{I}} \\ & + \underbrace{(\lambda_r^2 \cos \lambda_r z_c - 2\lambda_r |\lambda_i| \sin \lambda_r z_c) \exp(-|\lambda_i| z_c)}_{\text{II}} \\ & + \underbrace{\frac{2(\pi^2 - \Delta z^2 \lambda_r^2)}{\pi \bar{m} z_b \Delta z}}_{\text{III}} = 0. \end{aligned} \quad (19)$$

Since $|\cos \lambda_r z_t|$, $|\sin \lambda_r z_t|$, $|\cos \lambda_r z_c|$ and $|\sin \lambda_r z_c|$ are all ≤ 1 and $\exp(-|\lambda_i| z_c) < 1$, from (16) we have, allowing for small error under extreme cases,¹

$$\begin{aligned} |\text{I}| &\leq \lambda_r^2 \\ |\text{II}| &\leq \lambda_r^2 \end{aligned} \quad (20)$$

Thus for (19) to be satisfied we may write

$$\text{Max}[\text{Re}(\Psi')] = \text{Max}(\text{I}) + \text{Max}(\text{II}) + \text{III} > 0,$$

where Max denotes the maximum value using the range (20):

$$\text{Max}(\text{I}) = \text{Max}(\text{II}) = \lambda_r^2.$$

Thus we have

$$2\lambda_r^2 + \frac{2\pi}{\bar{m} z_b \Delta z} - \frac{2\Delta z \lambda_r^2}{\pi \bar{m} z_b} > 0,$$

which yields

$$\lambda_r^2 < \frac{\pi^2}{\Delta z (\Delta z - \pi \bar{m} z_b)}, \quad (21)$$

if

$$\Delta z > \pi \bar{m} z_b. \quad (22)$$

¹ The precise maximum for terms I and II is $\{ |1 + 4\epsilon^2| \cos [\tan^{-1}(-2\epsilon)] \} \exp(-|\lambda_i| z_c) \lambda_r^2$, where $\epsilon = |\lambda_i|/\lambda_r$. Inequality (20) is true when $\epsilon=0$. For $\epsilon=0.1$ which is our assumption the maximum is $[1.02 \exp(-|\lambda_i| z_c)] \lambda_r^2$. Obviously if $|\lambda_i|$ becomes large the exponential factor would become much less than 1.

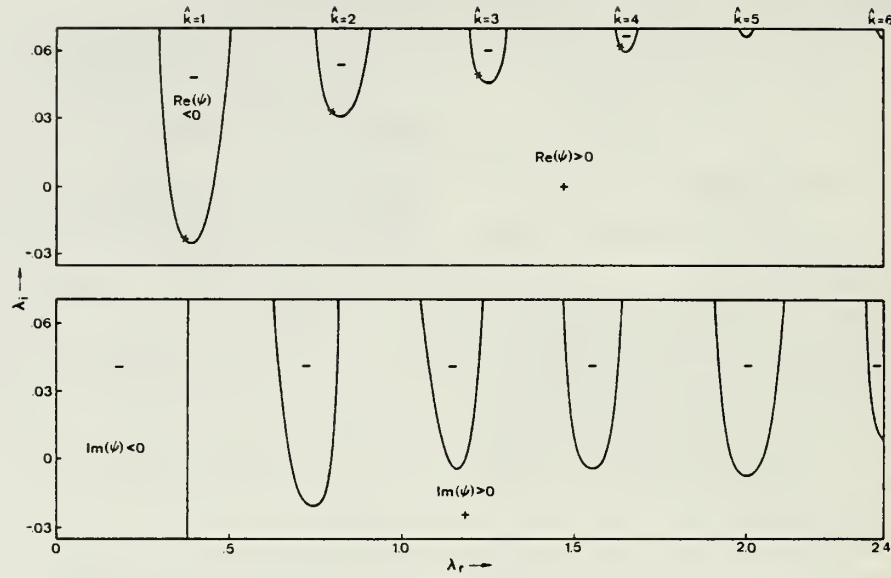


FIG. 3. Values of $\text{Re}(\Psi)$ and $\text{Im}(\Psi)$ as a function of λ_r [km^{-1}] and λ_i [km^{-1}]. The crosses in the $\text{Re}(\Psi)$ diagram are solutions for which $\text{Re}(\Psi) = \text{Im}(\Psi) = 0$.

Choosing the minimum values (Min) in (20), we have

$$\text{Min}[\text{Re}(\Psi')] = \text{Min}(I) + \text{Min}(II) + III < 0,$$

or

$$-2\lambda_r^2 + \frac{2\pi}{\bar{m}z_b\Delta z} - \frac{2\Delta z\lambda_r^2}{\pi\bar{m}z_b} < 0,$$

giving

$$\lambda_r^2 > \frac{\pi^2}{\Delta z(\Delta z + \pi\bar{m}z_b)}. \quad (23)$$

So (21) and (23) give the upper and lower bounds for λ_r . It is interesting to note that $\lambda_r \rightarrow \pi/\Delta z$ in the limit of $\bar{m} \rightarrow 0$, corresponding to a vertical wavelength of twice the heating scale, which is the most efficiently excited wavelength for forced waves (Chang, 1976). However, $\lambda_r = \pi/\Delta z$ cannot be a solution for any finite \bar{m} because it does not satisfy (14).

Now we shall use the values $z_t = 15$ km, $z_c = 1$ km, $\Delta z = 14$ km, $z_b = 0.4$ km, $m = 5.8$ which leads to $\bar{m} = 9$. The value of m is calculated by fitting (13) to Reed and Recker's (1971) observed heating and vertical velocity profiles for the wave trough, for which an estimate of

$$mz_b \approx 2.32 \text{ km}, \quad (24)$$

can be made assuming that $S_t = 1.22 \times 10^{-4} \text{ s}^{-2}$ based on a tropospheric value of $\Gamma = 3^\circ \text{C km}^{-1}$. Eq. (24) is a good approximation as long as $z_b < 4$ km, so the particular choice of z_b is not crucial. From Reed and Recker's data $w_b \approx 0.29 \text{ cm s}^{-1}$ so that the maximum heating is $\sim 6.8^\circ \text{C day}^{-1}$. Substituting these values into (21)–(23) we obtain

$$\frac{\pi}{6.14} = 0.512 > |\lambda_r| > \frac{\pi}{18.8} = 0.167 \text{ km}^{-1},$$

so the vertical wavelength, $L = 2\pi/\lambda_r$, is limited by the following bounds:

$$13 \text{ km} < L < 40 \text{ km}.$$

Thus waves with a vertical wavelength shorter than 13 km will not be excited by wave-CISK. If such waves are first excited by another mechanism, the above result indicates that they *cannot be maintained* by wave-CISK.

5. Eigenvalues and eigenfunctions

a. Growth rates

The stability equation (14) will now be solved using the graphical method with the accuracy of the solutions improved by a numerical iteration technique. The graphical method is illustrated in Fig. 3, where the real and imaginary parts of $\Psi(\lambda)$ given by (14) with $r=0$, $a=0$ and $m=6$ are plotted as a function of λ_r and λ_i . Here the constants used are $H=7$ km, $z_t=15$ km, $z_c=1$ km and $z_b=0.4$ km. The intersections of the zero $\text{Re}(\Psi)$ and zero $\text{Im}(\Psi)$ lines give the eigenvalue solution λ . It is seen that there exist many solutions with the most (and only) unstable solution having the smallest λ_r or the longest wavelength. The solutions are labeled by an integer k with increasing k indicating increased λ_r or decreased vertical wavelength.

The four longest vertical wavelength solutions are shown in Fig. 4 as a function of heating strength m . It is seen that $|\lambda_i| \ll \lambda_r$ and that the growth rates as represented by $-\lambda_i$ increase with m while the vertical wavelengths are almost constant. This diagram also indicates that the $k=1$ solution is most unstable throughout the range $m=4$ to $m=10$, which cor-

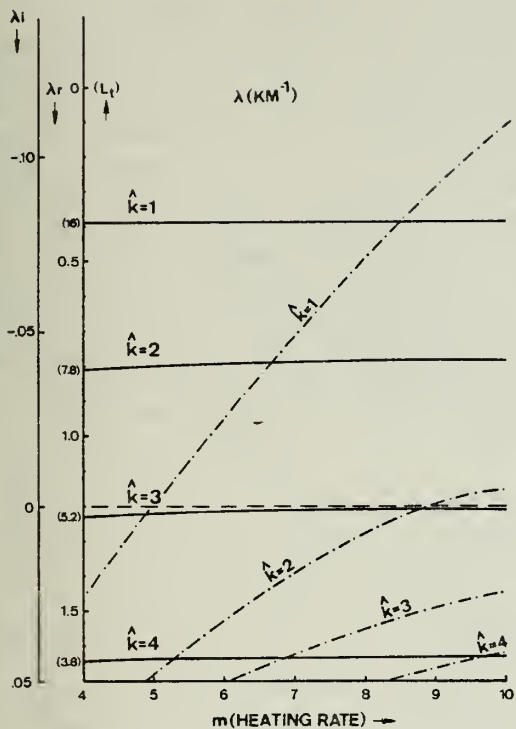


FIG. 4. The four longest vertical wavelength solutions as a function of the heating rate m . The solid curves are λ_r and the dash-dotted curves λ_i . The corresponding vertical wavelength $L_r = 2\pi/\lambda_r$ is given in the parentheses of the λ_r coordinate. The ratio of static stabilities between stratosphere and troposphere is 1.

responds to maximum heating rates of 4.7 and 11.7°C day⁻¹ if $w_b = 0.29$ cm s⁻¹. In fact, it is the only unstable solution up to $m = 9$. For this solution the value of λ for $m = 5.8$ is $0.388 - 0.026i$ [km⁻¹], which is well within the range predicted by (21) and (23).

The sensitivity of the eigenvalues with respect to the vertical heating profile (13) is shown in Fig. 5 in which the $\hat{k} = 1$ to $\hat{k} = 4$ solutions with $m = 6$ are given as a function of a . It is clear that the vertical wavelengths are all insensitive to a . For the growth rates the $\hat{k} = 1$ solution is almost independent of a , but the other solutions all increase with a . There is an indication that as a increased to > 5 the shortest vertical wavelength becomes the most unstable solution. However, for the realistic range of $0 \leq a \leq -1$, which represents the statistical mean state of the heating function in the tropical atmosphere, $\hat{k} = 1$ is the only unstable solution.

Solutions for a different static stability S_s in the stratosphere are obtained by including the radiation condition for $z > z_t$ as the third boundary condition. In this case the reflection coefficient is derived by continuity requirements of w and ϕ across z_t :

$$r = \frac{1 - (S_s/S_t)^{1/2}}{1 + (S_s/S_t)^{1/2}} \exp(-2i\lambda_t z_t), \text{ for } S_s > S_t.$$

The result for $S_s/S_t = 2.5$ is shown in Fig. 6. It is

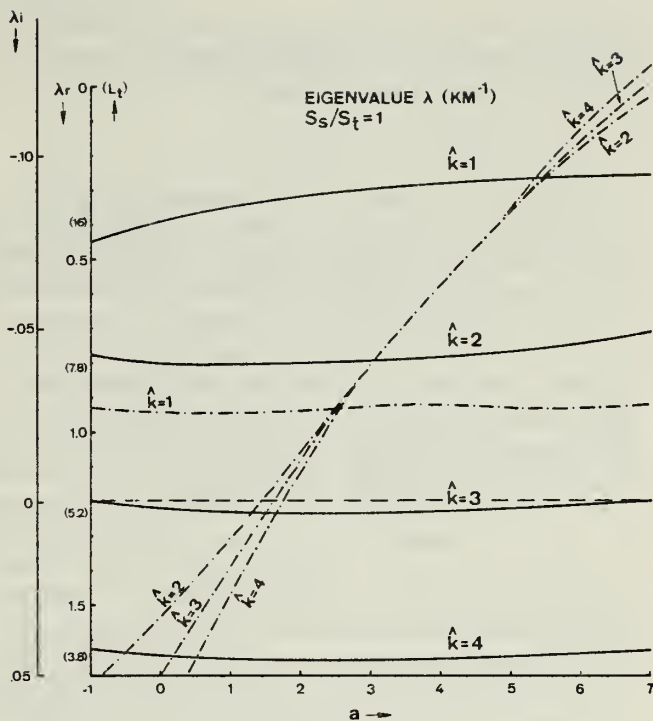


FIG. 5. As in Fig. 4 except that the solutions are given as a function of the heating profile parameter a .

seen that the general conclusions drawn from Fig. 5 remain valid, although waves with a shorter vertical wavelength become more unstable than the $\hat{k} = 1$ waves beginning at $a = 2$ which corresponds to a maximum

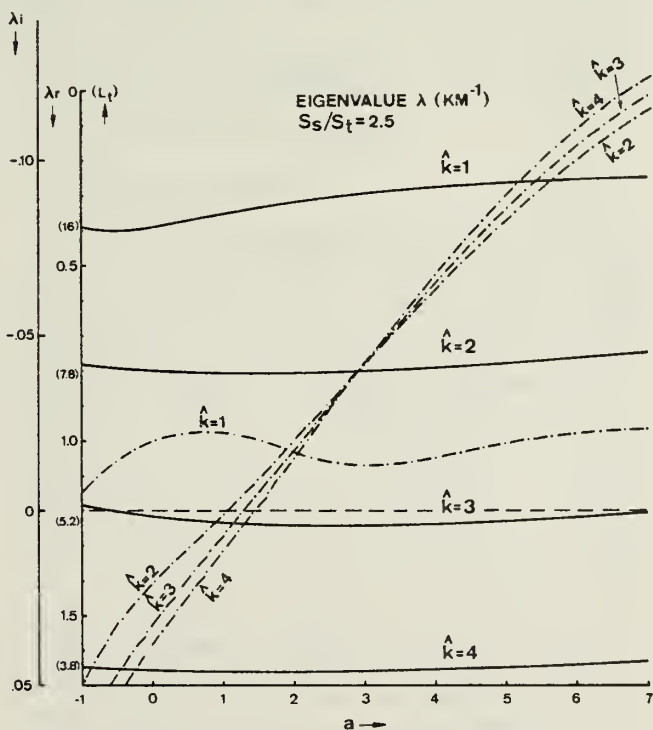


FIG. 6. As in Fig. 4 except that the solutions are given as a function of the heating profile parameter a and that the ratio of static stabilities between stratosphere and troposphere is 2.5.

heating level of ~ 12 km or 200 mb, much above all observed levels. So our result is basically insensitive to the vertical heating distribution.

b. Vertical profiles

The vertical structure of \hat{w} , corresponding to the λ for $k=1$ and $a=0$ in Fig. 6, is shown in Fig. 7 for two heating intensities $m=6$ and 10. It can be seen that the tropospheric amplitude reaches a maximum between 6 and 9 km and has a minimum at the tropopause for both cases. In the stratosphere the amplitude for $m=6$ increases at a slow rate with height due to the density factor, but the kinetic energy actually decreases with height. This decrease is due to the instability of the waves which results in $\lambda_i < 0$. The decrease of the wave kinetic energy is much faster for the more unstable $m=10$ case, so that even its amplitude decreases with height. The vertical phase distributions for both cases are almost the same and indicate that there is virtually no vertical propagation in the troposphere in contrast to a downward propagation in the stratosphere. The vertical wavelength computed from $2\pi/\lambda_r$ is 16.2 km in the troposphere and 10.2 km in the stratosphere, because the value

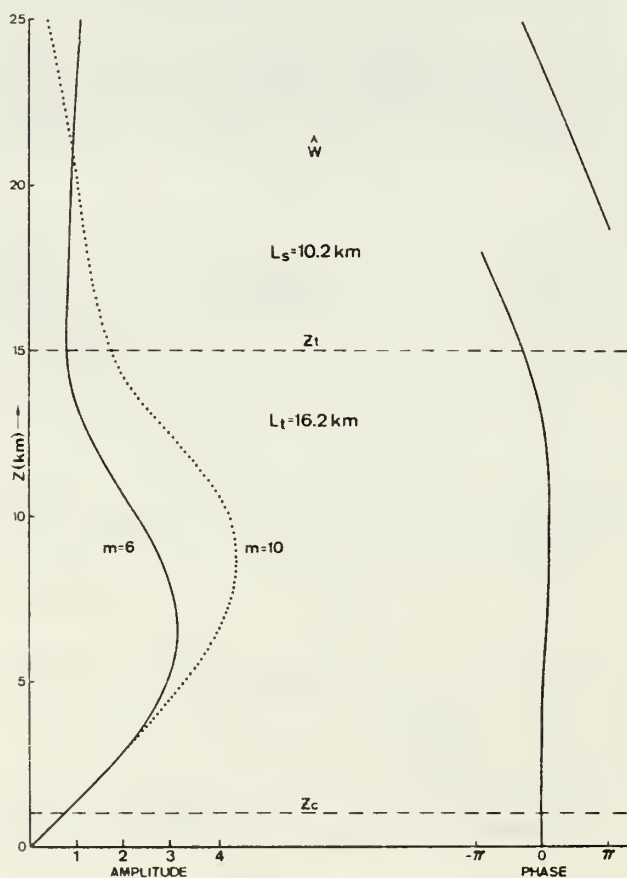


FIG. 7. Amplitude and phase of \hat{w} as a function of height for $m=6$ (solid lines) and $m=10$ (dotted lines). The phase lines for both cases are approximately the same.

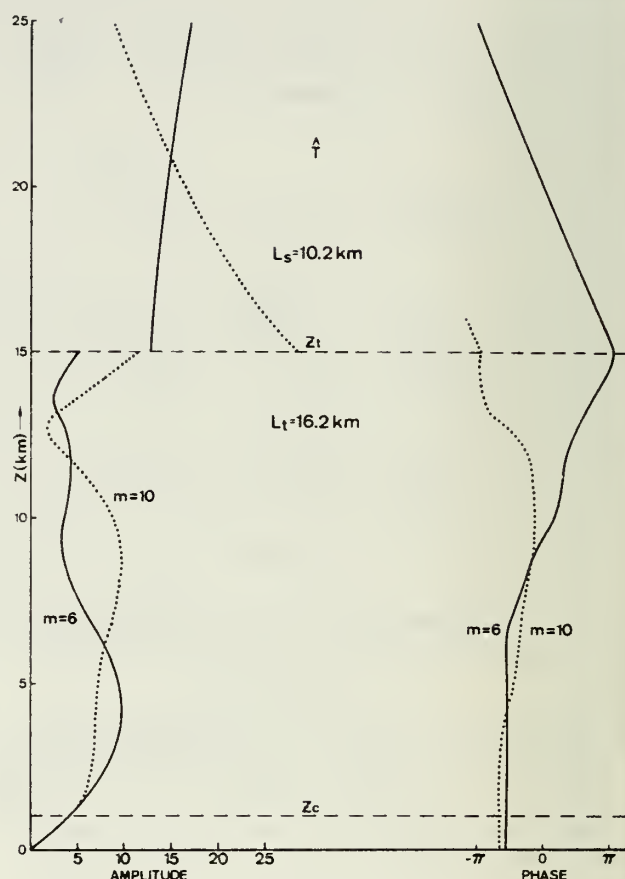


FIG. 8. As in Fig. 7 except for \hat{T} .

of λ_r is increased in the stratosphere by approximately a factor of $(S_s/S_t)^{1/2}$, as can be seen from (10).

Vertical structures of other variables can be computed utilizing the basic equations (1)–(5) and the solutions to the meridional structure equation (6). Here only the temperature structure for the Kelvin wave case ($n=-1$) will be shown. From (4) and (8) we have

$$\hat{T}_{n=-1} = - \frac{i \left(\hat{w} S - \frac{R}{H} \frac{\hat{Q}}{c_p} \right) H}{k R (g h)^{1/2}}. \quad (25)$$

It is obvious from (25) that the amplitude of the temperature perturbation decreases as the zonal wave-number k increases. The $\hat{T}_{n=-1}$ structure corresponding to the \hat{w} in Fig. 7, is shown in Fig. 8. It can be seen that the amplitude distribution is quite sensitive to the strength of the heating. The discontinuity at z_t is due to the layered static stability distribution assumed in our model. The large temperature perturbations in the stratosphere are, of course, due to the large static stability there. Figs. 7 and 8 are constructed using nondimensional units. The two figures may be compared by letting the unit for the \hat{w} amplitude be

cm s^{-1} ; in this case the corresponding unit for the amplitude will be $\alpha^{-1} [^{\circ}\text{C}]$, where $\alpha = k \times$ (radius of the earth) is the number of waves around the equator. For these units the amplitude of \hat{w} is quite close to the typically observed values of "matured" tropical waves, with maximum $\sim 3 \text{ cm s}^{-1}$ for $m=6$ and $\sim 4.2 \text{ cm s}^{-1}$ for $m=10$. On the other hand, the maximum \hat{T} perturbation in the troposphere is almost 10°C for wavenumber (α) 1 and even larger in the stratosphere. Lindzen (personal communication) has suggested that these enormously large temperature fluctuations indicate that large damping effect of vertical momentum transport due to cumulus convection must be important. However, for shorter waves the temperature perturbation is proportionally smaller. If we consider a zonal wavelength of 4000 km, then $\alpha \approx 10$ and the temperature fluctuations are all $< 1^{\circ}\text{C}$ in the troposphere, in good agreement with observations and with Holton (1971)'s numerical calculations. In fact, this magnitude estimate may explain why atmospheric Kelvin waves, which have a \hat{T} amplitude $\sim 2^{\circ}\text{C}$ in the lower stratosphere, are not observed in the troposphere. For such waves the vertical velocity in the troposphere would be an order of magnitude smaller than for the easterly waves which have a typical zonal wavelength $\sim 3000 \text{ km}$ and a maximum vertical velocity $\sim 3 \text{ cm s}^{-1}$. On the other hand, damping effect of a certain magnitude must play a role for the easterly waves to explain the complete absence of them in the stratosphere. Although these estimates are based on Kelvin waves only, for other wave modes a relationship between the tropospheric temperature amplitude and the zonal scale must also exist at latitudes somewhat away from the equator because of the following scaling arguments. Wallace (1971) and Holton (1972b) have shown that, for weak, tropical, synoptic-scale motions with a depth scale comparable to the scale height, a diabatic heating rate of $5\text{--}10^{\circ}\text{C day}^{-1}$ is almost completely balanced by the adiabatic cooling. Thus the temperature fluctuation is one order of magnitude smaller than either term. This balance may be attributed to the smallness of the Rossby number which is $\sim O(1)$ or larger for tropical synoptic-scale motions. For planetary-scale motions the length scale is one order larger so that the Rossby number is $\sim O(10^{-1})$ at intermediate tropical latitudes, and the scale analysis indicates that the pressure and temperature perturbations must be increased by one order of magnitude.

The phase diagrams in Figs. 7 and 8 indicate that in the lower troposphere and the entire stratosphere the temperature leads the vertical velocity by $\sim \frac{1}{4}$ cycle. In the middle and upper troposphere (7–12 km for $m=6$ and 5–12 km for $m=10$), they are in phase except near the tropopause (12–14 km), where they are out of phase. These phase relationships are consistent with the energetics because the conditions for

wave growth are

$$\int_0^{\infty} \overline{w'T'} dz > 0,$$

$$\int_0^{\infty} \overline{Q'T'} dz > 0.$$

From (25) and (10) it can be shown that these conditions are satisfied when $\lambda_i < 0$ and

$$\int_0^{\infty} S \text{Re}(\hat{w}) dz < R \int_0^{\infty} \hat{Q} dz / (Hc_p).$$

The latter condition implies that the diabatic heating rate exceeds the adiabatic cooling rate which, of course, is responsible for the continuous growth of the waves with time.

c. Equatorial trapping scales

The meridional scale of the unstable waves may be estimated from the Hermite solutions of the meridional equation (6). The north-south, e -folding width is

$$y_e = \text{Re}[2(gh)^{1/2}/\beta]^{\frac{1}{2}},$$

and the maximum amplitude for the mixed Rossby-gravity mode ($n=0$) occurs at

$$y_0 = \text{Re}[(gh)^{1/2}/\beta]^{\frac{1}{2}}.$$

The maximum for the Kelvin mode occurs at the equator. From results obtained for the $k=1$ waves, $\lambda \approx 0.388 - 0.026i \text{ [km}^{-1}]$ so that $(gh)^{1/2} \approx 25.5 - 1.7i \text{ [m s}^{-1}]$ from (10). It follows that $y_e \approx 1480 \text{ km}$ and $y_0 \approx 1050 \text{ km}$ with $\beta = 2.21 \times 10^{-11} \text{ m}^{-1} \text{ s}^{-1}$. Both of these are reasonable values in terms of the trapping of waves on the equatorial beta-plane.

6. Concluding remarks

We have shown that tropical waves cannot remain unstable with respect to wave-CISK if the vertical wavelength is much smaller than the vertical scale of heating. This result holds for a number of reasonable heating profiles that have been observed or theoretically derived. The dispersive relationship of the growth rates of various equatorial beta-plane modes has been shown by Lindzen (1974) to be unsatisfactory in selecting the horizontal scale of tropical waves. From the computed eigenvalues it can be shown that, even under the extremely intense heating case of $m=10$, the growth rates for Rossby waves, mixed Rossby-gravity waves, and the longer zonal-scale Kelvin waves are all very small. This result is similar to that obtained by Chang and Piwowar (1974) for the Ekman-CISK and indicates that wave-CISK is not responsible for the initial selection mechanism of the tropical waves. Once the waves are excited

by some other mechanism, however, the internal wave convergence could induce organized cumulus convection and release wave-CISK as an energy source. The present calculation indicates that under such cases the shorter vertical-scale waves will still not be maintained by wave-CISK. There is no definite explanation to the fact that the gravity modes and the shorter zonal scale Kelvin modes, which are usually not observed in the tropical atmosphere, are most unstable. However, these waves have very short periods and various arguments have been given against their occurrence on a regular basis. For example, if one considers the lifting process² of CISK (Ooyama, 1969; Holton, 1972b), the short periods will be insufficient for a low-level air parcel to reach its condensation level. In any case, the result that wave-CISK can neither excite nor maintain waves with short vertical wavelengths remains valid independent of these considerations. The concern about short vertical-scale excitation due to wave-CISK in a tropical numerical model may thus be relieved. The resonant forcing of tropical waves by a fundamental wave-CISK frequency associated with the zonally-symmetric, mixed Rossby-gravity mode as hypothesized by Lindzen (1974) also does not appear to be plausible, because the equivalent depth would be too large to give a fundamental periodicity near 5 days.

The calculated vertical structure of \hat{w} and \hat{T} applies to all waves maintained by heating and is not restricted to wave-CISK. The eigenvalue λ found by the wave-CISK equation used here may alternatively be viewed as being excited by a specified forcing [as in the model by Chang (1976)] with a small linear damping. The damping coefficient would then appear in the complex Doppler-shifted frequency in the same way as an imaginary frequency due to instability. The computed magnitudes of \hat{w} and \hat{T} suggest that the observed planetary-scale Kelvin waves are likely to be a result of forcing rather than instability, because a small forcing function can explain the amplitudes in the stratosphere and troposphere. However, an instability consistent with the present CISK parameterization should eventually amplify the waves to a finite amplitude \hat{w} comparable to that observed for large-scale, cumulus-associated tropical motions, but with a temperature amplitude too large to be realistic. The small low-level vertical velocities of these waves is also an indication that CISK is unlikely to be important. On the other hand, the tropospheric amplitude of the synoptic-scale waves may quite possibly be supported by a CISK-type process. These waves have a wavelength ~ 2000 – 4000 km and a period ~ 5 days which lead to a phase speed relative to the ground of ~ 5 – 9 m s⁻¹. Such a phase

speed would make the waves greatly attenuated before reaching the stratosphere, because the Doppler-shifted phase speed is very small near and below the tropopause and the damping can become very efficient (Lindzen, 1971).

Acknowledgments. The author wishes to thank Profs. R. T. Williams and R. L. Elsberry for reading the manuscript and making helpful suggestions. This research was supported by the Atmospheric Science Section, National Science Foundation, under Grant DES75-10719. Parts of the material in this paper were presented at the AMS Ninth Technical Conference on Hurricanes and Tropical Meteorology, May 1975, Miami, Fla.

REFERENCES

- Antsipovich, V. A., A. I. Snitkovsky and A. I. Falkovich, 1975: On the orders of the values of the meteorological elements obtained in the A/B-array in the period of GATE. GATE Rept., No. 14, Preliminary Scientific Results, Vol. 2, 99–116. [Available from WMO, Geneva].
- Arakawa, A., and W. H. Schubert, 1974: Interaction of a cumulus cloud ensemble with the large-scale environment, Part I. *J. Atmos. Sci.*, **31**, 674–701.
- Chang, C.-P., 1971: On the stability of low-latitude quasi-geostrophic flow in a conditionally unstable atmosphere. *J. Atmos. Sci.*, **28**, 270–274.
- , 1976: Forcing of stratospheric Kelvin waves by tropospheric heat sources. *J. Atmos. Sci.*, **33**, 740–744.
- , and T. M. Piwowar, 1974: Effect of a CISK parameterization on tropical wave growth. *J. Atmos. Sci.*, **31**, 1256–1261.
- Hayashi, Y., 1970: A theory of large-scale equatorial waves generated by condensation heat and accelerating the zonal wind. *J. Meteor. Soc. Japan*, **48**, 140–160.
- , 1973: Spectral analysis of tropical disturbances appearing in a GFDL general circulation model. *J. Atmos. Sci.*, **31**, 180–218.
- Holton, J. R., 1969: A note on the scale analysis of tropical motions. *J. Atmos. Sci.*, **26**, 770–771.
- , 1971: A diagnostic model for equatorial wave disturbances: The role of vertical shear of the mean zonal wind. *J. Atmos. Sci.*, **28**, 55–64.
- , 1972a: Waves in the equatorial stratosphere generated by tropospheric heat sources. *J. Atmos. Sci.*, **29**, 368–375.
- , 1972b: *An Introduction to Dynamic Meteorology*. Academic Press, 319 pp.
- , 1973: On the frequency distribution of atmospheric Kelvin waves. *J. Atmos. Sci.*, **30**, 499–501.
- Kuo, H.-L., 1965: On formation and intensification of tropical cyclones through latent heat release by cumulus convection. *J. Atmos. Sci.*, **22**, 40–63.
- , 1974: Further studies of parameterization of the influence of cumulus convection on large-scale flow. *J. Atmos. Sci.*, **31**, 1232–1240.
- Lamb, V. R., 1973: The response of a tropical atmosphere to middle latitude forcing. Ph.D. thesis, University of California, Los Angeles, 151 pp.
- Lindzen, R. S., 1967: Planetary waves on beta planes. *Mon. Wea. Rev.*, **95**, 441–445.
- , 1971: Equatorial planetary waves in shear: Part I. *J. Atmos. Sci.*, **28**, 609–622.
- , 1974: Wave-CISK in the tropics. *J. Atmos. Sci.*, **31**, 156–179.
- , L. Shapiro, D. Stevens and E. Sarachik, 1975: Tropical waves and oscillations. Paper presented at the Ninth Technical Conference on Hurricanes and Tropical Meteorology, Miami. (Abstract: *Bull. Amer. Meteor. Soc.*, **56**, 313–314).

²Lindzen *et al.* (1975) have alternatively considered that the CISK is not a lifting process but a low-level organizing process which does not require lifting.

- Madden, R., and E. Zipser, 1970: Multi-layered structure of the wind over the equatorial Pacific during the Line Island Experiment. *J. Atmos. Sci.*, **27**, 336-342.
- Matsuno, T., 1966: Quasi-geostrophic motions in the equatorial area. *J. Meteor. Soc. Japan*, **44**, 25-43.
- Nitta, T., 1970: A study of generation and conversion of eddy available potential energy in the tropics. *J. Meteor. Soc. Japan*, **48**, 524-528.
- Ooyama, K., 1969: Numerical simulation of the life cycle of tropical cyclones. *J. Atmos. Sci.*, **26**, 3-40.
- , 1971: A theory on parameterization of cumulus convection. *J. Meteor. Soc. Japan*, **49**, 744-756.
- Petrosiants, M. A., A. I. Snitkovsky and A. I. Falkovich, 1975: On the evolution of the ITCZ. GATE Rept. No. 14, Preliminary Scientific Results, Vol. 1, 12-28. [Available from WMD, Geneva].
- Reed, R. J., and E. E. Recker, 1971: Structure and properties of synoptic-scale wave disturbances in the equatorial western Pacific. *J. Atmos. Sci.*, **28**, 1117-1133.
- Schubert, W. H., and R. J. Reed, 1975: Vertical motion and vorticity in the A/B scale area: Phase II. GATE Rept. No. 14, Preliminary Scientific Results, Vol. 1, 137-144. [Available from WMO, Geneva].
- Wallace, J. M., 1971: Spectral studies of tropospheric wave disturbances in the tropical western Pacific. *Rev. Geophys. Space Phys.*, **9**, 557-612.
- Williams, K. T., and W. M. Gray, 1973: Statistical analysis of satellite observed trade wind cloud clusters in the western North Pacific. *Tellus*, **25**, 313-336.



Reprinted from JOURNAL OF THE ATMOSPHERIC SCIENCES, Vol. 33, No. 5, May 1976
American Meteorological Society
Printed in U. S. A.

Forcing of Stratospheric Kelvin Waves by Tropospheric Heat Sources

CHIH-PEI CHANG

Forcing of Stratospheric Kelvin Waves by Tropospheric Heat Sources

CHIH-PEI CHANG

Department of Meteorology, Naval Postgraduate School, Monterey, Calif. 93940

(Manuscript received 19 November 1975, in revised form 22 January 1976)

ABSTRACT

The problem of scale-selection of Kelvin waves in the stratosphere by forcing from tropospheric heating is analyzed using a simple linear model. The effect of vertical wind shear is excluded because the phase speed of the waves is fast relative to the range of the mean zonal wind in the vicinity of the tropopause at which level the upward energy flux due to forcing is evaluated. Results of this analysis modify Holton's (1973) theory in that 1) the forcing is most efficient for the longest zonal wavelength even if the heat sources are distributed randomly, and 2) the most favored vertical wavelength of the excited waves is about twice the vertical scale of heating. The calculated vertical wavelengths exceed slightly those observed and the discrepancies are discussed.

1. Introduction

There is ample evidence on the existence of atmospheric Kelvin waves in the equatorial stratosphere (Wallace and Kousky, 1968; and others). These waves propagate eastward and downward with a zonal wavenumber of 1–2, a periodicity of 10–15 days, and a vertical wavelength of 8–12 km. Their zonal wind component has a typical amplitude of 10 m s^{-1} at the equator while no appreciable fluctuation of the meridional wind component is observed. The zonal wind and pressure perturbations are both symmetric with respect to the equator and are close to geostrophic balance in the meridional direction, but the waves behave like internal gravity waves in the zonal and vertical directions. More detailed observational and theoretical descriptions of these waves are given in Wallace (1973) and Holton (1975). These waves are believed to play a very important role in the quasi-biennial oscillation of the equatorial stratosphere by supplying westerly momentum to the zonal mean flow (Lindzen and Holton, 1968; Holton and Lindzen, 1972).

The vertical structure of the Kelvin waves indicates that they are maintained by energy propagating from the troposphere. In addition, the possibility that they are forced by interaction with mid-latitude motions, as suggested by Mak (1969), is quite small because of the small meridional wind perturbations which rule out the importance of lateral energy fluxes. Dynamic instability also appears unlikely due to the very long zonal scale and the fast westerly phase speed of the waves.

Due to the presence of the large amount of deep cumulus convection in the tropical troposphere, it has

been suggested that a plausible energy source for these waves is the latent heat released by cumulus towers. There are two possible mechanisms by which the latent heating in the troposphere may maintain the Kelvin waves:

- 1) A two-way interaction such that the cumulus convection, which supplies energy to the waves, is itself controlled by the large-scale wave motion field. This scale interaction results in an unstable situation which is generally called the conditional instability of the second kind (CISK).

- 2) The waves are forced by cumulus heating which is controlled by processes unrelated to the waves. Hayashi (1970) and Lindzen (1974) have investigated the first mechanism and found that the growth rates of CISK are unsatisfactory in explaining the Kelvin waves. Holton (1972, 1973) studied the second mechanism with a numerical diagnostic model in which the diabatic heating due to cumulus convection is specified. Damping in the form of Rayleigh friction and Newtonian cooling are also included. He found that the wave response in the stratosphere to a tropospheric heat source resembling the Kelvin wave mode has a structure in close agreement with observations. However, the observed periodicity of the Kelvin waves must be specified although no corresponding peak in the cloud brightness spectra can be found. On the other hand, his numerical calculations suggest that the vertical scale of the excited waves is close to that of the specified forcing. In equatorial wave theory (Holton and Lindzen, 1968) the vertical scale determines the wavenumber-frequency relationship. By postulating a red-noise spectral distribution of the tropospheric heat sources, Holton suggested that the

vertical scale and the large low-frequency variance of the forcing result in a band-pass selectivity of the Kelvin waves.

Holton's theory may indeed be valid, especially because an oscillation of the monsoon heating in South Asia, with a quasi-periodicity of about 15 days, has been observed during the northern summer, although it is not clear whether this periodicity exists in other seasons. The purpose of this paper is to point out that the atmosphere acts like a band-pass filter even if the heat sources of the troposphere are distributed randomly in the frequency domain. The relationship between the vertical scale of the response and that of heating will also be examined.

2. The forced model

The zonal mean wind in the tropical stratosphere has considerable vertical shear which may influence the upward propagation of wave energy (Lindzen, 1971). However, due to the fast phase speed of the Kelvin waves the shear is probably not very significant at the tropopause level for which our discussion will be most relevant. The zonal mean wind will therefore be neglected in our simple analysis. The effect of damping will also be excluded. The linearized zonal momentum, meridional momentum, hydrostatic, thermodynamic energy and continuity equations on an equatorial beta-plane, with a single zonal wave-number k , a Doppler-shifted phase speed c , and no perturbation in the meridional velocity may then be written

$$-ikcu = -ik\phi, \quad (1)$$

$$\beta yu = -\frac{\partial \phi}{\partial y}, \quad (2)$$

$$\frac{\partial \phi}{\partial z} = \frac{RT}{H}, \quad (3)$$

$$-ikcT + w\Gamma = \frac{Q}{c_p}, \quad (4)$$

$$iku + e^{z/H} \frac{\partial}{\partial z} (e^{-z/H} w) = 0, \quad (5)$$

where u , w , T , ϕ and Q are the perturbation zonal velocity, vertical velocity, temperature, geopotential and the diabatic heating rate, respectively; H is a constant scale height, Γ the static stability, c_p the specific heat at constant pressure, R the gas constant, β the meridional gradient of the vertical component of earth's vorticity, y the meridional coordinate, and $z = -H \ln(p/p_0)$ is the vertical coordinate with p the pressure and p_0 a reference pressure.

Eqs. (1)–(2) give the meridional structure of the

Kelvin waves:

$$u, \phi \propto \exp\left(-\frac{\beta y^2}{2c}\right), \quad (6)$$

where the condition $c > 0$ is required to satisfy the trapping condition on an equatorial β -plane. If a height-dependence factor, $\exp(z/2H)$, is separated from the perturbation quantities, Eqs. (1) and (3)–(5) may be combined to form a single equation in w :

$$\frac{\partial^2 w'}{\partial z^2} + \lambda^2 w' = \frac{Q'}{c^2}, \quad (7)$$

where

$$\left. \begin{aligned} \lambda^2 &= \frac{S}{c^2} - \frac{1}{4H^2} \\ w' &= w e^{-z/(2H)} \\ Q' &= \frac{R}{c_p H} Q e^{-z/(2H)} \\ S &= \frac{R}{H} \Gamma \end{aligned} \right\}. \quad (8)$$

The parameter λ is a measure of the vertical wave-number. If the heating function Q' is given, (7) can be solved with suitable boundary conditions. In our problem the following boundary conditions are used:

$$w = \begin{cases} 0, & \text{at } z=0 \end{cases} \quad (9a)$$

$$\begin{cases} C_1 e^{i\lambda z} + C_2 e^{-i\lambda z}, & \text{at } z=z_t \end{cases} \quad (9b)$$

where

$$C_1 = r C_2.$$

Here z_t is the height of tropopause and the condition (9b) results from the requirement that latent heating vanishes at z_t . The parameter r is a reflection coefficient which, in the absence of vertical wind shear, is given by the model specification of the static stability distribution. The solution to (7) at $z = z_t$ may now be written as

$$w(z_t) = -\frac{r e^{i\lambda z_t} + e^{-i\lambda z_t}}{\lambda(1+r)} \int_{z_c}^{z_t} \sin(\lambda z) \frac{Q'}{c^2} dz, \quad (10)$$

where z_c is the height of the cloud base.

3. The energy flux at tropopause

We will consider the vertical energy flux $\overline{\phi' w'}$, where the overbar denotes the zonal average and $\phi' = \phi \exp(-z/2H)$, at the tropopause level (z_t), to be a measure of the efficiency of forcing. Despite the actual existence of the vertical shear of the zonal mean flow in the stratosphere, the response of the waves should be largely determined by this quantity.

At z_t the solution is given by (9b) and only the C_2 term needs to be considered for upward energy propagation or downward phase propagation.

Eqs. (1) and (5) may now be rewritten as

$$\begin{aligned} -ikcu' &= -ik\phi', \\ iku' - \left(i\lambda + \frac{1}{2H} \right) w' &= 0, \end{aligned}$$

where $u' = u \exp(-z/2H)$. From these relationships it follows immediately that

$$\phi' = cu' = \frac{c}{k} \left(\lambda - \frac{i}{2H} \right) w'.$$

Since $H \approx 7$ km for the atmosphere, $\lambda \gg 1/(2H)$ if the vertical wavelength $\ll 88$ km. This is the case for all practical purposes so we may write

$$\phi' \approx \frac{c\lambda}{k} w'.$$

From the definition of λ given in Eq. (8) we may also write

$$c\lambda \approx S^{\frac{1}{2}},$$

which leads to

$$\phi' \approx \frac{S^{\frac{1}{2}}}{k} w',$$

and

$$\overline{\phi' w'} \approx \frac{S^{\frac{1}{2}}}{k} \overline{w'^2}. \quad (11)$$

Eq. (11) indicates that, if the amplitude of the vertical velocity perturbation at the tropopause level is fixed, the upward energy flux will be inversely proportional to the zonal wavenumber. Examination of (7) reveals that w' depends only on λ (c is uniquely determined by λ) as long as Q is independent of k . Thus for given vertical scale the forcing at the tropopause level becomes maximum for the longest horizontal wavelength. This result obviously remains the same if one considers the upward momentum flux $\overline{u' w'}$, because $u' = \phi'/c$.

In order to examine the selection of vertical scales, we assume a heating function

$$Q' = \begin{cases} mSq(y) \sin\pi \left(\frac{z - z_c}{\Delta z} \right), & z \geq z_t \geq z_c \\ 0, & z > z_t \text{ or } z < z_c \end{cases} \quad (12)$$

where m specifies the strength of the heating and $\Delta z = z_t - z_c$ is a measure of the vertical scale of the heating. The function $q(y)$ which specifies the meridional distribution of heating will be assumed to

take the form of (6) for the time being. The vertical profile as given by (12) resembles closely that of the typical observations (Chang, 1976). For the simple case, we shall first assume that the static stability parameter S has a constant tropospheric value

$$S = S_t$$

throughout the atmosphere. In this case $r=0$ and on upward energy propagation at $z=z_t$ is allowed. The solution (10) at z_t is now found to be

$$w' = \hat{w} \exp[-i\lambda z_t - \beta y^2/(2c)], \quad z = z_t, \quad (13)$$

where

$$\hat{w} = -\frac{m\pi\Delta z}{\lambda} \frac{\lambda^2 + 1/(4H)^2}{\pi^2 - \lambda^2\Delta z^2} \sin\left[\frac{\lambda}{2}(z_t + z_c)\right] \cos\left(\frac{\lambda\Delta z}{2}\right) \quad (14)$$

denotes the amplitude of the solution in this simple model. We note here that no actual singularity exists in (14). The vertical energy flux at the equator at $z = z_t$ is thus

$$\overline{\phi' w'} = \frac{S^{\frac{1}{2}}}{2k} \hat{w}^2.$$

From (14) if one assumes $\lambda \gg 1/(4H^2)$, it can be shown that this energy flux reaches maximum at

$$\lambda = \frac{\pi}{\Delta z},$$

where

$$\hat{w}^2 \approx \frac{m^2\pi^2}{16} \sin^2\left[\frac{\pi}{2\Delta z}(z_t + z_c)\right].$$

The tropospheric forcing is therefore most efficient at a vertical wavelength

$$L_z \equiv \frac{2\pi}{\lambda} = 2\Delta z,$$

or twice the vertical scale of the heating. This result is somewhat similar to those of Green (1965) and Lindzen (1966). A plot of the energy flux profile at z_t is given in Fig. 1 in which it is assumed that $z_t = 15$ km and $H = 7z_c$. If we measure the vertical scale of Holton's (1972, 1973) heating function the value Δz can be found to be ~ 11 km, which predicts a maximum response of 22 km vertical wavelength in the troposphere. Since in reality the stratospheric static stability is about three times that of the troposphere, using (8) we may estimate that the stratospheric vertical wavelength corresponding to a 22 km tropospheric value would be

$$L_s \approx L_t \left(\frac{S_s}{S_t} \right)^{-\frac{1}{2}} = 22 \times 3^{-\frac{1}{2}} \approx 12.8 \text{ km},$$

where the subscript s denotes stratosphere. If we assume $\Delta z \approx 14$ km, then $L_s \approx 16.3$ km.

It may be of some interest to consider the effect of different static stability between stratosphere and troposphere on the solution (13), because the "efficiency" of reflection of wave energy at $z=z_t$ may be scale-dependent. In this case we have

$$S=S_s, \text{ for } z>z_t,$$

$$S=S_t, \text{ for } z\leq z_t.$$

Another boundary condition is now needed and the simplest form available is the radiation condition above z_t , i.e.,

$$w'=A \exp[-i\lambda_s z - \beta y^2/(2c)], \text{ for } z>z_t, \quad (15)$$

where λ_s is the vertical wavenumber in the stratosphere. The continuity conditions of w' and ϕ' across z_t lead to

$$r = \frac{1 - (S_s/S_t)^{1/2}}{1 + (S_s/S_t)^{1/2}} \exp(-2i\lambda_t z_t), \text{ for } S_s > S_t,$$

where λ_t is the vertical wavenumber in the troposphere. The solution (10) at z_t in the form of (15) is

$$A = \frac{2\lambda_t \exp[i(\lambda_s - \lambda_t)z_t] \hat{w}}{(\lambda_s + \lambda_t) - (\lambda_s - \lambda_t) \exp(-2i\lambda_t z_t)},$$

where \hat{w} is given by (14) with all λ replaced by λ_t . The vertical energy flux at the equator and z_t is now

$$\overline{\phi'w'} \approx \frac{S^{\frac{1}{2}}}{2k} A A^* \approx \frac{S^{\frac{1}{2}}}{2k} E \hat{w}^2,$$

where

$$E = 2[(1 + S_s/S_t) + (1 - S_s/S_t) \cos 2\lambda_t z_t]^{-1}$$

is the effect of different static stabilities above and below z_t and the asterisk denotes complex conjugate. For $S_s = 3S_t$, E varies between a maximum of 1 when $\lambda_t = 0, \pi/z_t, 2\pi/z_t, \dots$, and a minimum of 0.33 when $\lambda_t = \pi/(2z_t), 3\pi/(2z_t), 5\pi/(2z_t), \dots$. Assuming $z_t = 15$ km and $\Delta z = 14$ km, the variation of E is plotted in the upper section of Fig. 1 and the modified energy flux profile is indicated by the dashed curve in the lower section. It is seen that the most efficient forcing is slightly larger than twice the scale of heating. Hence we may conclude that the variation in static stability between troposphere and stratosphere does not cause great effect in the vertical scale of the most favored response.

4. Concluding remarks

We have shown that for randomly distributed tropospheric heat sources the Kelvin waves of the

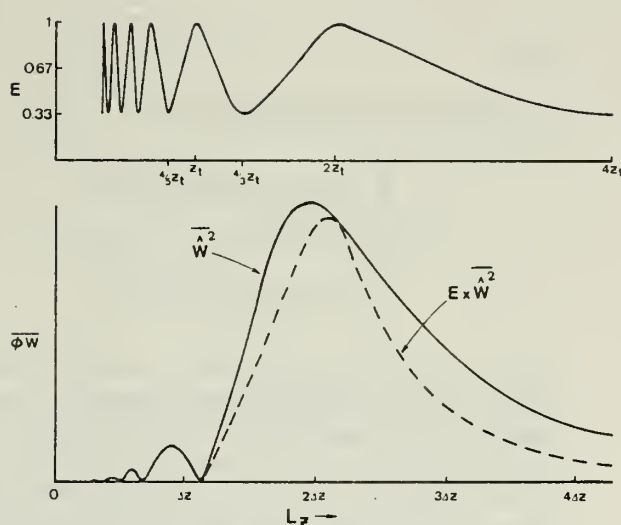


FIG. 1. Profile of vertical wave energy flux $\overline{\phi'w'}$ as a function of vertical wavelength L_z . The solid curve in the lower diagram is for the case $S_s = S_t$ and the dashed curve for the case $S_s = 3S_t$. The upper diagram is the effect on E of the difference in static stability on the vertical wave energy flux profile for the case $S_s = 3S_t$.

largest zonal scale are excited most efficiently in the absence of damping. This may explain why most of the Kelvin waves observed in the lower stratosphere are of zonal wavenumber 1 and some are of wavenumber 2. The vertical wind shear has been excluded from our analysis but it should not significantly alter this conclusion.

The finding that the most favored vertical wavelength is about twice the vertical scale of heating gives a reasonable estimate for Kelvin waves in the lower stratosphere, although the calculated wavelength of 13–16 km is slightly larger than those observed. Several influences which are excluded in our model may alter this aspect. For example, Lindzen (1971) found that the focusing effect of the vertical wind shear in the stratosphere would reduce the vertical scale of the waves. A two-scale expansion technique can be similarly applied to our forced model and the resultant prevailing vertical wavelength in the stratosphere should be reduced.

Another effect which has been excluded is the actual north-south distribution of the heating function. The meridional structure equation (6) indicates that the meridional scale of the waves is coupled with the vertical scale through the phase speed c . The variation of the meridional scale with the vertical scale may be considered slow because the e -folding width of the Gaussian distribution is proportional only to the square root of c , which is approximately proportional to the vertical wavelength. In the real atmosphere the meridional heating profile $q(y)$ in (12) does not adjust to different vertical scales as we have assumed in our calculations. A proper treatment of this problem is, perhaps, to multiply the previously

calculated response by the projection

$$P = \frac{\int_0^\infty q(y) \exp[-\beta y^2/(2c)] dy}{\int_0^\infty \exp[-\beta y^2/(2c)]^2 dy} \quad (16)$$

Here we could specify $q(y)$ as we did for the vertical heating profile, although there appears to be more observational uncertainty. For the purpose of the present qualitative discussion, however, this is not strictly necessary. We know that the latent heating is largely confined to the tropics, so that the meridional extent of $q(y)$ must be quite limited. Therefore, the effect of (16) should be such that waves whose vertical scales are larger than that corresponding to the meridional scale of $q(y)$ will suffer from having a large portion of their north-south domain unsupported by heating. If we assume that the meridional scale of $q(y)$ can be represented by an e -folding width $y_d \approx 1500$ km of a Gaussian distribution about the equator, and that $S_t = 1.22 \times 10^{-4} \text{ s}^{-2}$ which corresponds to $\Gamma = 3 \text{ K km}^{-1}$, then those waves with a tropospheric vertical wavelength

$$L_z > \pi \beta S_t^{-1} y_d^2 \approx 14.2 \text{ km},$$

or a stratospheric wavelength

$$L_s > 8.2 \text{ km},$$

will have their amplitude reduced by (16). The reduction will be more severe for longer vertical wavelengths. This obviously would also shorten the previously calculated most favored vertical scales of the Kelvin waves.

Acknowledgments. The author wishes to thank Profs. J. R. Holton and R. S. Lindzen for discussion and

Profs. R. T. Williams and G. J. Haltiner for reading the manuscript. This research was supported by the Atmospheric Sciences Section, National Science Foundation, under Grant DES75-10719. Parts of the material in this paper were presented at the AMS Ninth Conference on Hurricanes and Tropical Meteorology, May 1975, Miami, Fla.

REFERENCES

- Chang, C.-P., 1976: Vertical structure of tropical waves maintained by internally induced cumulus heating. *J. Atmos. Sci.*, **33**, 729-739.
- Green, J. S. A., 1965: Atmospheric tidal oscillations: An analysis of the mechanics. *Proc. Roy. Soc. London*, **A288**, 564-574.
- Hayashi, Y., 1970: A theory of large-scale equatorial waves generated by condensation heat and accelerating the zonal wind. *J. Meteor. Soc. Japan*, **48**, 140-160.
- Holton, J. R., 1972: Waves in the equatorial stratosphere generated by tropospheric heat sources. *J. Atmos. Sci.*, **29**, 368-375.
- , 1973: On the frequency distribution of atmospheric Kelvin waves. *J. Atmos. Sci.*, **30**, 499-501.
- , 1975: The dynamic meteorology of the stratosphere and mesosphere. *Meteor. Monogr.*, **15**, No. 37, 240 pp.
- , and R. S. Lindzen, 1968: A note on Kelvin waves in the atmosphere. *Mon. Wea. Rev.*, **95**, 385-386.
- , and —, 1972: An updated theory for the quasi-biennial cycle of the tropical stratosphere. *J. Atmos. Sci.*, **29**, 1076-1080.
- Lindzen, R. S., 1966: On the relation of wave behavior to source strength and distribution in a propagating medium. *J. Atmos. Sci.*, **23**, 630-632.
- , 1971: Equatorial planetary waves in shear: Part I. *J. Atmos. Sci.*, **28**, 609-622.
- , 1974: Wave-CISK in the tropics. *J. Atmos. Sci.*, **31**, 156-179.
- , and J. R. Holton, 1968: A theory of the quasi-biennial oscillation. *J. Atmos. Sci.*, **25**, 1095-1107.
- Mak, M.-K., 1969: Lateral driven stochastic motions in the tropics. *J. Atmos. Sci.*, **26**, 41-64.
- Wallace, J. M., 1973: General circulation of the tropical lower troposphere. *Rev. Geophys. Space Phys.*, **11**, 191-222.
- , and V. E. Kousky, 1968: Observational evidence of Kelvin waves in the tropical stratosphere. *J. Atmos. Sci.*, **25**, 900-907.

Reprinted from JOURNAL OF THE ATMOSPHERIC SCIENCES, Vol. 33, No. 8, August 1976
American Meteorological Society
Printed in U. S. A.

Comments on "Instability Theory of Large-Scale Disturbances in the Tropics"

C.-P. CHANG

Department of Meteorology, Naval Postgraduate School, Monterey, Calif. 93940

4 February 1976 and 25 March 1976

In a recent paper by Kuo (1975), a condition was used in a CISK parameterization to explain the time and length scales of the observed mixed Rossby-gravity waves and the Kelvin waves in the tropics. This condition, as stated by Kuo on p. 2231, is that "the depletion of moisture through precipitation must be replenished

by evaporation from the surface during a complete period of the disturbance." Eq. (15b) in his paper specifies this condition as follows:

$\tau (E + \text{rate of moisture convergence}) \geq \text{maximum total precipitation given by deep cumulus convection during a period,}$

where τ is the period of the wave disturbances and E the evaporation rate. On p. 2234 he derived the limiting period τ_0 for which the equal sign in (15b) holds. This is given by his Eq. (23):

$$\tau_0 = \frac{P_t}{E},$$

where P_t is the average maximum total precipitation over a period. This maximum total precipitation, according to the argument on p. 2232, is always produced by the disturbance "once the convective instability is activated by the large-scale flow," because the "convection will proceed as an overturning process and produce the maximum amount of precipitation possible for the given air mass." The value of P_t was estimated by subtracting the vapor contents of the outflow column from the inflow column as was schematically illustrated in his Fig. 3. The computed τ_0 was then used as a cutoff period in the CISK parameterization [Eq. (24)] in such a way that the heating function is proportional to the factor τ/τ_0 if $\tau < \tau_0$. The implication of his analysis is that, "disturbances with periods $< \tau_0$ cannot be supported fully by deep cumulus convection initiated by such disturbances because the moisture content of the atmosphere will be depleted by the convective process."

The above arguments are, however, inconsistent with an essential part of the CISK parameterization used in the paper, namely that the large-scale heating rate is proportional to the vertical velocity W_b at a low reference level z_b when $W_b > 0$. In this parameterization when the wave amplitude at an early stage of the development is small, W_b is small and so is the heating rate, which implies that the precipitation rate is small. As the waves grow, W_b increases and the precipitation rate in turn increases. Since the total precipitation of a

continuous wave chain cannot exceed the total evaporation in the tropical belt, the restraining effect is such that the precipitation rate must not exceed the evaporation rate, or $3.75 \text{ g cm}^{-2} \text{ day}^{-1}$ according to the calculations quoted by Kuo. Therefore the total moisture availability in the tropics should constrain the maximum amplitude the waves can grow to, rather than the period of the waves. The intensity of the *cumulus-scale* convection is determined by the large-scale moisture convergence below z_b in the CISK theory because this convergence provides the high θ_E for the ascending air. For more sophisticated parameterization theories, such as that of Arakawa and Schubert (1974) which is a form of the convective adjustment, the same inconsistency would occur. In these theories the effect of cumulus convection is also entirely a response to the large-scale forcing and therefore its intensity, as reflected by the net large-scale heating, should be controlled by the large-scale flow.

On the other hand, another condition mentioned by Kuo [Eq. (15a)] is a valid one, and may be quite important in selecting the wave scales. This condition requires "a disturbance of sufficiently long duration and high intensity able to lift the lower atmosphere above the condensation level, thereby activating the deep cumulus convection." In other words, waves with short periods are unlikely to grow. Kuo's Eq. (24), which contains a cutoff period may, in a way, be viewed as a crude representation of this condition although the precise requirement can only be treated as a nonlinear problem. Based on this condition alone, waves whose Doppler-shifted phase speed equals zero for $z \leq z_b$ are most favored for development. This seems to be the case in the tropical western Pacific where the usually observed warm-core synoptic-scale waves have a typical easterly phase speed of $5\text{--}8 \text{ m s}^{-1}$, quite close to the low-level mean zonal wind.

REFERENCES

- Arakawa, A., and W. H. Schubert, 1974: Interaction of a cumulus cloud ensemble with the large-scale environment, Part I. *J. Atmos. Sci.*, **31**, 674–701.
Kuo, H. L., 1975: Instability theory of large-scale disturbances in the tropics. *J. Atmos. Sci.*, **32**, 2229–2245.

Viscous Internal Gravity Waves and Low-Frequency Oscillations in the Tropics

CHIH-PEI CHANG

Department of Meteorology, Naval Postgraduate School, Monterey, Calif. 93940

(Manuscript received 10 January 1977, in revised form 11 March 1977)

ABSTRACT

In this paper we deal with the interpretation of observed oscillations in the tropical troposphere and stratosphere within the framework of the equatorial wave theory. A difficulty with this problem arises when one compares the short vertical wavelength (or equivalent depth) predicted by the classical theory and the observed large vertical scales associated with the low Doppler-shifted frequencies of the tropospheric oscillations. In this analysis it is shown that the inclusion of simple linear damping, justified by budget studies which revealed the important role of cumulus momentum transport, has a strong influence at low frequencies on the forced equatorial waves and results in two types of dispersive relationships. The first type is characteristic of the regular internal gravity waves which have fast phase speeds and weak vertical attenuation. The second type is dominated by the viscous damping time scale and has slow phase speeds and strong vertical trapping. The theory predicts that the stratospheric oscillations may be identified with the first type and the tropospheric oscillations with the second. In the case of Kelvin waves the results can be used to explain consistently both the observed stratospheric Kelvin waves and the planetary-scale Kelvin-like oscillations in the troposphere including the 40–50 day oscillation and the monsoon and Walker circulations. Possible implications with respect to other waves in the tropics are also discussed.

1. Introduction

Based on spectral and cross-spectral analyses of long time series (5–10 years) of tropical station data, Madden and Julian (1971, 1972) detected a global-scale oscillation in the tropical troposphere with a periodicity of 40–50 days. A degree of stationarity of this oscillation in time was also established by them by examining the limited amount of station pressure data available from the 1890's. Their results indicate that this oscillation is most prominent in the zonal velocity component and the surface pressure, with the maximum amplitude situated along the equator. There are some time and spatial variations within a 40–50 day cycle as depicted in Fig. 1 which is reproduced from a schematic diagram constructed by Madden and Julian (1972), but basically the oscillation propagates eastward at a fairly steady phase speed and, at most times, exhibits a zonal wave-number 1 structure. Madden and Julian (1972) argued that enhanced deep cumulus convection is usually associated with large-scale upward motion and the oscillation appears as two vertical circulation cells along the equatorial zonal plane.

The above structure resembles that of a theoretical atmospheric Kelvin wave (Holton and Lindzen, 1968) in several ways: the direction of propagation, the meridional structure and the absence of large amplitude in the meridional wind component. However, for a

given phase speed as slow as that observed, Kelvin wave theory would predict a fairly short vertical wavelength which does not appear to agree with that of the observed oscillation. This discrepancy, which has been a major difficulty for the theoretical understanding of the 40–50 day oscillations, has also been encountered by several meteorologists in their efforts to interpret various types of large-scale tropical wave motions using the equatorial wave theory. In a linear analysis Lindzen (1967) has shown that for synoptic (and larger) time scales, waves on an equatorial beta-plane generally propagate in the vertical as internal gravity waves with rather short vertical wavelengths. This result was evident in a study of the response of the tropical atmosphere to stationary heating by Webster (1972, 1973). In a two-level (750 and 250 mb) numerical model he found that the equatorial response in an easterly basic current has a horizontal structure that is characteristic of Kelvin waves. However, his analytical solution for the case of an idealized basic flow possesses very short vertical wavelength [$\sim O(1 \text{ km})$] and appears to suggest that higher vertical resolution is required for the numerical model.

The short vertical wavelength predicted by the equatorial wave theory arises from the internal gravity wave character of these waves. Since for pure gravity waves the phase speed c is given by $c = (gh)^{1/2}$, where

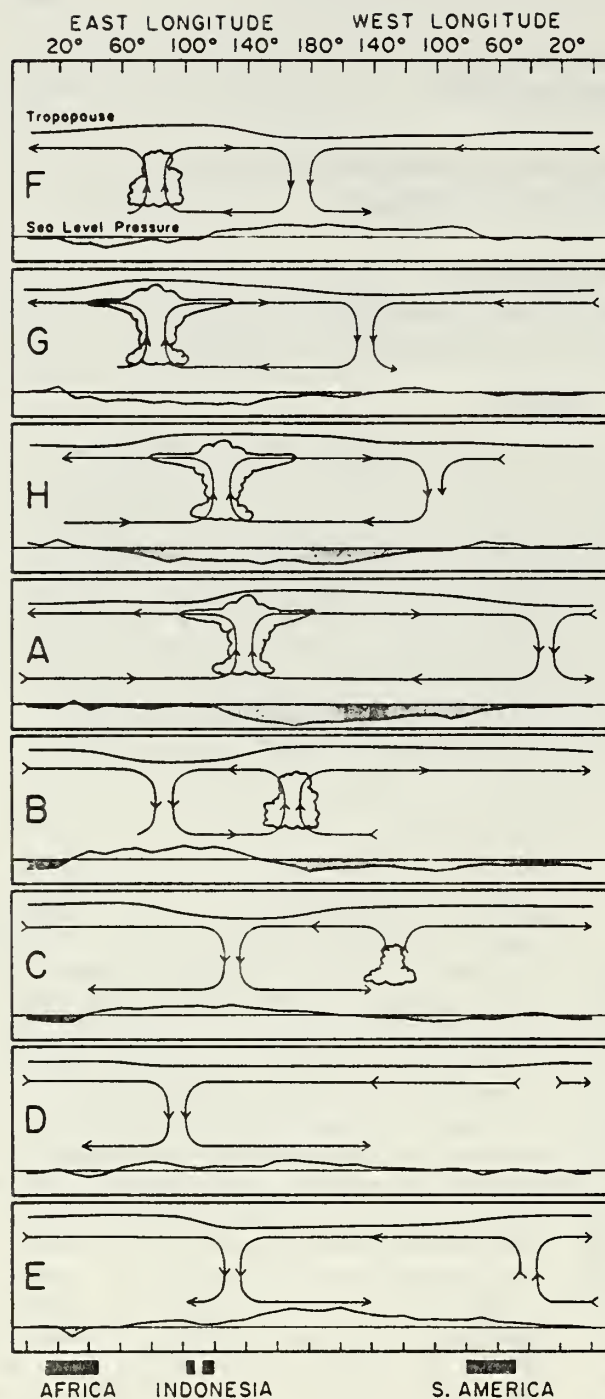


FIG. 1. Schematic depiction of the time and space (zonal plane) variations of the circulation cells associated with the 40-50 day oscillation. The mean pressure disturbance is plotted at the bottom of each chart with negative anomalies shaded. Regions of enhanced large-scale convection are indicated schematically by the cumulus and cumulonimbus clouds. The relative tropopause height is indicated at the top of each chart. (From Madden and Julian, 1972.)

g is the gravitational constant and h a depth scale for the motion (usually called the equivalent depth), the vertical wavelength tends to be proportional to

the phase speed. Within the range of large-scale tropical motions in the tropical troposphere the phase speed is usually slow compared to the external gravity wave phase speed, so the vertical wavelength is consequentially small compared to that given by the scale height. The observed Kelvin waves (Wallace and Kousky, 1968) and mixed Rossby-gravity waves (Yanai and Maruyama, 1966) in the lower stratosphere have rather large Doppler-shifted phase speeds (relative to the mean zonal wind) so that their observed vertical wavelengths are in better agreement with the theory. In Table 1 we summarize the comparison between the observed vertical wavelengths and that given by the equatorial wave theory for three major zonal wind oscillations in the tropics: the stratospheric Kelvin wave, the 40-50 day oscillation and the planetary-scale stationary motion which could include the east-west overturning Walker circulation along the equatorial plane (Bjerknes, 1969; Webster, 1973) or the winter monsoon (Krishnamurti *et al.*, 1973; Webster, 1973). The theoretical vertical wavelength is calculated using the Doppler-shifted phase speed with the mean zonal flow specified by an averaged tropospheric easterly speed of -5 m s^{-1} . This specification is based on the evidence that all these oscillations, including the stratospheric Kelvin wave, are generated by energy sources in the troposphere.

The equatorial wave theory used in Table 1 is basically inviscid because it does not include a significant frictional effect in the free atmosphere. In a numerical diagnostic study of the seasonal-mean circulation at 200 mb during the northern summer, Holton and Colton (1972) found that a very strong damping term (corresponding to linear damping time scale of ~ 1 day) is needed in the linearized barotropic vorticity equation to balance the generation of planetary-scale vorticity by horizontal divergence. Since the planetary-scale divergence field is largely a result of the strong condensation heating in the middle troposphere due to the vigorous cumulus convection associated with the summer monsoon, Holton and Colton hypothesized that the vertical mixing of vorticity and momentum by cumulus convection could account for this strong damping. This hypothesis is also consistent with several budget studies of synoptic-scale, cumulus-related tropical motions (Reed and Recker, 1971; Williams and Gray, 1973; Reed and Johnson, 1974; Chu, 1976; and others), and the numerical diagnostic study by Chang *et al.* (1975). Recently Stevens *et al.* (1977) also show that this strong damping mechanism is responsible for reducing the theoretically calculated amplitude of the tropical waves forced by heating to the observed magnitude. Thus the inclusion of this mechanism in the equatorial wave theory seems to be necessary for the proper

TABLE 1. Comparison of observed tropical zonal oscillations and the inviscid equatorial wave theory. The theoretical vertical wavelengths are based on the observed Doppler-shifted phase speeds which assume a basic zonal wind of $\bar{u} = -5 \text{ m s}^{-1}$. See text for details.

Oscillations	Observations					Theory
	Period (days)	Zonal wavenumber	Ground phase speed (m s^{-1})	Doppler-shifted* phase speed (m s^{-1})	Vertical wavelength (km)	Vertical wavelength (km)
Stratospheric Kelvin waves (Wallace and Kousky, 1968)	10-15	1-2	25-45	30-50	10-15(strat) 17-26(tropo)	17-29
40-50 day oscillations (Madden and Julian, 1972)	40-50	1	9-11	14-16	15-30	8-9
Stationary planetary circulations (monsoon and Walker)	∞	1-2	0	5	15-30	3

* $\bar{u} = -5 \text{ m s}^{-1}$.

interpretation of the observed tropical motions forced by cumulus heating.

The purpose of this paper is to study the effect of the strong damping mechanism called for by previous budget studies on tropical wave dynamics. The simplest form of linear drag will be used to represent this effect as was done by Holton and Colton (1972). We will show that this effect in some cases is more than just an expected reduction in the amplitude of the thermally forced waves or a near-trivial correction in the frequency equation. Moreover, in these cases it can account for most of the discrepancies in Table 1 and provide a consistent theoretical basis for the interpretation of the tropical oscillations in both the stratosphere and the troposphere.

2. Basic equations

Since the vertical structure equation of all equatorial waves is identical to that for two-dimensional gravity waves, we will consider only the Kelvin wave case for the purpose of simplicity. Setting the meridional velocity zero we may write the linearized zonal momentum, meridional momentum, hydrostatic, thermodynamic energy and continuity equations on an equatorial beta-plane, with a single zonal wavenumber k and constant phase speed c relative to the basic zonal flow as

$$-ikcu = -ik\phi - Du, \quad (1)$$

$$\beta yu = -\frac{\partial \phi}{\partial y}, \quad (2)$$

$$\frac{\partial \phi}{\partial z} = \frac{RT}{H}, \quad (3)$$

$$-ikcT + w\Gamma = \frac{Q}{c_p} - DT, \quad (4)$$

$$iku + e^{z/H} \frac{\partial}{\partial z} (e^{-z/H} w) = 0, \quad (5)$$

where u , w , T , ϕ and Q are the perturbation zonal velocity, vertical velocity, temperature, geopotential and the diabatic heating rate, respectively; H is a constant scale height, Γ the static stability, c_p the specific heat at constant pressure, R the gas constant, β the meridional gradient of the vertical component of earth's vorticity, y the meridional coordinate; and $z = -H \ln(p/p_0)$ is the vertical coordinate with p the pressure and p_0 a reference pressure. The damping effect is represented by the linear drag coefficient D in the zonal momentum equation. A Newtonian cooling term with the same coefficient is included in the thermodynamic energy equation in order to facilitate the analysis.

Eqs. (1)-(2) give the meridional structure of the Kelvin waves:

$$u, \phi \propto \exp(-\beta y^2/2\hat{c}), \quad (6)$$

where

$$\hat{c} \equiv c + iD/k,$$

and the condition $\text{Re}(\hat{c}) = c > 0$ is required to satisfy the trapping condition on an equatorial β -plane. If a height-dependence factor, $\exp(z/2H)$, is separated from the perturbation quantities, Eqs. (1) and (3)-(5) may be combined to form a single equation in w :

$$\frac{\partial^2 w'}{\partial z^2} + \lambda^2 w' = \frac{Q'}{\hat{c}^2}, \quad (7)$$

where

$$\lambda^2 \equiv \frac{S}{\bar{c}^2} - \frac{1}{4H^2}, \quad (8)$$

$$w' \equiv w e^{-z/(2H)},$$

$$Q' \equiv \frac{R}{c_p H} Q e^{-z/(2H)},$$

$$S \equiv -\frac{R}{H} \Gamma.$$

The parameter λ is a measure of the vertical wave-number. If the heating function Q' is given, (7) can be solved with suitable boundary conditions. In our problem the following boundary conditions are used:

$$w = \begin{cases} 0, & \text{at } z=0 \\ C_1 e^{i\lambda z} + C_2 e^{-i\lambda z}, & \text{at } z=z_t \end{cases} \quad (9a)$$

where

$$C_1 = r C_2.$$

Here z_t is the height of tropopause and the condition (9b) results from the requirement that latent heating vanishes at z_t . The parameter r is a reflection coefficient which, in the absence of vertical wind shear, is given by the model specification of the static stability distribution. The solution to (7) may be written in the form

$$w(z) = -\frac{r e^{i\lambda z} + e^{-i\lambda z}}{\lambda(1+r)} \int_{z_c}^{z_t} \sin \lambda z \frac{Q'}{gh} dz, \quad z \geq z_t, \quad (10a)$$

$$w(z) = -\frac{\sin \lambda z}{\lambda(1+r)} \int_z^{z_t} (r e^{i\lambda z} + e^{-i\lambda z}) \frac{Q'}{gh} dz - \frac{r e^{i\lambda z} + e^{-i\lambda z}}{\lambda(1+r)} \times \int_{z_c}^z \sin \lambda z \frac{Q'}{gh} dz, \quad z_t > z > z_c, \quad (10b)$$

$$w(z) = -\frac{\sin \lambda z}{\lambda(1+r)} \int_{z_c}^{z_t} (r e^{i\lambda z} + e^{-i\lambda z}) \frac{Q'}{gh} dz, \quad z_c \geq z \geq 0. \quad (10c)$$

Here z_t is the height of cloud top and z_c the height of cloud base. Chang (1976) has used the above equations to show that, in the case of $D=0$, the vertical energy flux of Kelvin waves due to pressure work is

$$\overline{\phi' w'} \approx -\frac{S^{\frac{1}{2}}}{k} \overline{w'^2}, \quad (11)$$

where the overbar denotes the zonal average and $\phi' = \phi \exp(-z/2H)$. Eqs. (11) and (7) indicate that for this case the upward forcing of Kelvin waves is most efficient for long waves. Augmented by the fact that waves with a vertical scale equal to twice that of forcing are most efficiently excited (Green, 1965

and Lindzen, 1966), Chang (1976) was able to show that the Kelvin wave response given by the inviscid theory agrees with the observed stratospheric Kelvin waves.

If we consider downward phase propagation (upward energy propagation) only, $\text{Re}(\lambda) > 0$. For ~ 7 km and vertical wavelength $\ll 88$ km, Eq. (8) may be approximated by

$$\bar{c} \lambda = S^{\frac{1}{2}}. \quad (1)$$

In the inviscid case, $D=0$ and $\bar{c}=c$ so that λ is purely real. In the case of $D \neq 0$, $\bar{c} = c_r + i c_i$ where $c_r = c > 0$ and $c_i = D/k > 0$; thus λ becomes complex, i.e., $\lambda = \lambda_r + i \lambda_i$. Here λ_i describes the exponential increase ($\lambda_i > 0$) or decrease ($\lambda_i < 0$) of the amplitude with height. Eq. (12) now becomes quadratic and has the following roots:

$$c_{rI,II} = \frac{S^{\frac{1}{2}} \pm (S - 4\lambda_r^2 c_i^2)^{\frac{1}{2}}}{2\lambda_r} > 0, \quad (12)$$

$$\lambda_{iI,II} = \frac{-S^{\frac{1}{2}} \pm (S - 4\lambda_r^2 c_i^2)^{\frac{1}{2}}}{2c_i} < 0. \quad (14)$$

The subscripts I and II are being used to denote the plus and minus roots, respectively. It is obvious that $c_{rI} > c_{rII}$ and $|\lambda_{iI}| < |\lambda_{iII}|$, hence the first solution (which shall be called Mode I) has a fast horizontal phase speed and can propagate more efficiently into higher levels while the second solution (Mode II) is slower and attenuates faster above the source region. In addition, Eqs. (13) and (14) indicate that the waves are excitable only if

$$\lambda_r < \frac{S^{\frac{1}{2}}}{2c_i} \left(= \frac{k S^{\frac{1}{2}}}{2D} \right), \quad (15)$$

so that the effect of damping causes a short-wave cutoff in the vertical or a long-wave cutoff in the horizontal.

If we take the inviscid limit of $D \rightarrow 0$, Eqs. (13) and (14) reduce to

$$\left. \begin{aligned} c_{rI} &= S^{\frac{1}{2}}/\lambda_r \\ \lambda_{iI} &= 0 \end{aligned} \right\}. \quad (16)$$

$$\left. \begin{aligned} c_{rII} &= 0 \\ \lambda_{iII} &= -\infty \end{aligned} \right\}. \quad (17)$$

Comparing (16) and (12) it is seen that Mode I corresponds to the regular inviscid solution. Substituting (17) into (1)–(5) leads to a trivial solution of vanishing wave amplitude. Thus Mode I may be called the “regular mode” and Mode II the “viscous mode,” because the latter is non-trivial only when $D \neq 0$.

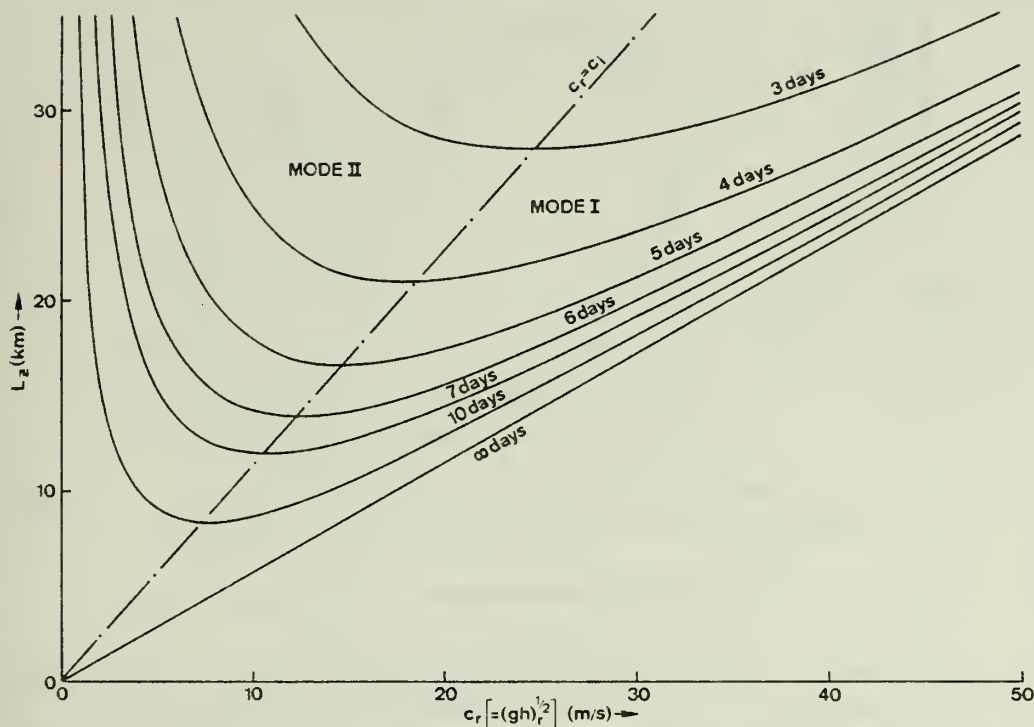


FIG. 2. Real Doppler-shifted phase speed c_r as a function of vertical wavelength L_z and damping time. For the convenience of application to other types of equatorial waves, the abscissa can also be designated by $(gh)_r^{1/2}$, where h is the equivalent depth.

Fig. 2 shows the real phase speed c_r as a function of vertical wavelength $L_z (= 2\pi/\lambda_r)$ and the viscous damping time scale $1/D$. For $D=0$ (damping time scale ∞) the dispersion relationship of Mode I is a straight line of $c_r \propto L_z$, typical of the internal gravity waves. In addition, the vertical coordinate ($c_r=0$) represents the trivial solution of Mode II. For $D \neq 0$ the two modes are represented by the quadratic curves. The effect of damping on Mode I is a relatively small modification with L_z increasing as c_r increases. The modification for Mode II is more substantial and L_z generally decreases as c_r increases. The two modes are separated by the line $c_r = c_i$. For Mode I $c_r > c_i$, i.e., the inertial time scale is faster than the damping time scale. The reverse is true for Mode II.

The imaginary vertical wavenumber λ_i is shown in Fig. 3 as a function of vertical wavelength and damping time scale. Here the magnitude of λ_i decreases with increasing L_z for Mode I and increases with L_z for Mode II. The $c_r = c_i$ curve again provides the partition of the two modes.

From Figs. 2 and 3 it can be seen that, if a certain vertical wavelength is most efficiently excited by a given forcing function, both modes will be excited for $D \neq 0$. The regular mode will have fast zonal phase speed and less vertical attenuation, while the viscous mode will have slow zonal phase speed and is more trapped in the vertical away from the source region.

3. Response of specified heating

The Kelvin wave response of the tropical atmosphere can be calculated if the vertical heating function Q' in (7) is known. As in Chang (1976) we will use the vertical heating profile

$$Q' \propto Sq(y) \sin \pi \left(\frac{z - z_c}{\Delta z} \right), \quad z_t \geq z \geq z_c$$

$$Q' = 0, \quad z > z_t \text{ or } z < z_c$$

where the function $q(y)$, which specified the meridional distribution of heating, is assumed to take the form of (6). Solution (10) will be evaluated by specifying the vertical scale of the heating $\Delta z \equiv z_t - z_c = 14$ km, $D = 2.3 \times 10^{-6} \text{ s}^{-1}$ (damping time = 5 days) and $S_s = 3S_t$, where S_s and S_t are the static stability for the stratosphere and troposphere, respectively.

Since Mode I is less trapped in the vertical we expect that it may be more prominent away from the source region. Using (10a) we display the vertical wave energy flux due to pressure work, $\overline{\phi'w'}$, at z_t as a function of vertical wavelength L_z and zonal wavenumber $s (= ka)$, where a is the radius of the earth, in Fig. 4. The cross-hatched area in the lower part of the diagram indicates the short vertical wavelength cutoff required by (15). The maximum response occurs at zonal wavenumber 1–2 and vertical wavelength 30–35 km. As expected, this result is similar to that

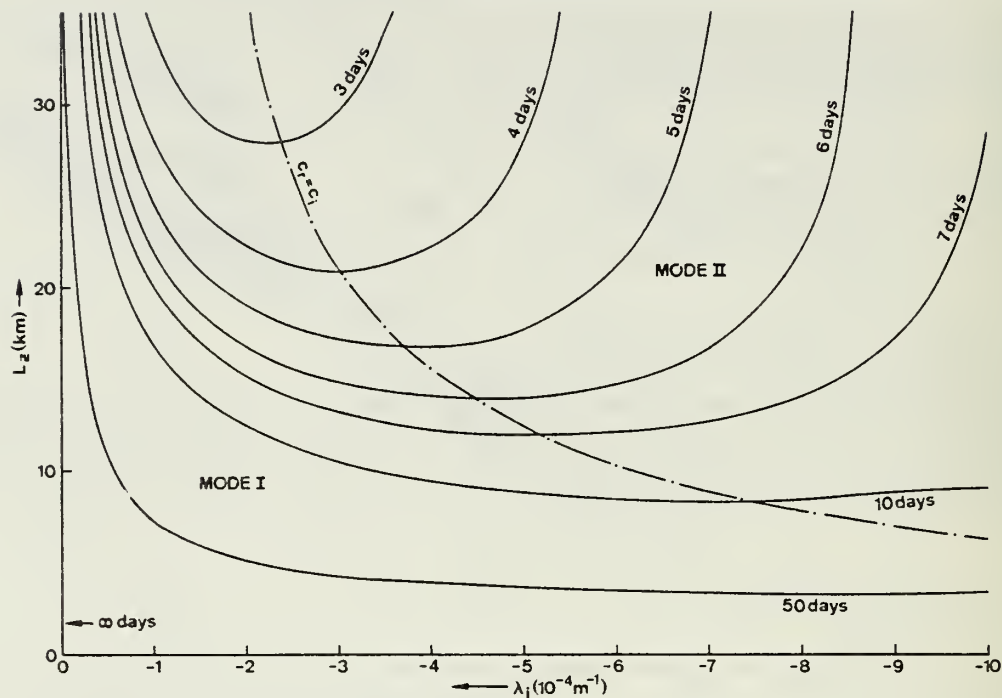


FIG. 3. Imaginary vertical wavenumber λ_i , as a function of vertical wavelength and damping time.

obtained by Chang (1976) except that the vertical wavelength is slightly longer and wavenumber 2 becomes comparable in importance to wavenumber 1. This vertical wavelength range, according to Fig. 2, implies a Doppler-shifted phase speed $\sim 50 \text{ m s}^{-1}$, in reasonable agreement with the observed stratospheric Kelvin waves.

For the highly trapped Mode II the vertically-integrated tropospheric kinetic energy is considered an appropriate measurement for the response spectrum.

Fig. 5 shows this quantity as a function of L_z and s . Here the zonal scale selection clearly favors the lowest zonal wavenumber, but all vertical wavelengths beyond the short-wave cutoff have about the same response. Thus the most prominent viscous mode excited should be of zonal wavenumber 1 and vertical wavelength $\gtrsim 17 \text{ km}$. For vertical wavelength $\sim 17 \text{ km}$ the Doppler-shifted phase speed is $\sim 10 \text{ m s}^{-1}$ according to Fig. 2. These values agree quite well with the 40–50 day oscillation observed by Madden and Julian

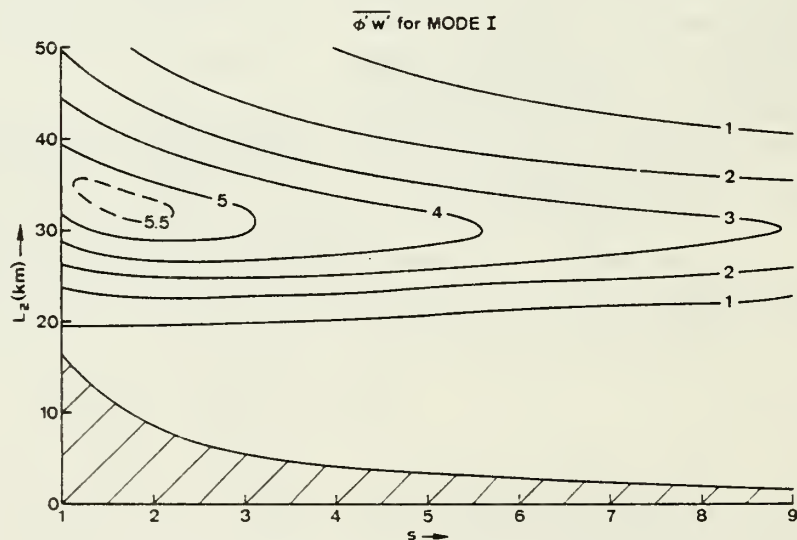
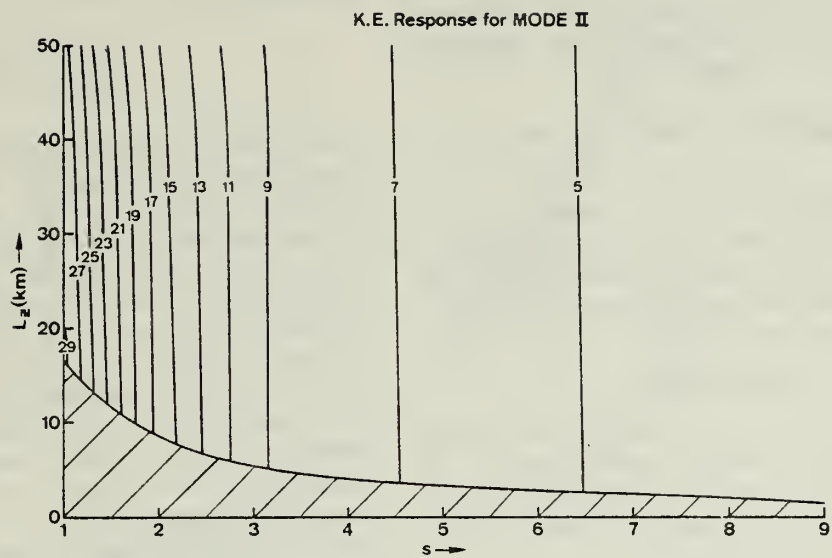


FIG. 4. Vertical wave energy flux due to pressure work at the tropopause level, $\phi'w'$, as a function of vertical wavelength L_z and zonal wavenumber s for Mode I. Units are arbitrary.



view of our result. This low-wavenumber preference for the thermally forced Kelvin wave response is related to (11) and the explanation has been given by Webster (1973) and Chang (1976).

4. Further comparison with the 40-50 day oscillation

As mentioned previously, the two solutions of (12) are separated by the curve $c_r = c_i$. Since for Mode I the inertial time scale is faster than the damping time scale, it follows that the main balance in Eq. (1) is between the first two terms, i.e.,

$$-ikcu \approx ik\phi.$$

In this case u and ϕ are in-phase and the wave is characteristic of the internal gravity waves. For Mode II the damping time scale is faster so that the main balance is between the last two terms, i.e.,

$$0 = -ik\phi - Du.$$

Thus u and ϕ have a quarter-cycle phase difference which is characteristic of a highly viscous wave motion. If we examine the schematic diagram of the 40-50 day oscillation (Fig. 1) depicted by Madden and Julian, it can be seen that, for most of the categories, u and ϕ have a phase relationship between in-phase and quarter-cycle difference. The important effect of damping is thus clearly indicated.

If the vertical scale is large, the main balance in the thermodynamic energy equation is between the adiabatic cooling and the diabatic heating. The residue is approximately balanced by the advective term for Mode I, i.e.,

$$-ikcT \approx \frac{Q}{c_p} - w\Gamma.$$

and T , w will have a quarter-cycle phase difference. For Mode II this residue is mainly balanced by the

damping term, i.e.,

$$w\Gamma - \frac{Q}{c_p} \approx DT.$$

In this case T , w will be in-phase if diabatic heating exceeds adiabatic cooling and half-cycle out-of-phase if adiabatic cooling dominates over diabatic heating. In Madden and Julian's (1972) observational study they found that the surface pressure is half-cycle out-of-phase with the 300 mb temperature and in-phase with the 100 mb temperature. Since vertical motion is close to in-phase with surface pressure as shown by Fig. 1, it may be inferred that T and w are in-phase at 300 mb and half-cycle out-of-phase at 100 mb. The former level is in the upper troposphere where diabatic heating must dominate for the motion to be self-sustaining, while the latter level is near the tropopause where the diabatic heating vanishes but the vertical motion may overshoot through the cloud top. The thermal structure of the 40-50 day oscillation thus also appears to be consistent with the viscous theory.

When damping is included, the meridional structure of the Kelvin waves as expressed by (6) contains a tilt of the wave axis because \hat{c} is complex, i.e.,

$$\begin{aligned} \exp\left(-\frac{\beta y^2}{2\hat{c}}\right) &= \exp\left(-\frac{\beta}{2} \frac{c_r}{c_r^2 + c_i^2} y^2\right) \exp\left(i \frac{\beta}{2} \frac{c_i}{c_r^2 + c_i^2} y^2\right) \\ &= \exp\left(-\frac{\beta \lambda_r}{2 S^{\frac{1}{2}}} y^2\right) \exp\left(i \frac{\beta \lambda_r c_i}{2 S^{\frac{1}{2}} c_r} y^2\right). \end{aligned} \quad (18)$$

Here the first part of the right-hand side gives a Gaussian distribution in the meridional direction with a Gaussian folding with y_G given by

$$y_G = \left(\frac{2 S^{\frac{1}{2}}}{\beta \lambda_r}\right)^{\frac{1}{2}} = \left(\frac{2}{-\beta c_r |D=0|}\right)^{\frac{1}{2}}.$$

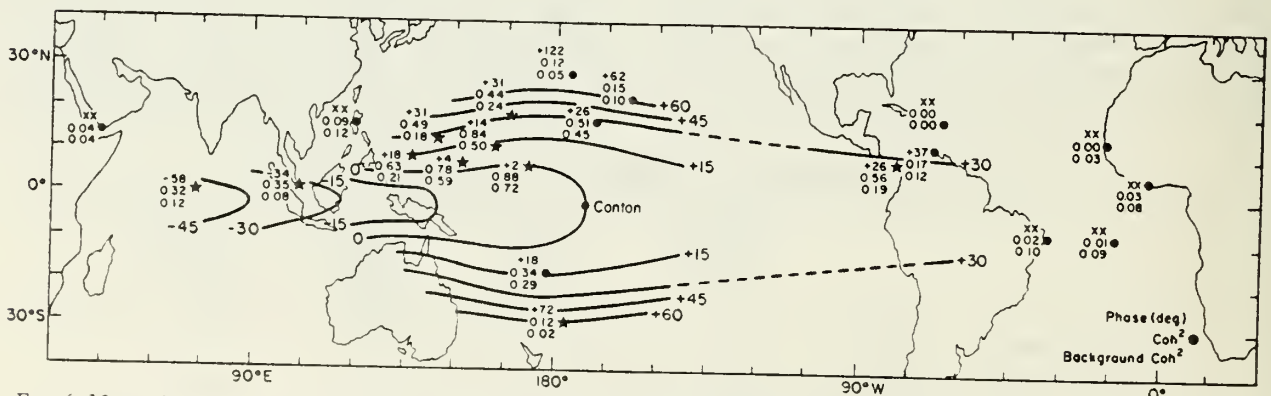


FIG. 6. Mean phase angles, coherence-squares and background coherence-squares for approximately the 36-50 day period range of cross spectra between all stations and Canton. The plotting model is given in lower right-hand corner. Positive phase angles at a station means the Canton series leads that of the station. Stations indicated by a star have coherence-squares above the background at the 95% level. Mean coherence-squares at Shemya (52°43'N, 174°6'E) and Campbell I. (52°33'S, 169°9'E) [not shown] are 0.08 and 0.02, respectively. Both are below their average background coherence-squares. (From Madden and Julian, 1972.)

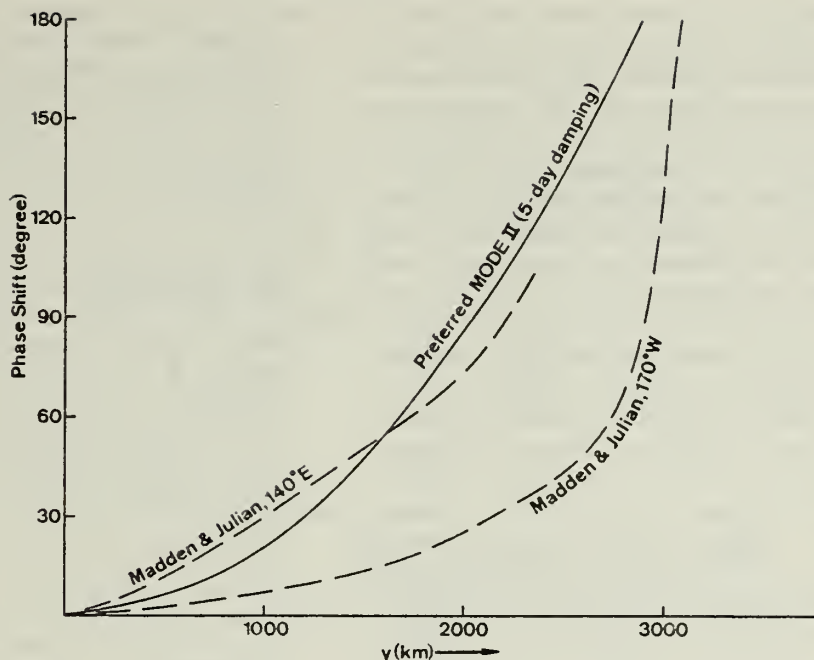


FIG. 7. Comparison of the meridional phase tilt of the 40–50 day oscillation at 140°E , 170°N , observed by Madden and Julian (1972), and the value of the most efficient Mode II response predicted by the viscous theory.

This meridional trapping scale is identical for both the regular and the viscous modes for a given vertical wavelength. In the case of the most efficient Mode II response discussed in the previous section, $|\gamma_0| = 1500$ km and agrees quite well with the observed 40–50 day oscillation. The second part of the right-hand side of (18) gives rise to a periodic variation of the waves in y^2 , and therefore a meridional tilt of the wave axis. It also implies a poleward phase propagation for the Kelvin waves because $c_r > 0$, $c_i > 0$ and $\lambda_r > 0$.

A strong meridional tilt was found by Madden and Julian for the 40–50 day oscillation using cross-spectral analysis of the surface pressure data. Their phase diagram, constructed by using the Canton Island series as the base series, is reproduced here in Fig. 6. Although the meridional phase tilt seems to vary in different geographical locations, near Canton Island and near the equator the tilt is primarily NW–SE north of the equator and NE–SW south of the equator. For eastward propagating waves this indicates a poleward phase propagation. In Fig. 7 the phase tilt of the 40–50 day oscillation deduced from Fig. 6 at two different longitudes, 170°W (near Canton Island) and 140°E (active convection area in Indonesia), are plotted along with that given by the viscous theory. Within the limitation of our simple theory and the approximations invoked, the theoretical result can be considered as fairly good in simulating the observed phase tilts.

5. Concluding remarks

We have shown that the inclusion of a damping term can result in two types of dispersive relationships for the forced Kelvin waves. The first type (Mode I) is characteristic of the regular internal gravity waves which propagate rapidly in the zonal direction and attenuate slowly in the vertical. The second type (Mode II) is dominated by the viscous damping time scale and has slower zonal phase speed and faster vertical attenuation. This viscous mode reduces to a trivial solution in the inviscid limit so its existence is supported only by damping. Assuming that the main thermal sources in the tropics are confined to the troposphere and have a red noise distribution which enhances the response of the viscous mode, this theory predicts that the stratospheric waves behave like the regular mode and the tropospheric waves behave like the viscous mode. Our theory includes features that are consistent with several results found by previous theoretical or numerical studies of the equatorial waves that incorporate the damping mechanism. Lindzen (1971) and Holton and Lindzen (1972) found that as a wave is propagating in weak vertical wind shear, the efficiency of damping would change inversely according to the change of the Doppler-shifted phase speed. This is consistent with our result that the slower moving waves are more trapped in the vertical. In a numerical diagnostic model of the Kelvin waves, Holton (1973) observed a maximum response in the tropospheric wavenumber 1 spectrum with period > 30 days. This response

seems to correspond to our viscous mode. Very recently Stevens *et al.* (1977) reported that with a parameterization of the cumulus damping, the tropical waves have very little vertical structure. This is again explainable by our theory because the vertical wavelength is increased as a result of damping.

In real atmosphere the damping due to cumulus convection and other processes is much more complicated than the simple linear drag term used in our analysis. However, the agreement with observed zonal wind oscillations such as the stratospheric Kelvin waves, the 40–50 day oscillations, and the stationary monsoon and Walker circulations strongly indicate that our theoretical interpretation is quite relevant to these oscillations. In addition, although the present analysis is limited to Kelvin waves only, the vertical structure equation applies to all equatorial waves. Hence it would be quite possible that the general result also applies to other thermally controlled tropical wave disturbances. This is particularly interesting in view of the large vertical scale and slow Doppler-shifted phase speed usually observed in the tropical tropospheric waves such as the easterly waves. In a discussion of the present results, Wallace (personal communication) suggested that they would also explain the seemingly non-dispersive westward propagation of the synoptic-scale cloud clusters observed in the time sections of tropical satellite pictures (Chang, 1970). In these sections the propagating cloud patterns have quite uniform phase speeds but the apparent wavelength varies over a large range. This non-dispersive character led Wallace (1972) to propose that, despite the strong vertical and longitudinal variations of the basic flow, they are more likely a result of advection by basic flow than a manifestation of some kind of Rossby waves. He argued that the difficulty of ascertaining a steering level is not as severe as that of explaining why the beta-effect does not produce dispersive phase speeds. However, to interpret these patterns as being passive cloud masses advected by the basic flow is also unsatisfactory due to the fact that they are frequently observed to be associated with active convections and that they sometimes decay and regenerate during the course of propagation. These difficulties are partially alleviated in the framework of the present theory because the viscous mode should have a much smaller Doppler-shifted phase speed and would appear as if they are advected by the basic easterly current at some levels.

Acknowledgments. The author wishes to thank Professors J. R. Holton, P. J. Webster and J. M. Wallace for discussion and Professors R. T. Williams and G. J. Haltiner for reading the manuscript. This work was supported by the Atmosphere Research Section, National Science Foundation, under Grant DES 75-10719.

REFERENCES

- Bjerknes, J., 1969: Atmospheric teleconnections from the equatorial Pacific. *Mon. Wea. Rev.*, **97**, 163–172.
- Chang, C.-P., 1970: Westward propagating cloud patterns in the tropical Pacific as seen from time-composite satellite photographs. *J. Atmos. Sci.*, **27**, 133–138.
- , 1976: Forcing of stratospheric Kelvin waves by tropospheric heat sources. *J. Atmos. Sci.*, **33**, 740–744.
- , F. T. Jacobs and B. B. Edwards, 1975: A diagnostic model for estimating large-scale flow patterns in the tropical upper troposphere from satellite cloud brightness data. *Mon. Wea. Rev.*, **103**, 536–549.
- Chu, J.-H., 1976: Vorticity in maritime cumulus clouds and its effects on the large-scale budget of vorticity in the tropics. Ph.D. thesis, University of California, Los Angeles, 123 pp.
- Egger, J., 1976: The linear response of the atmosphere to sea surface temperature anomalies in the tropical Pacific. Paper presented at the JOC Study Conference on Numerical Modelling for the Tropics, Exeter, England. [Available from Meteorologisches Institut, Der Universität, München, Theresienstrasse 37, D8000 München 2, FRG.]
- Green, J. S. A., 1965: Atmospheric tidal oscillations: An analysis of the mechanics. *Proc. Roy. Soc. London*, **A288**, 564–574.
- Holton, J. R., 1973: On the frequency distributions of atmospheric Kelvin waves. *J. Atmos. Sci.*, **30**, 499–501.
- , and D. E. Colton, 1972: A diagnostic study of the vorticity balance at 200 mb in the tropics during the northern summer. *J. Atmos. Sci.*, **29**, 1124–1128.
- , and R. S. Lindzen, 1968: A note on “Kelvin” waves in the atmosphere. *Mon. Wea. Rev.*, **96**, 385–386.
- , and —, 1972: An updated theory for the quasi-biennial cycle of the tropical stratosphere. *J. Atmos. Sci.*, **29**, 1076–1080.
- Krishnamurti, T. N., Kanamitsu, W. J. Koss and J. D. Lee, 1973: Tropical east-west circulations during the northern winter. *J. Atmos. Sci.*, **30**, 780–787.
- Lindzen, R. S., 1966: On the relation of wave behavior to source strength and distribution in a propagating medium. *J. Atmos. Sci.*, **23**, 630–632.
- , 1967: Planetary waves on beta planes. *Mon. Wea. Rev.*, **95**, 441–451.
- , 1971: Equatorial planetary waves in shear: Part I. *J. Atmos. Sci.*, **28**, 609–622.
- Madden, R. A., and P. R. Julian, 1971: Detection of a 40–50 day oscillation in the zonal wind in the tropical Pacific. *J. Atmos. Sci.*, **28**, 702–708.
- , and —, 1972: Description of global-scale circulation cells in the tropics with a 40–50 day period. *J. Atmos. Sci.*, **29**, 1109–1123.
- Reed, R. J., and R. H. Johnson, 1974: The vorticity budget of synoptic-scale wave disturbances in the tropical western Pacific. *J. Atmos. Sci.*, **31**, 1784–1790.
- , and E. E. Recker, 1971: Structure and properties of synoptic-scale waves in the equatorial western Pacific. *J. Atmos. Sci.*, **28**, 1117–1133.
- Stevens, D. E., R. S. Lindzen and L. Shapiro, 1977: A new model of tropical waves incorporating momentum mixing. Submitted to *Dynamics of Atmospheres and Oceans*.
- Wallace, J. M., 1972: On the general circulation of the tropics. Dynamics of the tropical atmosphere. NCAR Summer Colloquium Notes, 192–193. [Available from Advanced Study Program, NCAR.]
- , and V. E. Kousky, 1968: Observational evidence of Kelvin waves in tropical stratosphere. *J. Atmos. Sci.*, **25**, 900–907.
- Webster, P. J., 1972: Response of the tropical atmosphere to local steady forcing. *Mon. Wea. Rev.*, **100**, 518–541.
- , 1973: Temporal variation of low-latitude zonal circulations. *Mon. Wea. Rev.*, **101**, 803–816.
- Williams, K. T., and W. M. Gray, 1973: Statistical analysis of satellite-observed trade wind cloud clusters in the western North Pacific. *Tellus*, **25**, 313–336.
- Yanai, M., and T. Maruyama, 1966: Stratospheric wave disturbance propagating over the equatorial Pacific. *J. Meteor. Soc. Japan*, **44**, 291–294.

Reprint from the Review
PURE AND APPLIED GEOPHYSICS (PAGEOPH)
Formerly 'Geofisica pura e applicata'

Vol. 115, 5/6 (1977)

Pages 1089-1109

Some Theoretical Problems
of the Planetary-Scale Monsoons

by

Chih-Pei Chang



BIRKHÄUSER VERLAG BASEL

Some Theoretical Problems of the Planetary-Scale Monsoons

By CHIH-PEI CHANG¹⁾

Summary - Some important theoretical problems of the planetary-scale monsoons which have arisen from recent advances of observational studies are reviewed. These include: (1) the requirement of a strong damping mechanism in the planetary scale vorticity budget of summer monsoon and a similar but weaker requirement for the winter monsoon; (2) the localized barotropic instability of the summer monsoon which is a result of the strong zonal asymmetry of the planetary-scale flow and causes significant nonlinear energy conversions; and (3) the oscillations of the planetary-scale monsoons. It is pointed out that these problems are inter-related and their understanding is also important for the proper simulation of other scales of motion of the monsoon circulation.

Key words: Monsoon; Oscillation; vorticity budget; Barotropic instability.

1. Introduction

The monsoon circulation of both the northern summer and the northern winter (hereafter the word 'northern' will be neglected) are characterized by large planetary scale quasi-stationary waves in the subtropics and tropics. As have been shown by KRISHNAMURTI (1971a), KRISHNAMURTI, KANAMITSU, KOSS and LEE (1973b) and others, these waves are a result of the thermally direct overturnings induced by the differential heating associated with the land-sea distribution. The major component of the heating is the convective latent heat release which is most intense over the Tibetan and Mexican highlands during summer and the maritime continent of the Malaysia-Indonesia region during winter. Mainly due to the availability of the commercial aircraft data, the principal features of these zonal asymmetries have been best depicted by the wind analyses near 200 mb by KRISHNAMURTI and ROGERS (1970), KRISHNAMURTI *et al.* (1973b) and SADLER (1975). During summer these features include a strong anticyclone centered over the Tibetan plateau, a weaker anticyclone over Mexico and elongated troughs oriented northeast-southwest in the mid-Pacific and mid-Atlantic. These are all well presented in Fig. 1 which shows the time-mean streamfunction at 200 mb for June-August 1967 as determined by KRISHNAMURTI (1971a). During winter a large streamfunction high over the equatorial South China

¹⁾ Department of Meteorology, Naval Postgraduate School, Monterey, California 93940, U.S.A.

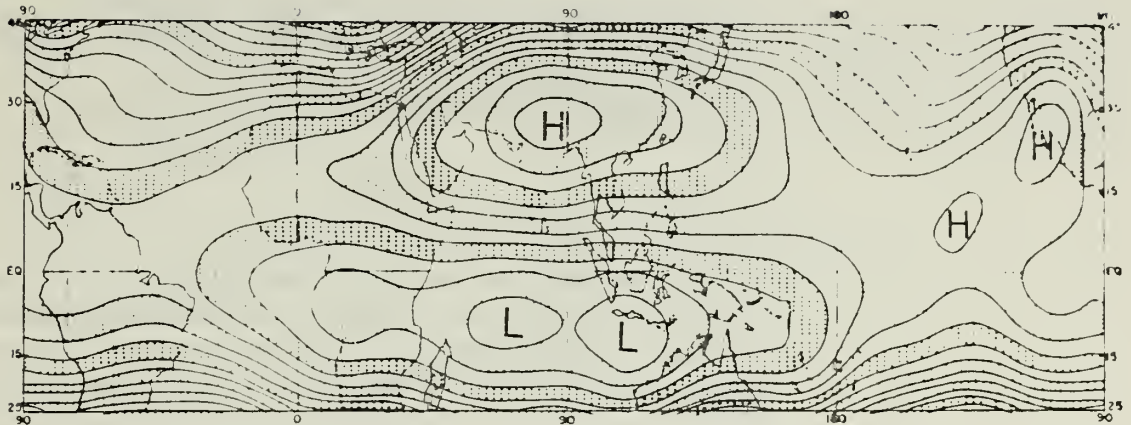


Figure 1

Summer mean (June–August 1967) 200-mb streamfunction, contour interval is $50 \times 10^5 \text{ m}^2 \text{ sec}^{-1}$. (From KRISHNAMURTI, 1971a.)

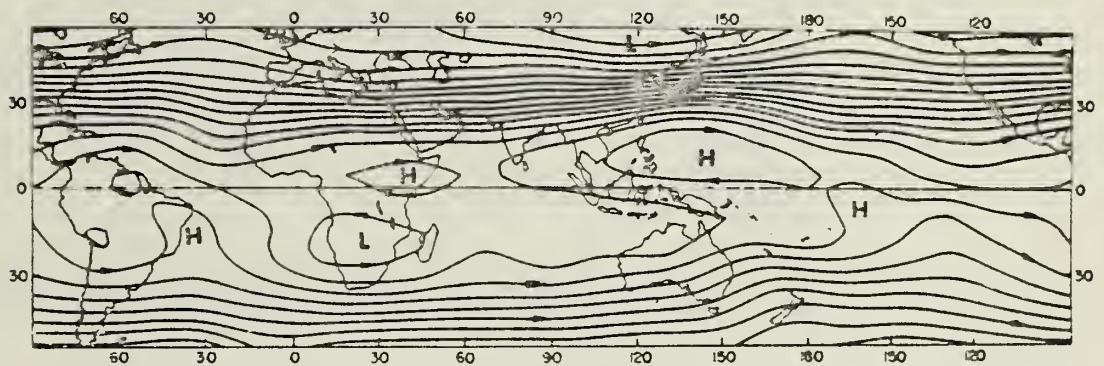


Figure 2

Winter mean (December–February 1971) 200-mb streamfunction, contour interval is $50 \times 10^5 \text{ m}^2 \text{ sec}^{-1}$. (From KRISHNAMURTI *et al.* 1973b.)

Sea and western Pacific replaces the Tibetan high to become the most pronounced planetary scale feature, with two weaker highs appearing over the equatorial eastern Africa and the northeastern South America and three oceanic troughs extending from the equator to the southern subtropics. These features are shown in Fig. 2 which is the 200 mb time-mean streamfunction for the winter of 1971 determined by KRISHNAMURTI *et al.* (1973b).

A number of interesting theoretical problems have arisen from the observed monsoon circulations. In this paper we will review some of the problems that are related to the planetary-scale monsoon. They include:

- (1) The requirement of a strong damping mechanism in the planetary scale vorticity budget.

- (2) The localized barotropic instability associated with the planetary-scale summer monsoon, and
- (3) Oscillations of the planetary-scale monsoons.

2. The requirement of a strong planetary scale damping mechanism

In a linear, one-level numerical model, HOLTON and COLTON (1972) used the barotropic vorticity equation to diagnose the budget of the seasonal-mean planetary scale vorticity at 200 mb during summer. They used the 200 mb mean divergence observed by KRISHNAMURTI (1971a, b) as the steady forcing function with a mean zonal flow also specified by the observed values. Figure 3 shows the velocity potential

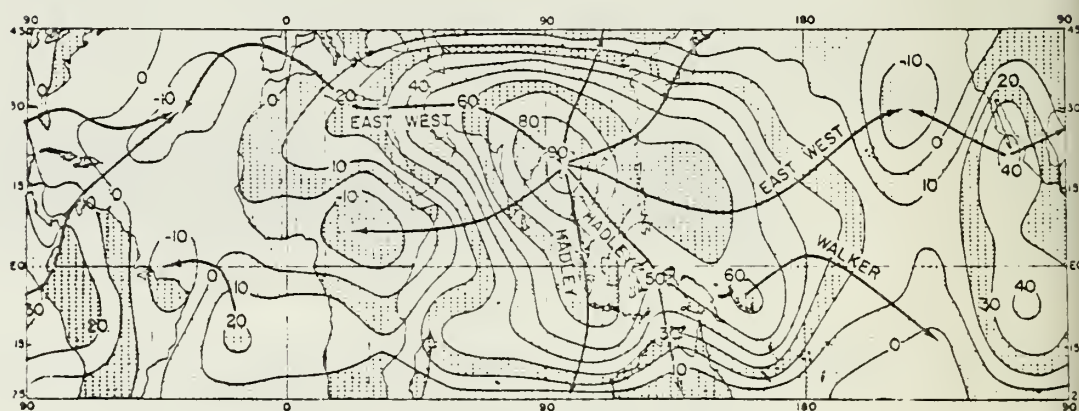


Figure 3

Summer mean (June–August 1967) 200-mb velocity potential, contour interval is $10 \times 10^5 \text{ m}^2 \text{ sec}^{-1}$. The few streamlines sketched indicate the direction of the mean divergence motions. (From KRISHNAMURTI, 1971a.)

computed by KRISHNAMURTI (1971a) which expresses the observed mean divergence field. Comparing this figure with Fig. 1, it is evident that the time-mean vorticity and divergence fields are approximately half-cycle out of phase. However, the resultant steady-state planetary scale vorticity field calculated by HOLTON and COLTON is about one-quarter cycle out of phase from the divergence field, unless a very strong damping term is added to the mean vorticity equation. This difficulty arises because, in the absence of strong damping, the main balance in the vorticity equation is between the generation by horizontal divergence and the advection by mean flow. This near-balance requires that the vorticity be one-quarter cycle out of phase from the divergence. The very efficient generation by the strong divergence also causes the amplitudes of the long waves to be significantly larger than those observed. Figure 4 (from HOLTON and COLTON, 1972) compares the diagnosed and observed amplitudes

and phases of the streamfunction for zonal wavenumber one as a function of latitude. When the linear damping coefficient is increased from a modestly strong value of $5 \times 10^{-6} \text{ sec}^{-1}$ to a very strong value of $1.5 \times 10^{-5} \text{ sec}^{-1}$, the discrepancy disappears and the phase and amplitude of the long waves become in close agreement with observations.

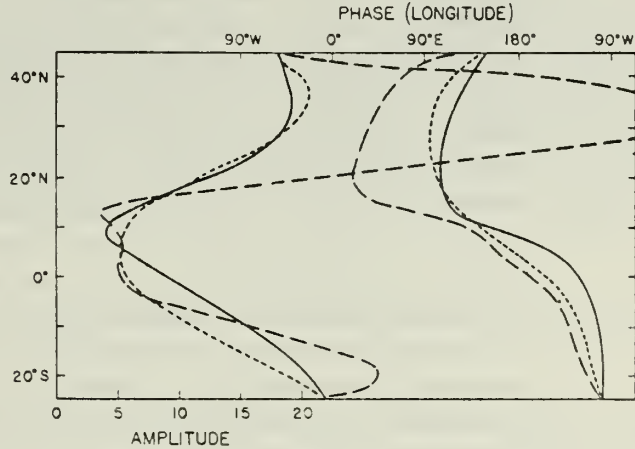


Figure 4

Amplitude in units of $10^6 \text{ m}^2 \text{ sec}^{-1}$ (left-hand curves) and phase (right-hand curves) of the streamfunction for zonal wavenumber 1 as a function of latitude. Solid curve is observed streamfunction; short and long dashes are the solutions computed by HOLTON and COLTON (1972) for damping rate of $1.5 \times 10^{-5} \text{ sec}^{-1}$ and $5 \times 10^{-6} \text{ sec}^{-1}$, respectively. (From HOLTON and COLTON, 1972.)

HOLTON and COLTON's (1972) findings suggest that a very strong sink with a damping time scale faster than 1 day is required to balance the linear vorticity budget of the seasonal-mean 200 mb planetary-scale flow during summer. This damping is much stronger than the normal dissipation process in the upper troposphere whose damping time is on the order of weeks. In looking for an explanation of this excessive damping requirement, they suggested that two possible mechanisms not included in their model may be responsible for the strong damping. The first is the vertical mixing of vorticity by cumulonimbus convection which is very strong over the Asian continent and Mexican highland during the northern summer. This mechanism has been suggested by RIEHL and PEARCE (1968), REED and RECKER (1971), WALLACE (1971), WILLIAMS and GRAY (1973) and others to balance the vorticity budget of the synoptic-scale easterly waves in the tropical troposphere. However, HOLTON and COLTON (1972) felt that it alone is still insufficient to account for the required fast damping. They then proposed the second mechanism which is related to the day-to-day fluctuations of the monsoon vorticity and divergence fields observed by KRISHNAMURTI (1971b). Considering deviations from the time mean, the complete divergence term in the time-mean vorticity equation is $\langle (\zeta + f)\delta \rangle = \langle \zeta \rangle \langle \delta \rangle + \langle \delta' \zeta' \rangle$ where ζ and f are the relative and planetary vorticities, respectively; δ is divergence and the primes are deviation from the time mean $\langle \rangle$. The last term, which was excluded in

HOLTON and COLTON's linear calculations, tends to be negative according to the observed out-of-phase correlation of the fluctuating vorticity and divergence fields. This term therefore may counteract the vorticity generation by the time-mean divergence. HOLTON and COLTON then speculated that the combination of this fluctuation correlation and the cumulus mixing mechanisms could be responsible for the less than one day damping time.

The requirement of a strong vorticity sink has also been confirmed by other numerical investigations that do not include the strong damping. As a follow up of the work of HOLTON and COLTON (1972), COLTON (1973) used a semi-spectral representation of the one-level nonlinear barotropic vorticity equation to study the scale interactions of the 200 mb summer monsoon flow forced by the observed mean divergence. As a consequence of the inclusion of only modest damping (time scale 5 days), the resultant planetary-scale waves have amplitudes considerably larger than the seasonal mean values. Westward phase shifts of 50° for the Tibetan high and 30° for the mid-Pacific trough, in comparison with the observed positions, are also produced by the model (Fig. 5). ABBOTT (1973) developed a 3-level nonlinear quasi-geostrophic hemispheric model to simulate the time-mean climatology of the summer

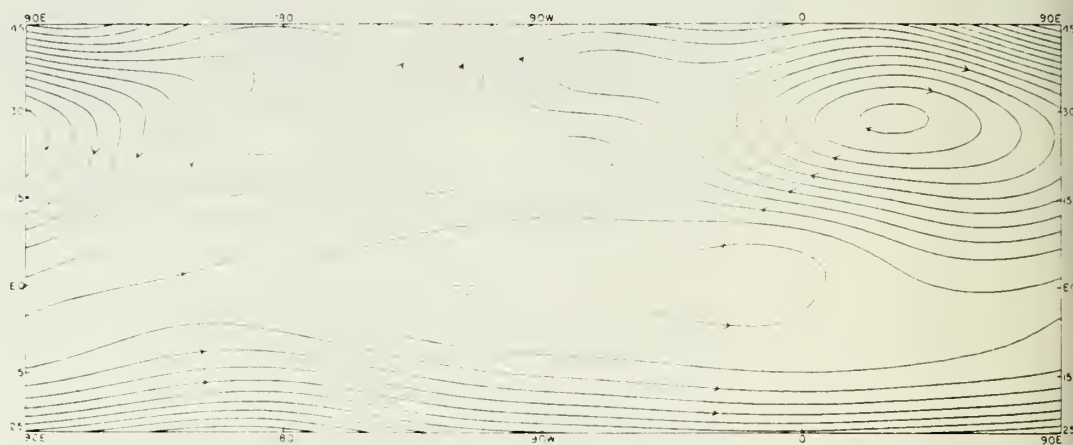


Figure 5

Streamfunction of the forced motion averaged over days 15 through 40 of the numerical integration by COLTON (1973). Contour interval is $50 \times 10^5 \text{ m}^2 \text{ sec}^{-1}$.

monsoon. To drive the monsoon circulation, he specified a steady heating distribution which was found by inverting the governing equations with the vorticity field giving by the observed time-mean values. This heating distribution (Fig. 6) in turn successfully simulates the principal features of the planetary-scale flow as well as the nonlinear energy exchanges. However, it is about a quarter cycle out of phase from that implied by the observed mean divergence field and the satellite cloud data. This apparently is also due to the absence of a strong damping mechanism in the model which forces a

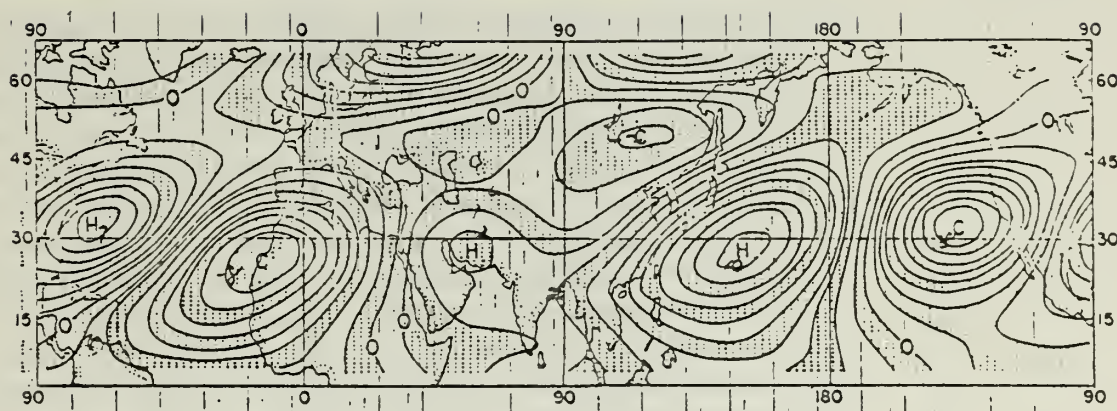


Figure 6

Time-independent horizontal distribution of the diabatic heating rate at 350 mb as computed by ABBOT (1973). Isopleths are at $5 \times 10^{-3} \text{ m}^2 \text{ sec}^{-1}$.

balance between the advection and generation of vorticity. In a 3-component semi-spectral primitive equation model, MURAKAMI (1974) also used a specified heating function to study the planetary scale monsoon flow during summer. Without the inclusion of the strong damping and allowing the specified heating to fluctuate with time, he was able to obtain the proper amplitude and phase of the long waves. However, the resultant divergence field in his model is somewhat different from that observed by KRISHNAMURTI (1971a). The greatest discrepancy occurs at 200 mb, where KRISHNAMURTI (1971a) found very strong divergence in the Tibetan high area during the 1967 summer, while in MURAKAMI's (1974) model this level is almost non-divergent. The model also produces a different horizontal distribution of long wave divergence compared to the observed 1967 distribution, with the Tibetan divergence center shifted slightly to the east and the mid-Atlantic convergence center shifted to the longitude of central Africa. Thus the magnitude of divergence forcing is much reduced and a phase shift between divergence and anticyclonic vorticity also results²). In addition, the advective effect is not properly treated because the zonal mean flow is not allowed to interact with the three interacting long waves. Hence it is unclear what is the main mechanism that produces the correct amplitude and phase of the vorticity field.

Looking for alternative sources for the strong damping, BARCILON and COOPER (1974) hypothesized that a thermal boundary layer effect could operate in the atmosphere during summer monsoon. In their simple analytical model a sinusoidal temperature variation is applied at the lower boundary which provides the planetary scale differential heating. A number of solutions were found for a balance between

²) However, MURAKAMI (personal communication) found that this horizontal distribution of divergence is in good agreement with the 1970 summer data.

the horizontal advection and vertical diffusion of heat in the thermodynamic energy equation, and one of them allows a half-cycle out of phase shift between the upper level vorticity and divergence. However, since the monsoonal differential heating in the real atmosphere is mainly due to the latent heat release of cumulus convection which is maximum in the middle-upper troposphere, it is uncertain whether BARCILON and COOPER's (1974) theory is completely applicable to the real atmosphere.

Another explanation for the observed vorticity-divergence phase relationship was offered by PAEGLE and PAEGLE (1976). They speculated that a high pressure region with strong pressure gradients may cause the geostrophic vorticity to become less than one-half of the negative planetary vorticity. This implies that the balance equation becomes non-elliptic and, under certain rather strong assumptions, leads to a rapid vorticity adjustment with strong horizontal divergence occurring in the negative relative vorticity region. However, the resultant steady-state absolute vorticity vanishes and this efficiently eliminates the generation of vorticity by divergence. Such large negative values of relative vorticity are not observed in the large-scale monsoon flow. In fact the minimum seasonal mean relative vorticity at 200 mb during the 1967 summer as observed by KRISHNAMURTI is $\sim -3 \times 10^{-5} \text{ sec}^{-1}$, which occurs in the vicinity of the Tibetan and Mexican highs near 30°N . This magnitude is considerably smaller than that of the Coriolis parameter. Thus it appears unlikely that this super-gradient effect is relevant to the planetary-scale monsoon problem.

To test the hypotheses proposed by HOLTON and COLTON (1972), CHANG and PENTIMONTI (1977) used a 3-level primitive equation model with a 4° finite-difference resolution in both the zonal and meridional directions. The zonal mean flow is included using a Newtonian term which maintains the proper north-south temperature gradient by continuously adjusting each temperature toward a thermal equilibrium determined by the zonally symmetric climatology. The zonally asymmetric motions are generated by a specified perturbation heating function whose horizontal distribution follows that of the 200 mb seasonal mean divergence observed by KRISHNAMURTI (1971b). It turns out that this heating distribution almost reproduces the observed mean divergence in the upper troposphere, which suggests that the choice of the forcing function is proper. Two experiments were carried out by integrating the model in time until 25 days after it reached the respective steady states. Both experiments include only weak damping (time scale > 7 days) in the free atmosphere but the heating function was held steady only in the first experiment and allowed to fluctuate in time with an amplitude equal to one-half of the time-mean heating in the second experiment. The fluctuation period was set to 10 days. Comparing the results of the two experiments, CHANG and PENTIMONTI found essentially no difference between the time-mean planetary scale fields except a slightly reduced amplitude for the fluctuating case. Figure 7 is their time-mean wind field at 250 mb (near the upper level of the model) for the fluctuating heating case. It can be seen that the simulated Tibetan and Mexican anticyclones are shifted about 30° and 25° , respectively, from the observed positions. These phase shifts are almost identical to those produced by

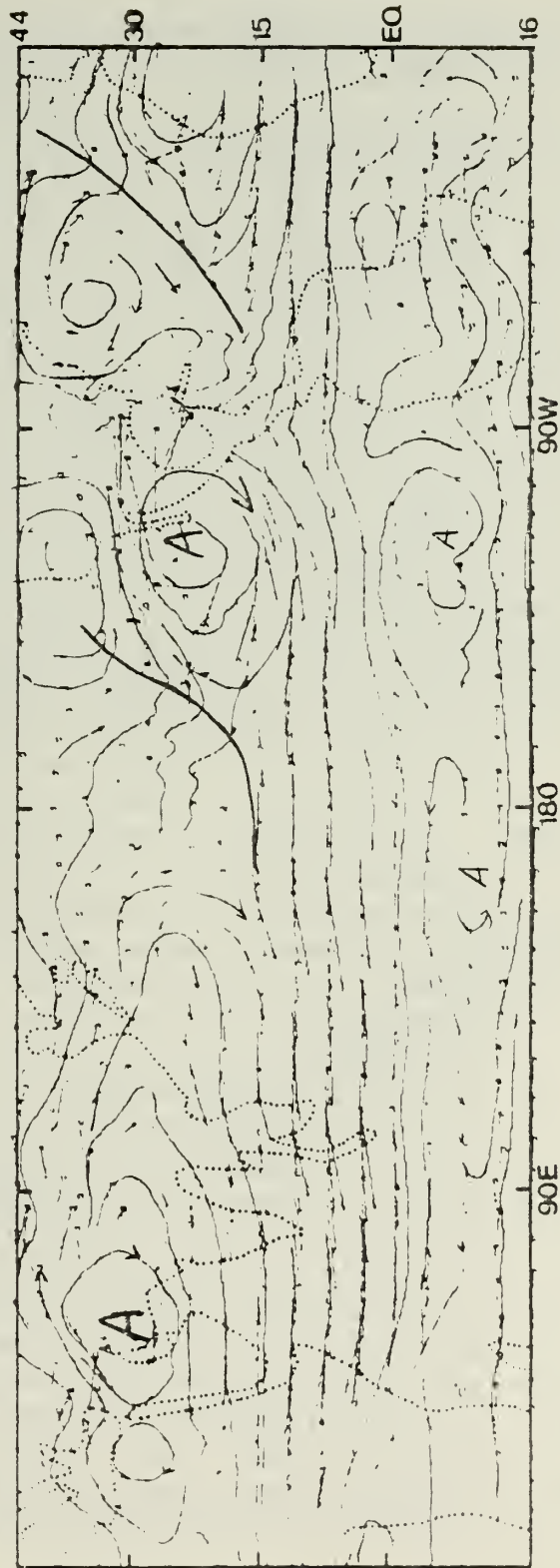


Figure 7
Time mean wind field at 250 mb forced by a fluctuating heating function as computed by CHANG and
PENTIMONII (1977)

their steady-heating case. Thus the fluctuating component as specified in the model is almost inconsequential in providing the damping needed for the phase shift problem. On the other hand, in both experiments the amplitudes of the long waves are not excessively large compared to observations. This result is similar to that of ABBOTT (1973) and seems to suggest that nonlinear processes could be responsible for part of the planetary-scale vorticity sink deduced by HOLTON and COLTON's linear calculations. The fluctuation of the planetary-scale flow apparently enhances these nonlinear conversions resulting in the further reduction of its time-mean amplitude.

A noteworthy feature in CHANG and PENTIMONTI's (1977) time-mean fields is that the positions of the upper tropospheric mid-oceanic troughs do not have significant phase errors as those of the anticyclones. As pointed out by KRISHNAMURTI, DAGGUPATY, FEIN, KANAMITSU and LEE (1973a), the damping due to cumulus transports should not operate over the relatively cloud-free oceanic areas. With the inclusion of nonlinear processes (and also large-scale vertical advections), the damping requirement implied by the phase errors of CHANG and PENTIMONTI's time-mean upper level anticyclones is weaker than that found by HOLTON and COLTON (1972). Perhaps a damping time longer than 1 day, which seems more reasonable than HOLTON and COLTON's value if interpreted as due to the cumulus transports, may be sufficient. In this case a numerical experiment similar to CHANG and PENTIMONTI's, but incorporating a moderately strong damping term with time scale order of a few days in the continental convective area only, may provide some insight as to whether cumulus transport processes are responsible for the missing vorticity sink.

The studies mentioned above all concern the summer monsoon only. During winter KRISHNAMURTI *et al.* (1973b) observed that the rotational component of the seasonal-mean flow of the active monsoon region is almost one order smaller than that of the summer monsoon, while the divergent component has a comparable magnitude. The reason for this appears to be the proximity of the winter monsoon convections to the equator, which reduces the efficiency of vorticity generation by horizontal divergence. However, the importance of a dissipation mechanism in the winter monsoon was also brought out in a few theoretical studies recently. In a linear study of the stationary forcing in the tropical atmosphere, WEBSTER (1972, 1973) found that the primary response in the equatorial region corresponds to the atmospheric Kelvin waves (HOLTON and LINDZEN, 1968). A theoretical calculation shows that the zonal wavelength of this Kelvin wave response is very long while its vertical wavelength is very short [$O(1 \text{ km})$]. The former agrees quite well with observed equatorial stationary circulations such as the winter monsoon, but the latter is one order of magnitude shorter than the observed vertical wavelengths. This discrepancy arises because the equatorial Kelvin waves behave like internal gravity waves in the zonal-vertical plane and their phase speed, c , is related to an equivalent depth scale h by the relationship $c = (gh)^{1/2}$. These stationary waves are imbedded in a mean easterly zonal current so that they have a Doppler-shifted phase speed of a few meters per second, which implies a very short vertical wavelength. To get around this problem

in simulating the observed stationary motions, WEBSTER (1972, 1973) adopted a two level numerical model with friction which is quite successful in reproducing many of the observed features.

Very recently CHANG (1977) re-examined this problem by incorporating linear damping terms in the thermally forced Kelvin wave equations. The dispersive relationship of the Kelvin waves may be written as $c\lambda = S^{1/2}$, where λ is the vertical wavenumber and S is a static stability parameter. The linear damping introduces an imaginary part to c which causes λ to become complex also. Consequently the dispersive relationship becomes quadratic and has two types of solutions. The first type arises when the inertial time scale is faster than the damping time scale. This solution resembles the regular internal gravity waves whose vertical wavelength decreases as the Doppler-shifted phase speed decreases. The second type, called the viscous mode by CHANG (1977), arises when the damping time scale dominates over the inertial time scale and its vertical wavelength increases as the Doppler phase speed decreases (Fig. 8). This solution is also much more trapped in the vertical so that it has appreciable amplitude only in the region of thermal forcing (troposphere). In the inviscid limit this solution reduces to a trivial solution with vanishing amplitude. For a reasonable range of physical parameters, CHANG (1977) calculated a vertical wavelength of > 17 kms for the stationary response, which is a significant improvement over the inviscid theory. The horizontal structure of this solution is also in good

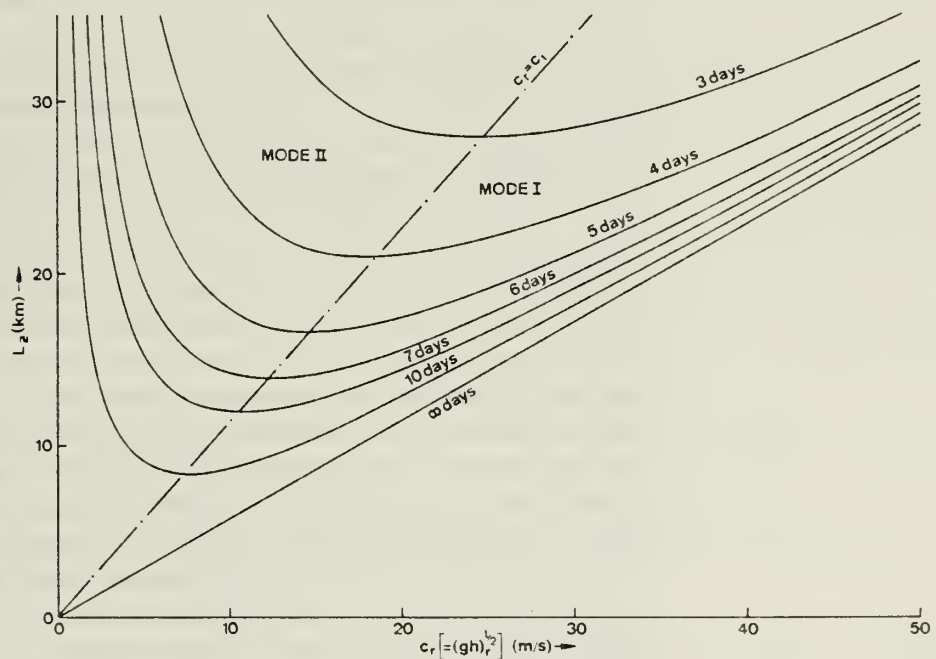


Figure 8

Real Doppler-shifted phase speed, c_r , as a function of vertical wavelength, L_z , and damping time for the Kelvin waves. (From CHANG, 1977.)

agreement with observations and WEBSTER's (1972, 1973) numerical model. This requirement of a damping mechanism with time scale on the order of 5 days is much weaker than that found by HOLTON and COLTON (1972) for the summer monsoon and could well be explained by cumulus transports. Detailed observational studies of the winter monsoon are needed to improve the theoretical understanding of this problem.

3. *Localized barotropic instability of the planetary scale summer monsoon*

As mentioned previously, the amplitude of stationary long waves during summer is better simulated by the nonlinear models than by the linear models when excessively large damping is excluded. This apparently is due to the barotropic energy conversions from planetary to both zonal and synoptic scales which are allowed in the nonlinear models only. Observational evidence of this type of energy conversion has been presented by KANAMITSU, KRISHNAMURTI and DEPRADINE (1972), who computed the wave-zonal flow and wave-wave energy exchanges for the tropical belt from 15°S to 15°N using the 1967 summer 200 mb wind data analyzed by KRISHNAMURTI and ROGERS (1970). In particular, they showed that the synoptic scale waves receive kinetic energy at a fairly significant rate (order of $10^{-5} \text{ m}^2 \text{ sec}^{-3}$) from both the zonal flow and the planetary-scale waves. A similar result for the equator to 30°N belt was also obtained by KRISHNAMURTI *et al.* (1973b).

Transient synoptic-scale wave disturbances have been observed in the tropical upper troposphere in all seasons. During summer, the most active season, the disturbances are found to occur primarily in two types of regions. One type is in the vicinity of the mid-oceanic troughs (RICK, 1959; SADLER, 1967; MILLER and CARLSON, 1970; FRANK, 1970) where the disturbances may assume the form of open waves or closed vortices. Occasionally these disturbances may develop in the vertical or be coupled with low level waves, and intensification leading to tropical cyclone development sometimes may also follow. Another region of transient wave activity is along the upper tropospheric easterly jet over the Indian ocean, where KRISHNAMURTI and ROGERS (1970) have reported fairly regular occurrences of synoptic-scale disturbances. Apparently these regions are where most of the barotropic energy conversion from zonal and planetary scales to the synoptic scale takes place. Thus it appears that the nonlinear energy transfers of the summer monsoon have a persistently localized nature. Another evidence of this is related to the linear barotropic instability criterion, which has been shown by MERILEES (1968) to be usually satisfied if nonlinear energy exchanges are very prominent. The upper tropospheric zonal mean flow of the summer monsoon does not satisfy this criterion, but regions of large negative gradients of relative vorticity (Fig. 9) where this instability criterion is satisfied locally can be found in the seasonal mean 200 mb analysis (KRISHNAMURTI, 1971b). These negative vorticity gradients occur mainly in the vicinity of the easterly jet and

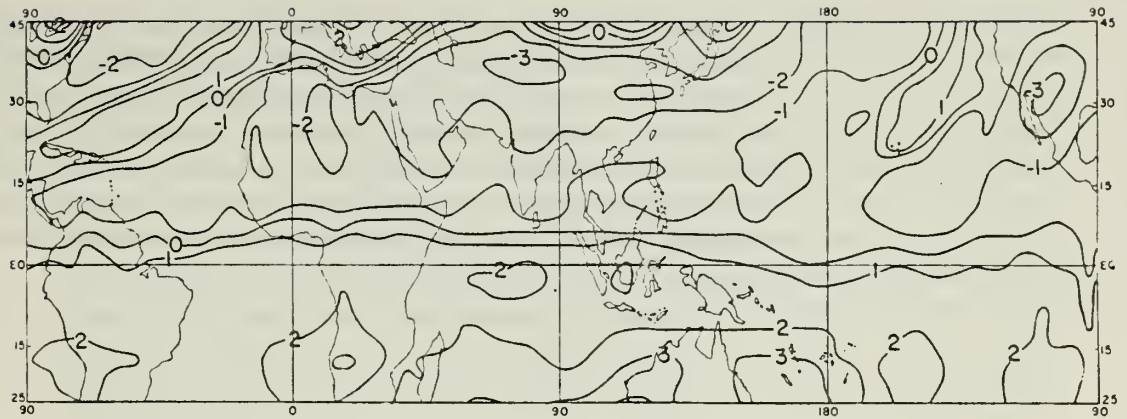


Figure 9

Summer mean (June–August 1967) relative vorticity at 200 mb, contour interval is 10^{-5} sec^{-1} . (From KRISHNAMURTI, 1971b.)

the mid-oceanic troughs, and on some individual days their magnitude may even greatly exceed the seasonal mean values. Therefore it is plausible that at least some of the transient synoptic wave activities in these regions is generated by the localized (and sometimes short term) barotropic instability, which is clearly a result of the zonal asymmetry of the planetary-scale summer monsoon.

The kinetic energy conversions from the planetary scale and the zonal flow to the synoptic scale in the upper troposphere have been simulated numerically by ABBOTT (1973) and KRISHNAMURTI *et al.* (1973a). The conversions produced by ABBOTT's (1973) model are roughly of the same order of magnitude as those computed by KANAMITSU *et al.* (1972). However, the conversions obtained by KRISHNAMURTI *et al.* (1973a) are about one order smaller. This appears to be related to their treatment of the Tibetan high as a fixed barrier which prevents vorticity transport across the boundary of the barrier. As a consequence, barotropic instability cannot be realized in the immediate vicinity of the Tibetan high and the total amount of energy extracted from the larger scales by the synoptic scale within a fixed period of time must be greatly reduced. Nevertheless, KRISHNAMURTI *et al.* (1973a) were able to simulate the gross features of the planetary scale waves in the upper troposphere, such as the mid-oceanic troughs and the Mexican high. Apparently once the strength, shape and position of the Tibetan high are fixed in the experiment, the interaction of the zonal mean flow and this blocking high is sufficient to produce mechanically many other features of the circulation.

In the numerical model by COLTON (1973), attention is focused on the development of the synoptic-scale disturbances in the easterly jet and in the mid-Pacific trough regions where the barotropic instability criterion is locally satisfied. Near the easterly jet the model produces disturbances that propagate westward at a phase speed slightly less than the local speed of the jet and continue to grow until they are well past the

longitude of the jet maximum. After reaching the maximum amplitude they begin to decay fairly rapidly. Many features of these disturbances resemble those analyzed by KRISHNAMURTI and ROGERS (1970) in the Indian Ocean and African region. In the mid-Pacific trough the model also produces waves and vortices whose movement and behavior are quite similar to those observed in daily synoptic charts. In both regions the growing disturbances exhibit a latitudinal tilt in opposition to the lateral shear of the quasi-steady basic flow, which is characteristic of the barotropically unstable waves.

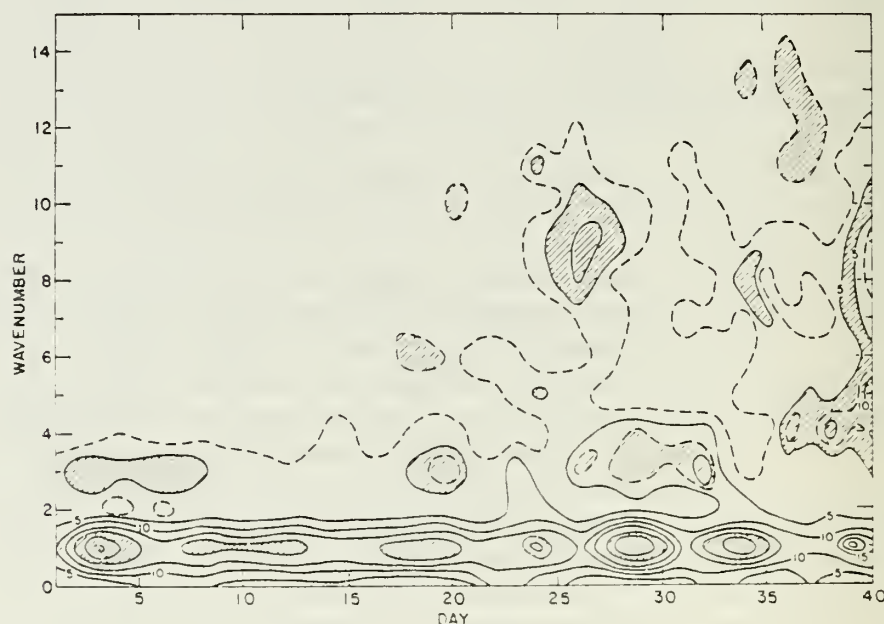


Figure 10

Zonal average kinetic energy at 20°N as a function of time and wavenumber as computed by COLTON (1973). Contour interval is $5 \text{ m}^2 \text{ sec}^{-2}$. Hatched areas are regions of energy maximum.

In studying the barotropic energy exchanges, COLTON (1973) also examined the time evolution of the computed kinetic energy spectrum. An example of this is given in Fig. 10 which shows the zonally averaged energy at 20°N as a function of time and wavenumber. A noteworthy feature is that when the energy of wavenumber 1 is at a maximum, the energy at the short waves is usually at a minimum, and vice versa. This suggests that energy exchanges take place continuously between the forced long waves and the transient disturbances. The disturbances remove energy from the planetary scale during the growing stage and feed energy back into the planetary scale during the decaying stage. As a consequence the amplitude of the time mean planetary-scale waves is smaller than that produced by a linear model. Since no dissipation is provided for the transient waves all energy extracted from the forced motion must either remain in the transient waves or be transferred back to the forced motion. COLTON

(1973) speculated that the actual damping of the planetary scale by the local barotropic instability may be more effective if some dissipation mechanism for the transient synoptic waves is included.

Although COLTON's (1973) model lacks a sufficient damping mechanism and therefore produces a basic flow that is somewhat too intense and has a phase shift problem, it nevertheless illustrates the interesting phenomenon of waves developing and decaying in a spatially varying basic flow which contains locally unstable and stable regimes. To gain further physical insight into this phenomenon, especially with respect to the easterly jet of the summer monsoon, TUPAZ, WILLIAMS and CHANG (1977) formulated a 1-level numerical model using the barotropic vorticity equation to study this problem from a linear instability point of view. In their model the basic zonal wind is approximated by a steady easterly Bickley (hyperbolic-secant-squared) jet which increases slowly from the inflow (eastern) boundary to a longitude in the middle of a rectangular domain, then decreases slowly downstream towards the outflow (western) boundary. The basic meridional wind is derived in such a way that the total basic flow is non-divergent. Periodic forcing is introduced on the inflow boundary and a radiation condition, whereby a wave is allowed to propagate its energy out of the domain, is applied at the outflow boundary. The model is integrated from zero interior perturbation streamfunction until the perturbation fields vary periodically in time at each grid point. At this quasi-steady state the waves move through the region and grow or decay in space only, in reaction to the local stability properties of the basic flow.

To compare the numerical results with the 'local growth rate' concept of the parallel flow theory, TUPAZ *et al.* (1977) developed a simple analytical model to calculate the effects of the local instabilities. This is done by considering an equation that allows for propagation and growth or decay, $\psi'_t + c(x)\psi'_x = n(x)\psi'$, where t is time, x the zonal coordinate, and ψ' the perturbation streamfunction. The local phase speed c and local growth rate n can be obtained from the parallel flow theory. When a periodic solution with a frequency ω and an amplitude $F(x)$ is introduced, the downstream variation of F with respect to a reference point x_0 may be written as

$$F(x) = F(x_0) \exp \left[-i \int_{x_0}^x \omega \, dx/c(x) \right] \exp \left[\int_{x_0}^x n(x) \, dx/c(x) \right].$$

In this equation the local wavelength is ω/c and the local spatial growth rate is n/c . Figure 11 compares the steady state envelope for ψ' of the numerical solution and the corresponding $F(x)$ for a case in which the central speed of the easterly jet is increased from 15 m sec^{-1} at $x = -10\,000 \text{ km}$ to 30 m sec^{-1} at $x = 0$ and then reduced to 15 m sec^{-1} at $x = 10\,000 \text{ km}$. The curve for $F(x)$ can be shifted up or down in the diagram by changing x_0 , but its shape does not change. Two $F(x)$ curves are included in Fig. 11, one for $x_0 = 280 \text{ km}$ and the other for $x_0 = 4200 \text{ km}$, both based on the local wavelength distribution measured from the numerical solution. It is evident from this figure that both the numerical solution and the local growth rate of the

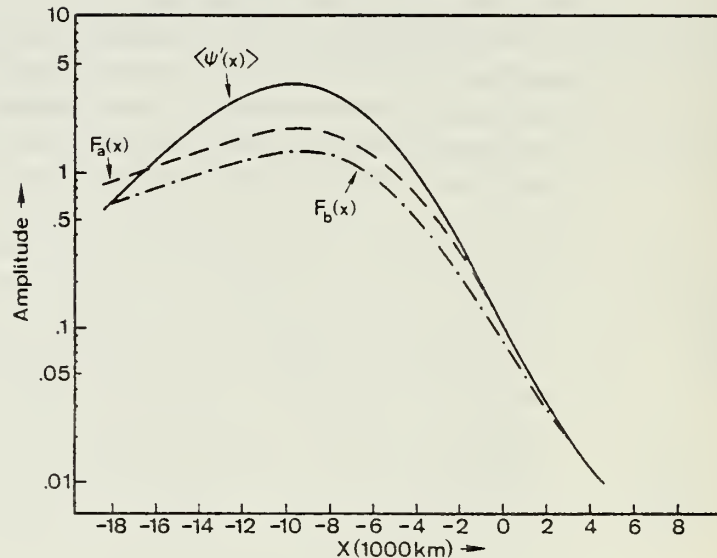


Figure 11

Comparison of wave packet envelopes in a locally unstable mean flow: $\langle \psi' \rangle$, computed from a numerical model; $F_a(x_0 = 280 \text{ km})$ and $F_b(x_0 = 4200 \text{ km})$, computed from an analytical model based on the parallel flow theory. (From TUPAZ *et al.* 1977.)

parallel flow theory put the maximum amplitude of the perturbations at $x = -9800 \text{ km}$, well past the jet maximum. This is in good agreement with the results obtained by COLTON (1973) and CHANG and PENTIMONTI (1977), and is qualitatively consistent with KRISHNAMURTI and ROGERS' (1970) observation that the most active disturbance area extends downstream from the jet maximum near the southern tip of India to central Africa (see Fig. 10.2, top panel, of KRISHNAMURTI, 1971b). This longitude of maximum amplitude corresponds to the neutral point of the basic flow, and is immediately understandable from the local growth rate concept: a wave coming in from the inflow boundary will grow as it moves downstream in the locally unstable region, until it reaches the neutral point where it begins to decay. However, the numerical solution has a larger maximum amplitude than that predicted by the local growth rate of the parallel flow theory. The waves actually grow faster in the unstable region and decay faster in the stable region. TUPAZ *et al.* (1977) evaluated the energy equation for the numerical model and found that the most important term for perturbation energy production is the Reynold stress term proportional to the meridional shear of the basic zonal wind. This term is also the only source term for a parallel flow model, and it depends on the phase structure of the perturbation field. Figure 12 compares the local phase tilt of the wave from the numerical model with that from the parallel flow theory at two longitudes: $x = 0 \text{ km}$ (jet maximum) and $x = -2800 \text{ km}$ (slightly downstream from jet maximum). At both places the phase tilt from the numerical model is significantly larger than that of the parallel flow theory.

Thus apparently the downstream variation of the basic flow augments the phase tilt of the waves which gives a larger growth rate in the unstable region. A similar situation is found in the stable region where the dynamic damping due to the continuous spectrum effect is enhanced by a stronger tilt in the same direction of the basic shear of the easterly jet. These results indicate that the barotropic energy exchanges associated with a zonally varying easterly jet which is locally unstable can actually be more prominent than those predicted by the local growth rate from the parallel flow theory. Hence the presence of the planetary-scale asymmetries during the summer monsoon strengthens the nonlinear energy conversions resulting in significant activity of synoptic-scale disturbances.

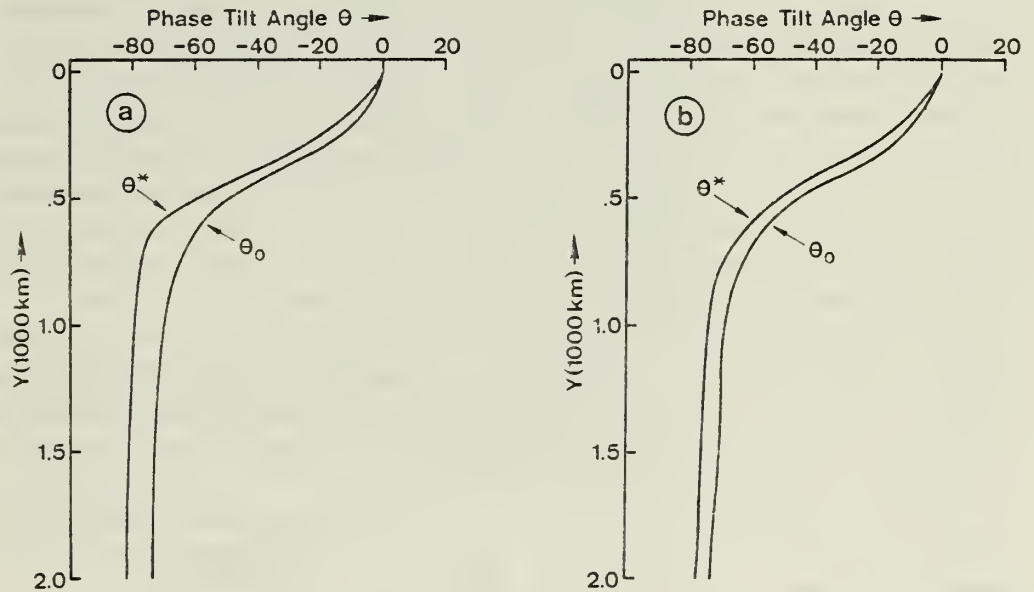


Figure 12

Comparison of the phase tilts of waves in a locally unstable mean flow computed by a numerical model (θ^*) and the parallel flow theory (θ_0) at two longitudes: (a) $x = 0$ where $\bar{u}(x, 0) = -30 \text{ m sec}^{-1}$ and (b) $x = 2800 \text{ km}$ where $\bar{u}(x, 0) = -27.3 \text{ m sec}^{-1}$. (From TUPAZ *et al.* 1977.)

Although TUPAZ *et al.* (1977) employed linear equations only, their results may also shed some light on the effects of the transient waves on the basic flow. The waves remove kinetic energy from the basic flow (both zonal and planetary scale) and most of this energy is removed on the downwind side of the jet maximum. Therefore it may be expected that in a nonlinear extension of their model the planetary scale will experience maximum damping west of the easterly jet maximum, which undoubtedly will affect the amplitude and phase of the forced planetary-scale waves.

4. Oscillations of the planetary-scale monsoons

The summer monsoon circulation is known to exhibit many fluctuations in a variety of time scales within each season. The most notable fluctuation is the alternating active and break periods of the monsoon. During the break periods most of the circulation characteristics may diminish or even reverse over the broad monsoon region. Less dramatic variations occur more frequently than the active-break cycles, although sometimes they are limited to local regions. Figure 13 shows the power spectrum of the 1967 summer 200 mb streamfunction over a region of the Tibetan high, analyzed by KRISHNAMURTI *et al.* (1973a). A pronounced oscillation periodicity is noted around 10–13 days and a secondary spectral peak occurs near 3 days. A similar spectral distribution for the tropospheric wind field of the 1962 summer was found by M. MURAKAMI (1976), where the main peaks occur at 10–15 days and 4–5 days. Both of these investigators felt that the shorter period oscillation may be a manifestation of the synoptic-scale westward propagating monsoon depressions. The longer period oscillation, on the other hand, appears to be related to the break monsoon and other broad-scale variations of the monsoon circulation. The 10–15 day periodicity of this oscillation has also been noted during many other years. For example, it is reflected in the daily rainfall data of 1963, 1971 (MURAKAMI, 1972), and 1972, 1973 (KRISHNAMURTI and BHALME, 1976).

After detecting a spectral peak near the 13-day periodicity in many parameters of the planetary-scale monsoon system of the 1967 summer, KRISHNAMURTI and BHALME (1976) calculated the phase relationship between the oscillation of these parameters. Their result suggests that in a 13-day cycle the sequential strengthening of the mon-

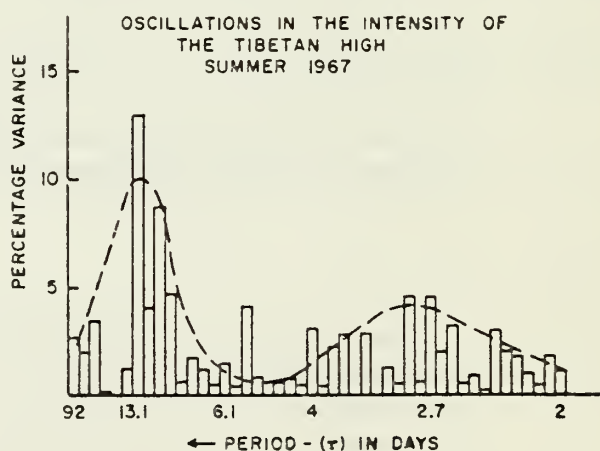


Figure 13

Percent variance spectrum of the intensity of the Tibetan High during June–August 1971. The dashed line is a smoothed envelope. (From KRISHNAMURTI *et al.*, 1973a.)

soon system including the monsoon trough, the cloud brightness, the surface Mascarene high, the upper Tibetan high and easterly jet, and the central Indian rainfall occur after the dry and moist destabilization of the lower troposphere. This will then be followed by a weakening of the system in the same sequence after dry and moist stabilization. On the other hand, M. MURAKAMI (1976) used a composite technique to study the 1962 summer monsoon, noting that it is difficult to verify the statistical significance of the cross-spectral quantities of this period range derived from a 3-month time series of daily data. He found that the intensification and weakening of convection and other low- and upper-level winds are closely in phase for the 15-day cycle during this season. In any case, there is strong evidence that many components of the planetary-scale monsoon are involved in this oscillation.

The observed 10–15 day oscillation raises an interesting question concerning its physical mechanism. KRISHNAMURTI and BHALME (1976) proposed that it may be a result of a cloud-radiative feedback mechanism in which the enhanced convection causes increased cloud cover which in turn reduces the incoming short-wave radiation and stabilizes the lower troposphere. This is then followed by decreased convection and cloudiness, and therefore increased short-wave radiative heating at the surface which renews the active convection. Another possible oscillation mechanism is revealed by a simple, domain-averaged, atmosphere-ocean interacting model by WEBSTER and LAU (1977). In their model the large heat capacity of the ocean causes it to respond slowly to the solar heating while the atmosphere temperature reaches a maximum due to heating at the land surface. After a period of time the ocean temperature peaks and this feeds back to the atmosphere through convection resulting in another temperature maximum. Although this process alone is unlikely to produce subsequent maxima without the participation of other mechanisms, it may still be relevant to some of the active-break cycles because RAMAMURTHY's (1969) survey (quoted in KRISHNAMURTI and BHALME, 1976) indicates that there are only one or two major breaks during most of the summer monsoon seasons. Other possible mechanisms for the planetary-scale oscillation may include interactions between hemispheres and between stationary and propagating long waves as mentioned by KRISHNAMURTI and BHALME (1976), and nonlinear vacillations between different scales. The latter mechanism produces a 5-day oscillation of the planetary scale in COLTON's (1973) barotropic model, which is purely dynamical and does not provide dissipation processes for the synoptic scale. If thermodynamics and synoptic damping are included, the interaction would become more complex and the oscillation period could be modified.

The planetary-scale circulation during the winter monsoon also exhibits significant variations, largely due to the influence of the cold air outbreaks from the Asian continent. These outbreaks often interfere with the main winter convective region in the maritime continent and cause widespread weather changes in the South China Sea and Malaysia–Indonesia region, including the development of strong synoptic-scale disturbance activity. Since this convective region provides the major energy

source for the thermally direct, planetary-scale east-west overturning and Hadley cells (KRISHNAMURTI *et al.* 1973b), its variations directly influence the circulations in the entire tropics and southern mid-latitudes during winter. These planetary-scale zonal and lateral teleconnections are reflected in the analyses by MURAKAMI and UNNINAYAR (1977) and KRISHNAMURTI *et al.* (1973b) despite their limited data base. The initiation and progress of theoretical studies in this area would depend heavily on the expansion of our present observational knowledge of this problem.

5. Concluding remarks

The three problems reviewed here are inter-related to each other. For example, the localized barotropic instability is a reflection of the strong nonlinear energy transfer which appears to be quite relevant to the damping of the planetary-scale flow during the summer monsoon. Also CHANG and PENTIMONTI's (1977) experiment indicates that these energy conversions are more pronounced when the planetary scale contains an appreciable oscillation. The enhanced upper tropospheric instability in summer due to both time and spatial variations of the planetary scale also has important ramifications for the synoptic-scale disturbances. At least in the mid-oceanic trough regions, the upper-level disturbances may develop in the vertical and could be related to some of the weather-producing easterly waves and tropical cyclones. A different type of problem arises for the winter monsoon during which the upper tropospheric synoptic-scale waves and zonal flow feed energy to the planetary scale (KRISHNAMURTI *et al.* 1973b). This on the one hand removes the nonlinear processes as a possible damping mechanism, and on the other hand requires an explanation for the energy source of the synoptic scale. Clearly much more effort is needed to answer these questions, whose importance lies in the fact that a thorough understanding of the planetary scale is crucial for the proper simulation of the entire multiple-scale monsoon circulation.

Acknowledgements

I wish to thank Professors R. T. Williams, J. R. Holton, P. J. Webster, T. Murakami, T. N. Krishnamurti and G. J. Haltiner for helpful discussion. This work was supported by the Atmospheric Science Section, National Science Foundation, under Grant DES75-10719, and by the Naval Environmental Prediction Research Facility.

REFERENCES

- ABBOTT, D. A. (1973), *Scale interactions of forced quasi-stationary waves at low latitudes*, Rept. 73-2, Dept. of Meteorology, Florida State Univ., Tallahassee, 190 p.
BARCILON, A., and COOPER, A. L. (1974), *A simple model for the east-west circulations found at 200 mb*

- during the summer of the northern hemisphere, Presented at Fall Annual Meeting, Amer. Geophys. Union, Abstract published in Transactions 56, 1123.
- CHANG, C.-P. (1977), *Viscous internal gravity waves and low-frequency oscillations in the tropics*, J. Atmos. Sci. 34, 901-910.
- CHANG, C.-P., and PENTIMONTI, R. J. (1977), *A numerical study of time-mean northern summer monsoon with steady and fluctuating heating*, Proc. Internatl. Sym. on Monsoons, New Delhi, India.
- COLTON, D. E. (1973), *Barotropic scale interactions in the tropical upper troposphere during the northern summer*, J. Atmos. Sci. 30, 1287-1302.
- FRANK, N. L. (1970), *On the nature of upper tropospheric cold core cyclones over the tropical Atlantic*, Ph.D. thesis, Florida State Univ., Tallahassee.
- HOLTON, J. R., and COLTON, D. E. (1972), *A diagnostic study of the vorticity balance of 200 mb in the tropics during the northern summer*, J. Atmos. Sci. 29, 1124-1128.
- HOLTON, J. R., and LINDZEN, R. S. (1968), *A note on "Kelvin" waves in the atmosphere*, Mon. Wea. Rev. 96, 385-386.
- KANAMITSU, M., KRISHNAMURTI, T. N., and DEPRADINE, C. (1972), *On scale interactions in the tropics during northern summer*, J. Atmos. Sci. 29, 698-706.
- KRISHNAMURTI, T. N. (1971a), *Tropical east-west circulations during the northern summer*, J. Atmos. Sci. 28, 1342-1347.
- KRISHNAMURTI, T. N. (1971b), *Observational study of the tropical upper troposphere motion field during the northern hemisphere summer*, J. Appl. Meteor. 10, 1066-1096.
- KRISHNAMURTI, T. N., and BHALME, H. N. (1976), *Oscillations of a monsoon system. Part I. Observational aspects*, J. Atmos. Sci. 33, 1937-1954.
- KRISHNAMURTI, T. N., DAGGUPATY, S. M., FEIN, J., KANAMITSU, M., and LEE, J. D. (1973a), *Tibetan high and upper tropospheric tropical circulations during northern summer*, Bull. Amer. Meteor. Soc. 54, 1234-1249.
- KRISHNAMURTI, T. N., KANAMITSU, M., KOSS, W. J., and LEE, J. D. (1973b), *Tropical east-west circulations during the northern winter*, J. Atmos. Sci. 30, 780-787.
- KRISHNAMURTI, T. N., and ROGERS, B. (1970), *200 millibar wind field June, July and August 1967*, Rept. 70-2, Dept. of Meteorology, Florida State Univ., Tallahassee.
- MERILEES, P. E. (1968), *An interpretation of barotropic instability in terms of the frequency of momentum convergence*, Mon. Wea. Rev. 96, 32-38.
- MILLER, B. L., and CARLSON, T. N. (1970), *Vertical motions and the kinetic energy balance of a cold low*, Mon. Wea. Rev. 98, 363-374.
- MURAKAMI, M. (1976), *Analysis of summer monsoon fluctuations over India*, J. Meteor. Soc. Japan 54, 15-31.
- MURAKAMI, T. (1972), *Equatorial stratospheric waves induced by diabatic heat sources*, J. Atmos. Sci. 29, 1129-1137.
- MURAKAMI, T. (1974), *Steady and transient waves excited by diabatic heat sources during summer monsoon*, J. Atmos. Sci. 31, 340-357.
- MURAKAMI, T., and UNNINAYAR, M. S. (1977), *Changes in atmospheric circulations during the northern hemisphere winter*, Submitted to Mon. Wea. Rev.
- PAEGLE, J., and PAEGLE, J. (1976), *On the realizability of strongly divergent supergradient flows*, J. Atmos. Sci. 33, 2300-2307.
- RAMAMURTHY, K. (1969), *Some aspects of the break in the Indian Southwest monsoon during July and August*, Forecasting Manual No. IV-18.3, India Meteor. Dept., Poona, 1-57.
- REED, R. J., and RECKER, E. E. (1971), *Structure and properties of synoptic-scale wave disturbances in the equatorial western Pacific*, J. Atmos. Sci. 28, 1117-1133.
- RICKS, E. (1959), *On the structure and maintenance of high-tropospheric cold-core cyclones of the tropics*, M. S. thesis, Univ. of Chicago.
- RIEHL, H. and PEARCE, R. P. (1968), *Studies on the interaction between synoptic and meso-scale weather elements in the tropics*, Rept. 126, Dept. of Atmospheric Science, Colorado State Univ., Ft. Collins.
- SADLER, J. C. (1967), *The tropical upper tropospheric trough as a secondary source of typhoons and a primary source of tradewind disturbances*, Final Rept., Contract AF19(628)-3860, Air Force Cambridge Research Labs., 44 p.
- SADLER, J. C. (1975), *The upper tropospheric circulation over the global tropics*, Rept. UHMET75-05, Dept. of Meteorology, Univ. of Hawaii, Honolulu, 35 p.

- TUPAZ, J. B., WILLIAMS, R. T., and CHANG, C.-P. (1977), *A numerical study of the locally unstable barotropic easterly jet*, Proc. Internl. Symp. on Monsoons, New Delhi, India.
- WALLACE, J. M. (1971), *Spectral studies of tropospheric wave disturbances in the tropical western Pacific*, Rev. Geophys. Space Phys. 9, 557-612.
- WEBSTER, P. J. (1972), *Response of the tropical atmosphere to local steady forcing*, Mon. Wea. Rev. 100, 518-541.
- WEBSTER, P. J. (1973), *Temporal variation of low-latitude zonal circulations*, Mon. Wea. Rev. 101, 803-816.
- WEBSTER, P. J., and LAU, K. M. W. (1977), *Simulation of the global monsoon sequence by a simple ocean-atmosphere interacting model*, Proc. Internl. Sym. on Monsoons, New Delhi, India.
- WILLIAMS, K. T., and GRAY, W. M. (1973), *Statistical analysis of satellite-observed trade wind cloud clusters in the western North Pacific*, Tellus 25, 313-336.

(Received 15th June 1977)

Initial Distribution List

	No. Copies
1. Defense Documentation Center Cameron Station Alexandria, Virginia 22314	2
2. Library, Code 0142 Naval Postgraduate School Monterey, California 93940	2
3. Research Administration, Code 012A Naval Postgraduate School Monterey, California 93940	1
4. National Science Foundation Division of Grants and Contracts Post-Award Project Branch Washington, D.C. 20550	2
5. Dr. Ron Taylor Meteorology Program National Science Foundation Washington, D.C. 20550	1
6. Dr. Richard Greenfield Global Atmospheric Research Program National Science Foundation Washington, D.C. 20550	1
7. Dr. Jay S. Fein Global Atmospheric Research Program National Science Foundation Washington, D.C. 20550	1
8. Professor C.-P. Chang, Code 63Cj Department of Meteorology Naval Postgraduate School Monterey, California 93940	5
9. Professor R. T. Williams, Code 63Wu Department of Meteorology Naval Postgraduate School Monterey, California 93940	2
10. Professor G. J. Haltiner, Code 63Ha Department of Meteorology Naval Postgraduate School Monterey, California 93940	1
11. Professor R. L. Elsberry, Code 63Es Department of Meteorology Naval Postgraduate School Monterey, California 93940	1

U18 1872

DUDLEY KNOX LIBRARY - RESEARCH REPORTS



5 6853 01068829 4

U18137